



**TRIBHUVAN UNIVERSITY
INSTITUTE OF ENGINEERING
PULCHOWK CAMPUS
DEPARTMENT OF CIVIL ENGINEERING**

**FINAL YEAR PROJECT REPORT
on
STUDY OF PAVEMENT RESPONSE TO VEHICLE
LOADING AND EVALUATION OF DAMAGE DUE TO
OVERLOAD**

By:

Roshit Raj Paudel (075BCE049)
Kamlesh Laha (075BCE069)
Pratik Subedi (075BCE105)
Pratiksha Khadka(075BCE106)
Sabit Timilsina(075BCE126)
Sailendra Katwal (075BCE131)

Supervisor:

Dr Pradeep Kumar Shrestha

APRIL 2023



**TRIBHUVAN UNIVERSITY
INSTITUTE OF ENGINEERING
PULCHOWK CAMPUS
DEPARTMENT OF CIVIL ENGINEERING**

FINAL YEAR PROJECT REPORT
on
**STUDY OF PAVEMENT RESPONSE TO VEHICLE
LOADING AND EVALUATION OF DAMAGE DUE TO
OVERLOAD**
**IN PARTIAL FULFILMENT OF THE REQUIREMENT FOR THE AWARD OF
BACHELOR DEGREE IN CIVIL ENGINEERING**
(Course Code: CE755)

By:

Roshit Raj Paudel (075BCE049)
Kamlesh Laha (075BCE069)
Pratik Subedi (075BCE105)
Pratiksha Khadka(075BCE106)
Sabit Timilsina(075BCE126)
Sailendra Katwal (075BCE131)

Supervisor:

Dr. Pradeep Kumar Shrestha

April 2023

COPYRIGHT

This project report is protected by copyright laws and is owned by the authors. © Roshit Raj Paudel, Kamlesh Kumar Laha, Pratik Subedi, Pratiksha Khadka, Sabit Timilsina, Sailendra Katwal. All rights reserved.

Any redistribution, reproduction, or display of part or all of the contents in any form is prohibited without the express written permission of the authors other than the following:

- You may print or download to local hard disk extracts for your personal and non-commercial use only.
- You may copy the content to individual third parties for their personal use, but only if you acknowledge the report as the source of the material.

You may not distribute or commercially exploit the content except with our written permission. Nor may you transmit it or store it on any other website or other forms of electronic retrieval system.

Head of Department
Department of Civil Engineering
Pulchowk Campus
Institute of Engineering
Lalitpur, Nepal



TRIBHUVAN UNIVERSITY
INSTITUTE OF ENGINEERING
PULCHOWK CAMPUS
DEPARTMENT OF CIVIL ENGINEERING

CERTIFICATE

This is to certify that this project work entitled “STUDY OF PAVEMENT RESPONSE TO VEHICLE LOADING AND EVALUATION OF DAMAGE DUE TO OVERLOAD” has been examined and declared successful for the fulfilment of academic requirement towards the completion of Bachelor Degree in Civil Engineering.

Project Supervisor
Dr Pradeep Kumar Shrestha

HOD , Department of Civil Engineering
Dr. Gokarna Bahadur Motra

External Examiner
Anil Marsani

Internal Examiner
Gopal Singh Bhandari

ACKNOWLEDGEMENT

We are grateful to the Department of Civil Engineering, Pulchowk Campus for providing us the opportunity and necessary environment to carry out our project work. We are indebted to our project supervisor, Dr. Pradeep Kumar Shrestha, for his invaluable guidance, and supervision suggestions that helped us complete the project work, and our Transportation Engineering professor Dr. Rojee Pradhananga for enriching our understanding in the field of transportation engineering.

We express our gratitude to our family members and friends for their unwavering support and encouragement during this journey.

We also thank everyone who directly or indirectly helped us during the project.

Roshit Raj Paudel (075BCE049)
Kamlesh Laha (075BCE069)
Pratik Subedi (075BCE105)
Pratiksha Khadka(075BCE106)
Sabit Timilsina(075BCE126)
Sailendra Katwal (075BCE131)

ABSTRACT

Flexible pavements are extensively utilized in roadway and airport construction due to their capacity to endure traffic loads and deformations. Finite element (FE) analysis has emerged as a prominent tool for projecting the performance of flexible pavements subjected to varying traffic loads and environmental conditions. In this report, an FE model of a flexible pavement was established and scrutinized through the use of the commercial software ABAQUS. The model encompassed numerous layers, including asphalt concrete, base, subbase, and subgrade layers. Validation of the FE model was done using IITPAVE. The linear model of the developed stress exhibited an increment in response with a rise in vehicular speed, whereas the viscoelastic model revealed a decline in stress with an increase in vehicular speed. It was found that the viscoelastic pavement has a higher response than linear elastic pavement and was concluded that the viscoelastic pavement is subjected to damage earlier than the linearly elastic pavement due to the development of more strain in viscoelastic pavement than in linearly elastic pavement. The findings of the FE analysis divulged that the pavement responses were heavily influenced by the individual properties of the various pavement layers and the traffic loads applied.

Additionally, the report addresses the issue of pavement failure due to overloaded vehicles on highways in Nepal, which reduces the road's service life. The findings indicate that the major cause of pavement failure is vehicle overload, with a decrease in remaining service life for the pavement ranging from 46 to 68 percent for an average value of overloading. The study also found that the required increase in asphalt overlaying due to vehicle overload is 15 to 21 percent for an average value of overloading. The CESAL values obtained through different methods provide fairly consistent estimates for the reduction in pavement service life and the increase in overlay thickness.

Roshit Raj Paudel (075BCE049)
Kamlesh Laha (075BCE069)
Pratik Subedi (075BCE105)
Pratiksha Khadka(075BCE106)
Sabit Timilsina(075BCE126)
Sailendra Katwal (075BCE131)

TABLE OF CONTENTS

| | |
|------------------------------------------------|------|
| List of Figures | viii |
| List of Tables | x |
| ABBREVIATIONS | xii |
| LIST OF SYMBOLS | xiii |
| 1. INTRODUCTION | 1 |
| 1.1 Introduction..... | 1 |
| 1.2 Problem Statement | 2 |
| 1.3 Objectives and Scope | 3 |
| 1.4 Limitations | 3 |
| 1.5 Organization of Report | 4 |
| 2. LITERATURE REVIEW | 5 |
| 2.1 Finite Element Modelling of Pavement | 5 |
| 2.2 Pavement Damage | 8 |
| 2.3 Material Behaviour of Pavement Layer | 10 |
| 3. METHODOLOGY | 13 |
| 3.1 Pavement Design | 13 |
| 3.2 Finite Element Modelling | 13 |
| 3.3 Analysis of Pavement Damage | 15 |
| 4. PAVEMENT DESIGN | 17 |
| 4.1 Traffic Study | 17 |
| 4.1.1 Future Traffic | 18 |
| 4.1.2 Axle Loading | 19 |
| 4.1.3 Vehicle Damage Factor..... | 19 |

| | |
|--------------------------------------------------------------------------|----|
| 4.2 Computation of Design Traffic..... | 22 |
| 4.2.1 Calculation of Forecasted Cumulative Number of Standard Axles..... | 23 |
| 4.3 Pavement Design | 24 |
| 4.3.1 Properties of Material | 25 |
| 4.3.2 Analysis of Pavement | 25 |
| 4.3.3 Results..... | 26 |
| 4.4 Final Design Parameters | 27 |
| 5. FEM MODELLING AND ANALYSIS | 28 |
| 5. 1 General Theory | 28 |
| 5.1.2 Material Behaviour of Pavement Layers | 29 |
| 5.1.3 Modelling of Moving Vehicle Load | 30 |
| 5.2 Model Validation | 32 |
| 5.2.1 Validated Model Description..... | 32 |
| 5.2.2 Validation..... | 32 |
| 5.3 Final Model Description | 34 |
| 5.3.1 General Description | 34 |
| 5.3.2 Boundary Condition..... | 35 |
| 5.3.3 Vehicle Modelling | 35 |
| 5.3.4 Material Characterization..... | 37 |
| 5.4 Response Analysis of Linear Model..... | 38 |
| 5.4.1 Stress (σ_y) on the pavement: | 39 |
| 5.4.2 Strain (ϵ) on the pavement..... | 41 |
| 5.4.3 Displacement (U_y) on the pavement: | 43 |
| 5.4 Response Analysis of Viscoelastic FEM Model..... | 44 |
| 5.5.1 Strain (ϵ) on the pavement..... | 45 |

| | |
|------------------------------------------------------------|----|
| 5.5.2 Stress (σ_y) on the pavement: | 48 |
| 5.5.3 Displacement (U_y) on the pavement: | 50 |
| 5.6 Comparison between Linear and Viscoelastic Model | 51 |
| 6. PAVEMENT DAMAGE ANALYSIS | 54 |
| 6.1 Introduction..... | 54 |
| 6.2 Survey Data..... | 55 |
| 6.3 Regulatory Standards in Nepal | 62 |
| 6.4 Study Process | 63 |
| 6.5 Equivalent Single Axle Load (ESAL) | 66 |
| 6.6 Methodology | 72 |
| 6.7 Calculation | 74 |
| 6.7 Results from Calculation..... | 86 |
| 7. CONCLUSION..... | 92 |
| 8. RECOMMENDATION | 93 |
| REFERENCES | 94 |
| ANNEX..... | 97 |

List of Figures

| | |
|---------------------------------------------------------------------------------------------------------|----|
| Figure 3.1: Flowchart for Pavement Design | 14 |
| Figure.3.2: Flowchart for FEM analysis | 15 |
| Figure 3.3: Flowchart for Pavement Damage Analysis | 16 |
| Figure 4.1: Survey stretch | 17 |
| Figure 5.1: Area of contact for wheel | 31 |
| Figure 5.2: Different Steps for FE Discretization | 31 |
| Figure 5.3: Model Used for Validation | 33 |
| Figure 5.4: Stress distribution in Model used for Validation | 34 |
| Figure 5.5: General Model with Loading | 34 |
| Figure 5.6: Area of contact of wheel | 36 |
| Figure 5.7: Stress at various positions of viscoelastic pavement under different velocities..... | 40 |
| Figure 5.8: Strain at various positions of viscoelastic pavement under different velocities..... | 42 |
| Figure 5.9: Displacement at various positions of viscoelastic pavement under different velocities | 44 |
| Figure 5.10: Strain at various position of viscoelastic pavement under different velocities | 47 |
| Figure 5.11: Stress at various positions of elastic pavement under different velocities | 49 |
| Figure 5.12: Displacement at various positions of elastic pavement under different velocities... | 51 |
| Figure 5.13: Response comparison for 110mm | 52 |
| Figure 5.14: Comparison of Responses at 410mm | 53 |
| Figure 6.1: Traffic Survey Stations Map | 55 |
| Figure 6.2: A Pie Chart Showing Vehicle Composition at Gurjudhara..... | 56 |
| Figure 6.3: Hourly Variation of Traffic Volume (Excluding Motorcycles) | 58 |
| Figure 6.4: Axle Load Survey..... | 58 |
| Figure 6.5: A bar graph comparing Eastbound to Westbound Loading Conditions..... | 59 |
| Figure 6.6: Flowchart for Statistical Analysis | 73 |
| Figure 6.7: Yearly CESAL for Bus (Case A) | 78 |
| Figure 6.8: Yearly CESAL for Bus (Case B) | 79 |
| Figure 6.9: Yearly CESAL for Bus (Case C) | 79 |
| Figure 6.10 Yearly CESAL Values for Case D | 80 |
| Figure 6.11: Yearly CESAL for heavy truck (Case A)..... | 80 |

| | |
|-----------------------------------------------------------------------------|----|
| Figure 6.12: Yearly CESAL for Heavy Truck (Case B)..... | 81 |
| Figure 6.13: Yearly CESAL for Heavy Truck (Case C)..... | 81 |
| Figure 6.14: Yearly CESAL for Heavy Truck (Case D) | 82 |
| Figure 6.15: Yearly CESAL for Multi-Axle Truck (Case A)..... | 82 |
| Figure 6.16 Yearly CESAL for Multi-Axle Truck (Case B) | 83 |
| Figure 6.17: Yearly CESAL for Multi-Axle Truck (Case C) | 83 |
| Figure 6.18: Yearly CESAL for Multi Axle Truck (Case D) | 84 |
| Figure 6.19: Yearly CESAL (Case A) | 84 |
| Figure 6.20: Yearly CESAL (Case B) | 85 |
| Figure 6.21: Yearly CESAL (Case C) | 85 |
| Figure 6.21: Yearly CESAL (case D) | 86 |
| Figure 6.23: Increasing asphalt thickness as increasing year (Case A) | 90 |
| Figure 6.24: Increasing asphalt thickness as increasing year (Case B) | 90 |
| Figure 6.25: Increasing asphalt thickness as increasing year (Case C) | 91 |

List of Tables

| | |
|--------------------------------------------------------------------------|----|
| Table 4.1: Vehicle Count | 18 |
| Table 4.2: Traffic growth rate forecast | 18 |
| Table 4.3 Results of Axle load survey | 19 |
| Table 4.4: Vehicle damage factor | 20 |
| Table 4.5: Trial thickness for design iterations..... | 25 |
| Table 4.6: Allowable strain..... | 26 |
| Table 4.7: Final Design Parameters | 27 |
| Table 5.1: Layer properties | 32 |
| Table 5.2: Comparison of values obtained by IITPAVE and ABAQUS..... | 33 |
| Table 5.3: TATA LPK 2518 Specifications | 35 |
| Table 5.4: Calculation of equivalent tyre dimensions | 36 |
| Table 5.5: Layer properties | 37 |
| Table 5.6 Prony Series for Generalized Maxwell Model | 37 |
| Table 5.8: Response of Viscoelastic pavement model on various speed..... | 38 |
| Table 5.9: Response of Viscoelastic pavement model on various speed..... | 45 |
| Table 6.1: Traffic Count Survey | 57 |
| Table 6.2: Loading Weight of Each Commodity Type..... | 60 |
| Table 6.3: Total Weight Recorded..... | 60 |
| Table 6.4: Results of Axle Load Surveys Done in Other Studies..... | 61 |
| Table 6.5: Loading Limit for Different Axles | 62 |
| Table 6.6: Vehicle Classification..... | 64 |
| Table 6.7: Values of k as suggested by LCPC..... | 68 |
| Table 6.8: Values of ALP | 69 |
| Table 6.9: Values of 1 through a_6 | 69 |
| Table 6.10: Values of a, b, c for thickness..... | 71 |
| Table 6.11: EALF for Heavy Bus | 74 |
| Table 6.12: EALF for Heavy Truck..... | 75 |
| Table 6.13: EALF for Multi Axle Truck | 76 |
| Table 6.14: CESAL calculation throughout the design life..... | 77 |
| Table 6.15: Reduction in Service life | 86 |

| | |
|------------------------------------------------------------|----|
| Table 6.16: Increased Asphalt thickness for method A | 88 |
| Table 6.17: Increased Asphalt thickness for Method B | 88 |
| Table 6.18: Increased Asphalt thickness for method C | 89 |

ABBREVIATIONS

| | |
|-------|---------------------------------------------|
| FEM | Finite Element Method |
| CFD | Computational Fluid Dynamics |
| DEM | Discrete Element Method |
| HMA | Hot Mix Asphalt |
| FEA | Finite Element Analysis |
| MEPDG | Mechanistic Empirical Pavement Design Guide |
| FE | Finite Element |
| ESAL | Equivalent Single Axle Load |
| CESAL | Cumulative Equivalent Single Axle Load |
| GVW | Gross Vehicle Weight |
| DoR | Department of Roads, Nepal |
| ALP | Axle Load Parameter |
| AADT | Average Annual Daily Traffic |
| MPa | Mega Pascal |
| PSI | Pounds per Square Inch |
| VDF | Vehicle Damage factor |

LIST OF SYMBOLS

| | |
|----------|-----------------------------------------------------------------------------------|
| [M] | Mass |
| [C] | Damping |
| [K] | Stiffness Matrices |
| { u } | Velocity |
| {P} | External Force Vectors |
| σ | Stress Tensor |
| E | Deviator Parts of Strain Tensor |
| Δ | Volumetric Parts of Strain Tensor |
| τ | Relaxation Time |
| N_R | Sub-Grade Rutting Life |
| E_V | Vertical Compressive Strain at the Top of the Sub-Grade |
| N_f | Fatigue Life of Bituminous Layer |
| E_T | Maximum Horizontal Tensile Strain at the Bottom of the Bottom Bituminous Layer |
| M_{Rm} | Resilient Modulus (MPa) Of the Bituminous Mix Used in the Bottom Bituminous Layer |
| N | Cumulative Number of Standard Axles to Be Catered for the Design in Terms of Msa |
| A | Initial Traffic in the Year of Completion of Construction in Terms of CVPD |
| D | Lane Distribution Factor |
| F | Vehicle Damage Factor (As Shown Above VDF Table) |

| | |
|------------------------|----------------------------------------------------------------------------|
| N | Design Life in Years = 20 Years |
| R | Annual Growth Rate of Commercial Vehicles |
| G_{∞} And G_i | Material Shear Modulus in Pa |
| K_{∞} And K_i | Material Bulk Modulus in Pa |
| τ | Relaxation Time |
| μ | Poisson Ratio |
| A_c | Contact Area Calculated by Dividing the Load on Each Tyre By Tyre Pressure |
| G_i | Material Constant |
| ϵ | Strain |
| ϵ_y | Vertical Strain |
| U_y | Displacement of the Pavement |

1. INTRODUCTION

1.1 Introduction

Pavement is a multi-layered system that transmits the vehicular loads into the underlying soil. The frequent loading and unloading of pavements with varying intensity and speeds makes their quality and strength deteriorate quickly. This deterioration is unavoidable, but it can be delayed by proper design and construction of pavements. The deterioration of pavements indicates the failure of pavement, which is based on structure (potholes, cracks, rutting, etc.) as well as serviceability. Pavement design has been the subject of extensive research and study. Various empirical design, semi-empirical and mechanistic empirical design methods have been developed throughout the years. The mechanistic-empirical methods like Road Note-31 (1984) AASHTO Design Guide (1993) and IRC-37 (2001) are widely used nowadays. The Department of Roads, Nepal has also developed the Guidelines for the Design of Flexible Pavements- 2014 (Second Edition 2021) based on these design methods.

With pavement being a multi-layered system, layered elastic theory is mostly used to analyse the response of the pavements. Various theories regarding multi-layered elastic models of pavement have been developed, starting from Burmister in 1945, who developed a solution for two layered elastic pavement which was extended to a three-layer system by Huang (1993). With the development of finite element methods, various computer programs have been developed such as BISAR (Shell, 1978), ELSYM5 (University of California, 1985), KENPAVE (Huang, 1993), IITPAVE (IIT, India), etc. Even though there are programs designed for pavement analysis, general FEM programs like ABAQUS, ANSYS, DYNA, etc. are widely used because they can handle complex pavement problems. These programs give more accurate results with wider control over the characteristics, parameters and the governing laws/models.

The study on pavement damage using Finite Element Method (FEM) is an emerging field with many papers being recently published. Pavements are modelled as two- or three-dimensional structures usually considering linear material properties. Looney et al. (1981) were among the first to develop the 2D FEM models to analyse the behaviour of flexible pavements using stiffness model. Zaghoul et. al (1994) were among the first to develop a three-dimensional model to

validate the application of 3D-DFEM to flexible pavement analysis. In recent times, use of FEM is being combined with machine learning techniques to develop data driven models that can predict the pavement performance. The combination of FEM along with Computational Fluid Dynamics (CFD), Discrete Element Method (DEM), etc. provides even more accurate and comprehensive analysis of pavement performance.

The analysis of pavement using FEM involves modelling the pavement model into the smaller elements and simulating the behaviour under different loading and environmental conditions by applying boundary conditions. The material properties used require accurate and reliable data obtained from laboratory tests. The FEM analysis of pavement usually assumes the materials to behave linearly although the use of viscoelastic and viscoelastic theory is also sometimes used. The viscoelastic theory is generally accepted to represent the real-world behaviour of pavement and provide accurate pavement response although the accuracy depends on the accuracy of material properties as determined by various lab tests. FEM analysis provides information about the stress and strain distribution of the model under various conditions. This information is critical to understand the response of pavement. This can be used to predict the fatigue life as well as failure of the pavement.

In addition to evaluating the pavement response to vehicular loads, statistical analysis can be employed to quantify pavement damage using available traffic data. By examining the vehicle count and axle loads on a specific road segment, the Equivalent Single Axle Load (ESAL) can be determined over the pavement's design life. This information can then be utilized in studies of pavement cost analysis and service life reduction. By using ESAL as a tool to quantify pavement damage, engineers and researchers can make informed decisions and provide effective solutions for pavement maintenance and design. Existing literature can provide further insight into the statistical analysis of pavement damage through the calculation of ESAL.

1.2 Problem Statement

Various indicators of damage in pavements of Nepal can be seen prematurely. Almost all of the major roads of Nepal do not last up to their intended service period and the major indicators of failure; potholes, ruts and cracks can be seen after a brief period of operation. This can be accounted to the faulty design, poor construction materials and method, etc. Among these, the overloading of vehicles and the lack of proper design methodology accounting for this overload

beyond the legal limit are significant. The study of pavement responses required for designing new design methodology and guidelines are also lacking in the context of Nepal. There is a serious need for experimental as well as analytical research of pavement response under various load conditions and various types of vehicles. This research project aims to quantify the damage caused by the overloads in the roads of Nepal as well as to close the gap in analytical research of the pavement responses to the major overloaded vehicles i.e., trucks under various speeds.

1.3 Objectives and Scope

Our study consists of two major parts, the FEM Study Part and Pavement Damage Part. The objectives of the project have been listed below:

- To assess the vehicle count for a selected stretch of road and design the pavement.
- To prepare a Finite Element Model for the designed pavement.
- To validate the Finite Element Model using existing linear analysis.
- To use the validated model to further find out the response of a pavement in its different layers to vehicle loading in both linearly elastic and viscoelastic conditions.
- To use the response of vehicle loading in subgrade rutting and fatigue cracking criteria.
- To study the different ways of calculating the ESAL for a stretch of road through various guidelines and then compare the results.
- To analyse axle-load survey results in the selected stretch of road and find out the reduction in service life through various methods and compare the results.
- To find the extra thickness of overlay required due to vehicle overload.

1.4 Limitations

The limitations of project are listed below:

1. There is a lack of proper and updated data regarding axle loads and overloading of vehicles.
2. The data used in analysis is obtained from secondary sources, so the results may not be as accurate when primary data can be used.
3. The material's non-linear behaviour is not taken into account directly, but instead adjusted based on data from an experimental research paper. As a result, the material's

- response may not accurately reflect the actual conditions experienced in Nepal.
4. It was not possible to find out the VDF of each and every vehicle traversing the road.
 5. Due to the unavailability of data, we had to choose a representative vehicle for each of the considered classes.

1.5 Organization of Report

This project report is presented in eight chapters. Brief description of the organization is as follows:

Chapter 1 contains the introduction of the project. This chapter discusses the deterioration of pavements due to overloading of pavement as well as the brief description of modelling of pavement for FEM analysis. The objectives, scope and limitations of the project are also discussed.

Chapter 2 includes the review of existing literature regarding FEM analysis of pavement and the statistical analysis and quantification of pavement damage along with some general literature review.

Chapter 3 explains the methodology followed in the project in brief.

Chapter 4 includes the design of pavement using the data available for further use in FEM analysis of the pavement.

Chapter 5 is about the description and analysis of Pavement model using ABAQUS. It contains the model validation, and the linear and nonlinear Finite Element Analysis of pavement designed the preceding chapter.

Chapter 6 has the quantification of pavement damage through statistical analysis of vehicle count and the overloading of vehicle.

Chapter 7 includes the discussion and conclusion of the project as a whole.

Chapter 8 provides recommendations for any future work.

2. LITERATURE REVIEW

2.1 Finite Element Modelling of Pavement

Finite Element modelling offers the best analysis for multi-layered pavement systems. FEM can be used to simulate the behaviour of pavement structures under various types of traffic loads and environmental conditions. This allows engineers and researchers to better understand the performance of different pavement designs and materials, and to optimize pavement performance and longevity.

The models can be 2 dimensional (2D) or 3 dimensional (3D) and various conditions and properties of materials can be used. Flexible pavements were commonly modelled as multi-layered linear elastic systems using the theory was originally developed by Burmister in 1943 for two-layered linear elastic systems. Looney et al. (1981) were among the first to develop the 2D FEM models to analyse behaviour of flexible pavements using stiffness model. Zaghoul et. al (1994) were among the first to develop a three-dimensional model to validate the application of 3D-FEM to flexible pavement analysis. The asphaltic concrete modelled was viscoelastic while other granular materials were modelled using Drucker-Prager model. Several three-dimensional models have been developed since then.

Al-Qadi et al (2008) proposed a viscoelastic model to accurately represent the properties of Hot Mix Asphalt (HMA). It is believed that the models using uniform tyre pavement contact stresses, static vehicle load and linear material properties are inconsistent with realistic conditions. So, to more accurately simulate the real-world conditions a model incorporating continuous moving vehicle load and viscoelastic model for HMA was proposed. The study focused on the damage caused by dual tyre configuration and wide based tyres. It was found that the longitudinal tensile strain at bottom of the HMA is critical in thin and medium thickness HMA. This model was verified using in situ pavement response of the tyres using ATLAS loading machine at the University of Illinois.

To improve the accuracy of FEM model on rutting, Wang et al. (2015) developed a modified 3D model using creep law as the strain hardening formulation. This model adopted repeated loading on the pavement to evaluate the influences of truck parameters on rutting. The results indicate that

the front axle is also as important as the rear axle for pavement rutting. Also, the study found that the rutting increases by 60% when the vehicle speed decreases from 80kmph to 60kmph. The study was validated by using laboratory results.

Beskou et al. (2016) modelled the pavement materials as elastic-viscoelastic with time dependent properties. The study investigated the sensitivity of pavement responses under dynamic loads to variations in material properties such as thickness, Modulus of Elasticity, Poisson's ratio and Shear Modulus. This study concluded that the asphalt layer has most significant influence on the pavement response under dynamic loads. There were four model which incorporated viscoelastic or viscoelastic nature of asphalt layer and elastic or elastoplastic Drucker-Prager material behaviour for the granular layers. The model was validated using numerical as well as field experimental results. This study recommended the use of viscoelastic model for practical application as it was the simplest and had the lowest computational time while producing similar results to other models as well as being closer to the test results.

Ghadimi et al. (2016) developed a 2D FEM model taking into account the shakedown effects under which the granular material behaviour changes from plastic to elastic as a function of number of loading cycles. The shakedown concept was implemented for the granular layer under asphalt concrete. This study compared their simulations, first modelled by Mohr-Coulomb equation, second modelled by modified Mohr-Coulomb to replicate shakedown effect and the third considering soil-asphalt interaction along with shakedown effect. The inclusion of SAI effect resulted in higher tensile strain at bottom of asphalt layer and lower compressive strain at the top of subgrade.

Alimohammadi et al. (2021) developed a FEM model to compare the rutting damage of pavements designed by Mechanistic-Empirical Pavement Design Guide (MEPDG) using the results of series of dynamic modulus tests. The models used viscoelastic simulations to predict the behaviour of asphalt. It was found that the MEPDG based on linear elastic theories may overestimate the rutting while finite element-based theory predicted the rutting behaviour more accurately. A series of calibration coefficients was proposed to modify and correct the MEPDG overlay design guidelines.

The study by Al-Ghazali et al. (2015) focused on investigating the effect of flexible pavement thickness on permanent deformation of paved and unpaved roads over sand dunes subgrade under repeated loads. The study utilized two approaches to evaluate the behaviour of flexible pavement

in permanent deformation of paved and unpaved roads over sand dunes subgrade under repeated loads: laboratory tests and FEM models. In laboratory tests, the behaviour of sand dunes subgrade layer was investigated by using it as a part of flexible pavement structure under repeated loads at relative density 55.7%. On the other hand, the FEM models were based on a three-dimensional finite element model for flexible pavements using ABAQUS. The results indicated that increasing the thickness of flexible pavement resulted in an increased number of passes that reached the same value of rutting (value of failure) and led to a decrease in displacement in subgrade and subbase layers. The findings from the ABAQUS program were very close to the results of laboratory tests. Therefore, the ABAQUS program was successful in simulating pavement structure models, which makes it a useful tool in the analysis of paved road behaviour.

The research conducted by Yoo et al. (2014) investigated the impact of different tyre types and vehicle configurations on pavement damage. The study found that wide-base tyres have a lower radial stiffness than conventional dual tyres, leading to higher contact pressure and more significant pavement damage. The study considered the four main failure mechanisms of pavement: fatigue cracking, primary and secondary rutting, and top-down cracking. The authors compared various tyre configurations and validated them through field measurements. Tensile strains at the bottom of the Hot Mix Asphalt (HMA) were measured under various tyre loading conditions, and a three-dimensional finite element (FE) model was developed to predict pavement responses caused by various tyre configurations, which was validated by field measurements. It was observed that wide base single tyres were more damaging on both thin and thick pavement sections. The study also found that tyre type and inflation pressure had a significant impact on pavement damage, with higher inflation pressure causing more damage to the pavement. The number and spacing of axles on the vehicle were also found to affect pavement damage, with more axles and closer spacing resulting in greater damage.

Hao Wang et al. (2011) conducted a study for predicting the contact stresses at static and various rolling conditions by simulating tyre pavement interactions. The ribbed radial-ply tyre was modelled as a composite structure (rubber and reinforcement), and the tyre material parameters were calibrated through load-deflection curves. The steady-state tyre rolling process was simulated using an arbitrary Lagrangian Eulerian formulation. The model results are consistent with previous measurements and validate the existence of non-uniform vertical contact stresses and localized tangential contact stresses. The analysis results show that the non-uniformity of vertical contact

stresses decreases as the load increases but increases as the inflation pressure increases. However, vehicle manoeuvring behaviour significantly affects the tyre–pavement contact stress distributions. For example, tyre braking/acceleration induces significant longitudinal contact stresses, while tyre cornering causes the peak contact stresses shifting towards one side of the contact patch. The model results provide valuable insights into understanding the realistic tyre–pavement interaction for analysing pavement responses at critical loading conditions.

2.2 Pavement Damage

Pais and Pereira (2016) study examined the consequences of traffic overloads on the design life of flexible pavements. The findings revealed that pavement design life can be reduced by almost half due to overloaded vehicles. The study also highlighted that when a pavement is overloaded by 5%, its design life is reduced from 15 years to 12.3 years. Similarly, overloading of 10% and 20% can reduce pavement design life to approximately 10 and 7 years, respectively. The impact of overloads on pavement performance was investigated by calculating the effect of all vehicles on pavement performance. To represent the effect of different types of vehicles with varying loads, all vehicles were converted into a representative axle, which in pavement design is referred to as a standard axle resulting in the Equivalent Single Axle Load (ESAL). By converting vehicle axles into ESAL, the study was able to consider a vehicle as a certain number of single axle loads. These findings can provide valuable insights for improving pavement design and maintenance to enhance the durability and safety of flexible pavements.

Amorim et al. (2015) proposed a model for calculating equivalent axle load factors. They developed a model for calculating equivalent axle load factors (EALFs) considering the type of axle, the type of wheel and the constitution of the pavement. The model was developed based on the tensile strain at the bottom of the asphalt layer that is responsible for bottom-up cracking in asphalt pavement. It also presents the influence of the type of wheel (single and dual) on pavement performance. The results of this work allowed the conclusion that the EALFs for single wheels are approximately 10 times greater than those for a dual wheel.

Wang, Zhao, and Wang (2015) evaluated the impact of overweight traffic on pavement life using a mechanistic-empirical analysis approach and found that weigh-in-motion data can be used to analyse this impact. The state-of-practice mechanistic-empirical pavement design and analysis

software (Pavement-ME) was used to predict pavement life under different traffic loading scenarios. A linear relationship was found between the overweight percentage and the reduction ratio of pavement life regardless of the variation in traffic loading and pavement structure. In general, it shows that a 1% increase of overweight truck may cause a 1.8% reduction of pavement life.

Jihanny et al. (2018) presented the analysis results of the weigh-in-motion survey data and the impact of overloaded trucks on the pavement. For the analysis, a simplified approach was used where axle loads were converted into representative single-axle loads based on 4th power formula by AASHTO 1993 equation. The vehicle damage factor of vehicles is presented and compared with the Highways National Standard to estimate the remaining service life of pavement and IRI value prediction¹. The analysis showed that the vehicle damage factor determined from weigh-in-motion data is extremely greater than the vehicle damage factor of the national standard in Indonesia.

Ojha (2015) conducted a comparative study on flexible pavement thickness between standard and overloading conditions using the AASHTO 1993. The impact of overload conditions on the road pavement showed an increase in layer thickness compared to thickness at the legal axle load limit. For S-N direction, the pavement thickness seemed to be increased up to 22.81% due to overloading with respect to standard condition. The total pavement thickness required for overloaded condition seemed to be 43.25 inches with 30.735 inches subbase, 7.797 inches base, and 4.718 inches bituminous wearing course but in standard condition total thickness required seemed to be 36.856 inches with 26.659 inches subbase, 6.355 inches base, and 3.842 inches bituminous wearing course.

According to Raheel et al. (2015), the load equivalency factor can be affected by factors such as axle overload, asphalt pavement thickness, and subgrade modulus. This paper quantifies the number of overloaded vehicles from data collected on a critical national highway and computes the impact of overloaded axle loads on road pavement in terms of ESALs. The truck factor was calculated according to the modified French Pavement Design Guide equation. It was found that the impact of axle configuration on the pavement is significant, i.e. truck factor for 2-axle vehicles was almost 3.33 times the 3-axle vehicles and 5.45 times the 6-axle semi-trailers. It was also

observed that the truck factor reduced by almost 47% with a twofold increase in asphalt layer thickness. The subgrade modulus had a very minimal effect on the truck factor.

2.3 Material Behaviour of Pavement Layer

The material behaviour of a pavement layer is an important factor in determining the performance of a pavement structure under various loads and environmental conditions. Different pavement layers can exhibit different material behaviours, which can be modelled using different constitutive equations.

Some common material behaviours of pavement layers include:

- **Elastic behaviour:** This is the simplest material behaviour, in which the pavement layer deforms elastically under load but returns to its original shape when the load is removed. This behaviour is modelled using Hooke's Law, which relates the stress in the material to the strain.
- **Viscoelastic behaviour:** This is a more complex material behaviour, in which the pavement layer deforms both elastically and viscously under load. This behaviour is modelled using a variety of constitutive equations, such as the generalized Maxwell model or the Burgers model.
- **Plastic behaviour:** This is a non-reversible material behaviour, in which the pavement layer deforms plastically under load and does not return to its original shape when the load is removed. This behaviour is modelled using a variety of constitutive equations, such as the Drucker-Prager model or the Mohr-Coulomb model.
- **Damage behaviour:** This is a material behaviour in which the pavement layer undergoes micro-cracking or other forms of damage under load, leading to a reduction in stiffness and strength over time. This behaviour is modelled using a variety of constitutive equations, such as the damage mechanics model or the cohesive zone model

For the finite element simulation of the pavement, pavement layers from road base to natural soil were considered isotropic linear elastic.

Flexible pavement refers to a type of road surface that is designed to be flexible and move slightly under traffic loads. It is made up of a subgrade, base course, and an asphalt or concrete surface

course, among other layers of materials. Low flexural strength and distribution of wheel load from the mineral grains of the pavement layers are characteristics of flexible pavement types.

During the design of road pavements, each type of vehicle is translated into Equivalent Standard Axle Load (ESAL) to consider their impact on road structure. There are different types of vehicles passing on the pavement during the life of pavement, among which heavy vehicles impose the most critical loading, causing damage in pavement structure which has large axle load.

The increasing axle load and/or total vehicle weight reduces the pavement service life and increases the departmental cost to keep pavement condition at an acceptable level. Greater increasing of Gross Vehicle Weight (GVW) led to significant decreasing of the pavement service life and more overlays. Additionally, it was also found that the effect of vehicle loads was decreased by increasing the asphalt layer thickness and subgrade stiffness and little effect on the impact of vehicle loads, if the pavement distress is fatigue cracking.

An axle load survey conducted by the Department of Roads (DoR) in 2010 has revealed that about 30% of commercial heavy vehicles are overloaded beyond the permissible axle load. In the context of Nepal highway, traffic volume along the major Highways is increasing rapidly. Relatively the movement of multi axle heavy vehicles is very common. Due to these overloaded heavy vehicles, the road pavement is deteriorating rapidly with rutting, fatigue cracking and potholes along the road section. In general, it is accepted that a 1% increase of overweight truck may cause 1.8% reduction of pavement life.

Any sort of physical destruction or deterioration to a paved surface, such as a road, parking lot, or footpath, is referred to as "pavement damage." Pavement deterioration is frequently brought on by:

- High traffic volume: High traffic volume can wear down the pavement over time, resulting in cracks, potholes, and other types of damage.
- Weather Condition: Extreme temperatures, precipitation, and snow can cause the pavement to expand and compress, which can result in cracking and other damage.
- Poor construction: Pavement that has been improperly built may be more vulnerable to damage and decay.
- Chemical damage: The pavement can erode and break down when exposed to chemicals

like oil, gasoline, and salt.

- Natural catastrophes: Earthquakes, floods, and landslides are few examples of the catastrophes that can seriously harm pavements.
- Lack of upkeep: Pavements can deteriorate over time if regular maintenance isn't performed, such as patching potholes and cracks and sealing the surface.

In pavement engineering, stress and strain are crucial ideas because they affect how well and how long pavements perform and last when subjected to traffic loads. Strain is the resultant deformation or elongation per unit length, whereas stress is the force exerted per unit area. Stress is commonly measured in Kilo Pascal (KPa) in the SI system of units (or alternatively, pounds per square inch (PSI) in US Customary Units) in pavement engineering, whereas strain is quantified as a dimensionless quantity.

Pavements endure both vertical and horizontal stresses as a result of traffic loading. Vehicle weight causes vertical strains, but lateral pressures applied by turning or changing lanes by moving vehicles create horizontal stresses. These stresses can weaken the pavement over time and increase the risk of failure by causing deformation or cracking in the pavement. Engineers should understand the stress-strain connection of the materials used in the pavement construction in order to design and build long-lasting pavements. A stress-strain curve, which represents the relationship between the applied stress and the resulting strain for a certain material, is often used to describe this relationship.

3. METHODOLOGY

This report consists of three major parts, pavement design, FEM Analysis and Statistical Analysis for pavement damage. The brief methodology followed in each of these parts are described below in brief along with appropriate flowcharts just to provide an overview. The detailed methodology can be found in their respective chapters.

3.1 Pavement Design

The general methodology carried out for the pavement design is presented in figure 3.1. It is summarized as follows:

1. Traffic data of a stretch of road from Gurjudhara to Naubise was collected.
2. The future forecasting of traffic in terms of cumulative number of standard axles was done.
3. The properties of materials were extracted from the values as suggested by the guidelines.
4. Horizontal and vertical strains derived from the performance models mentioned in the guidelines were computed.
5. A trial thickness of pavement was taken, and the computation of allowable horizontal and vertical strains were done using IITPAVE software. The trial iterations were done until the values given by IITPAVE were less than that of the computed allowable strain values.
6. The final pavement parameters were selected.

3.2 Finite Element Modelling

The general methodology carried out for the Finite Element (FE) Modelling of the pavement is presented in figure 3.2. It is summarized as follows:

1. The trial thickness of each pavement layer was extracted from pavement modelling, and the corresponding part was created in the FE software ABAQUS.
2. Properties like elasticity, density, Poisson's ratio, and viscoelasticity were assigned to each pavement layer.
3. The interaction between the pavement layers was then created, which allowed for the transfer of loads applied to one layer to another layer.
4. The mesh for the different pavement layers was generated, with the mesh near the surface

of the pavement being more refined than the layer below to capture stress and strain distribution more accurately.

5. Steps were created and time periods were assigned to each step according to the required velocity of the vehicle.
6. A load was created and applied to the surface of the asphalt layer in the appropriate step to simulate a running vehicle on the pavement. Additionally, a boundary condition was created and assigned to the initial step, which propagated to every step.
7. Once the geometry, material properties, mesh, interaction, and boundary conditions were defined, the pavement structure was analysed using ABAQUS.
8. Finally, the results of the analysis were extracted and interpreted, including the stress, strain, and displacement on the pavement.
9. The results thus obtained were validated by using the IITPAVE software.

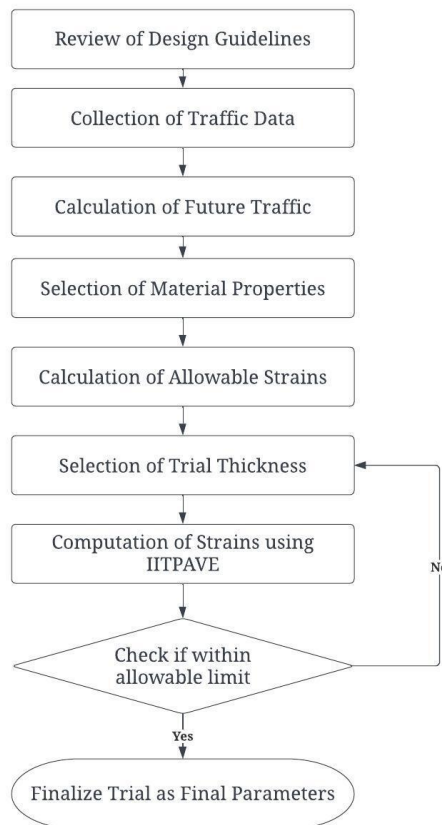


Figure 3.1: Flowchart for Pavement Design

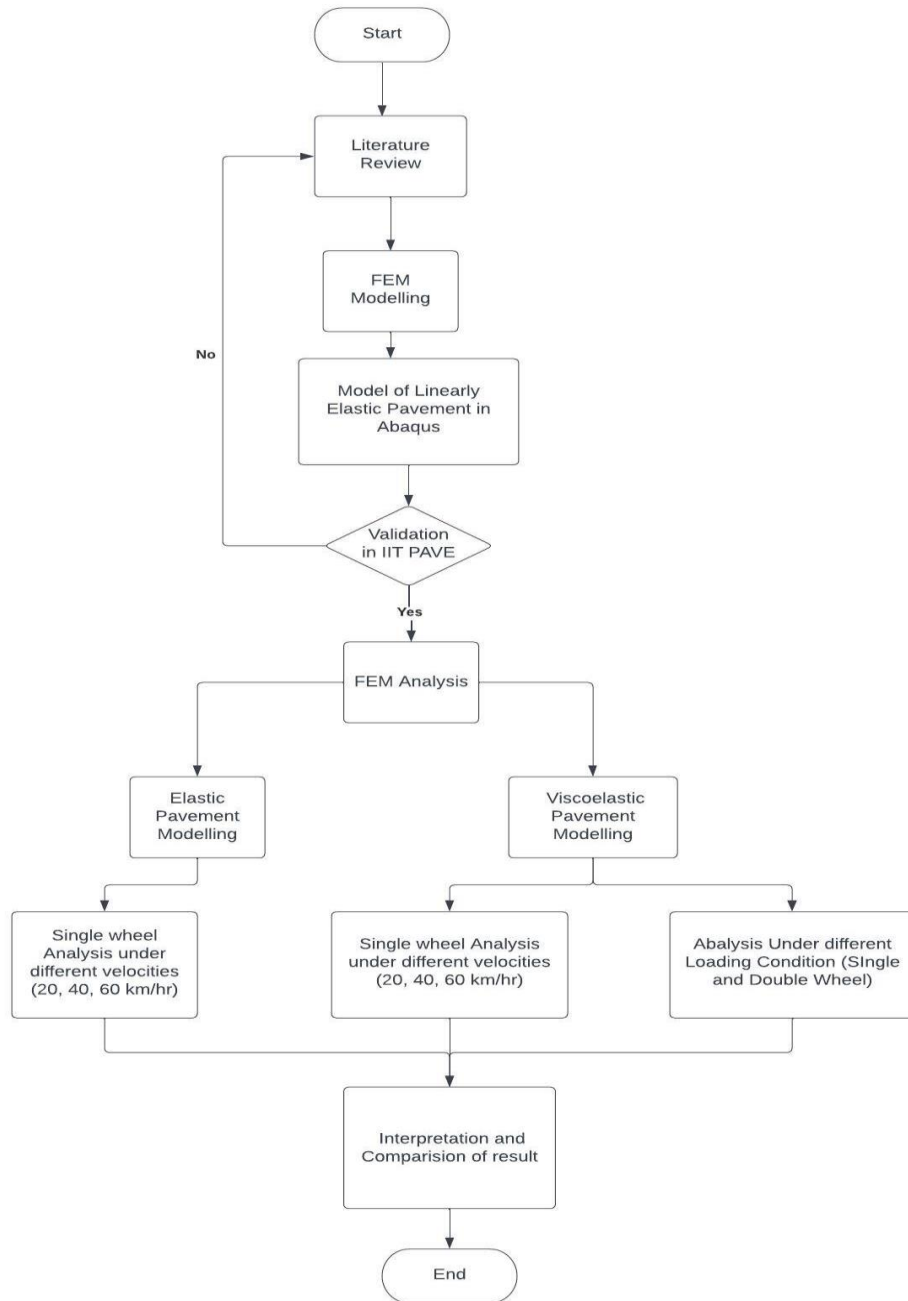


Figure.3.2: Flowchart for FEM analysis

3.3 Analysis of Pavement Damage

The general methodology followed for statistical analysis is as follows:

1. The main types of vehicles responsible for causing pavement damage were determined.
2. The values of EALF and CESAL were calculated by using four different methods for the design life of the pavement.

- The calculated values were further evaluated to determine the Remaining Service Life (RSL) and the increase in overlay thickness.

The detailed flowchart of this process is as follows:

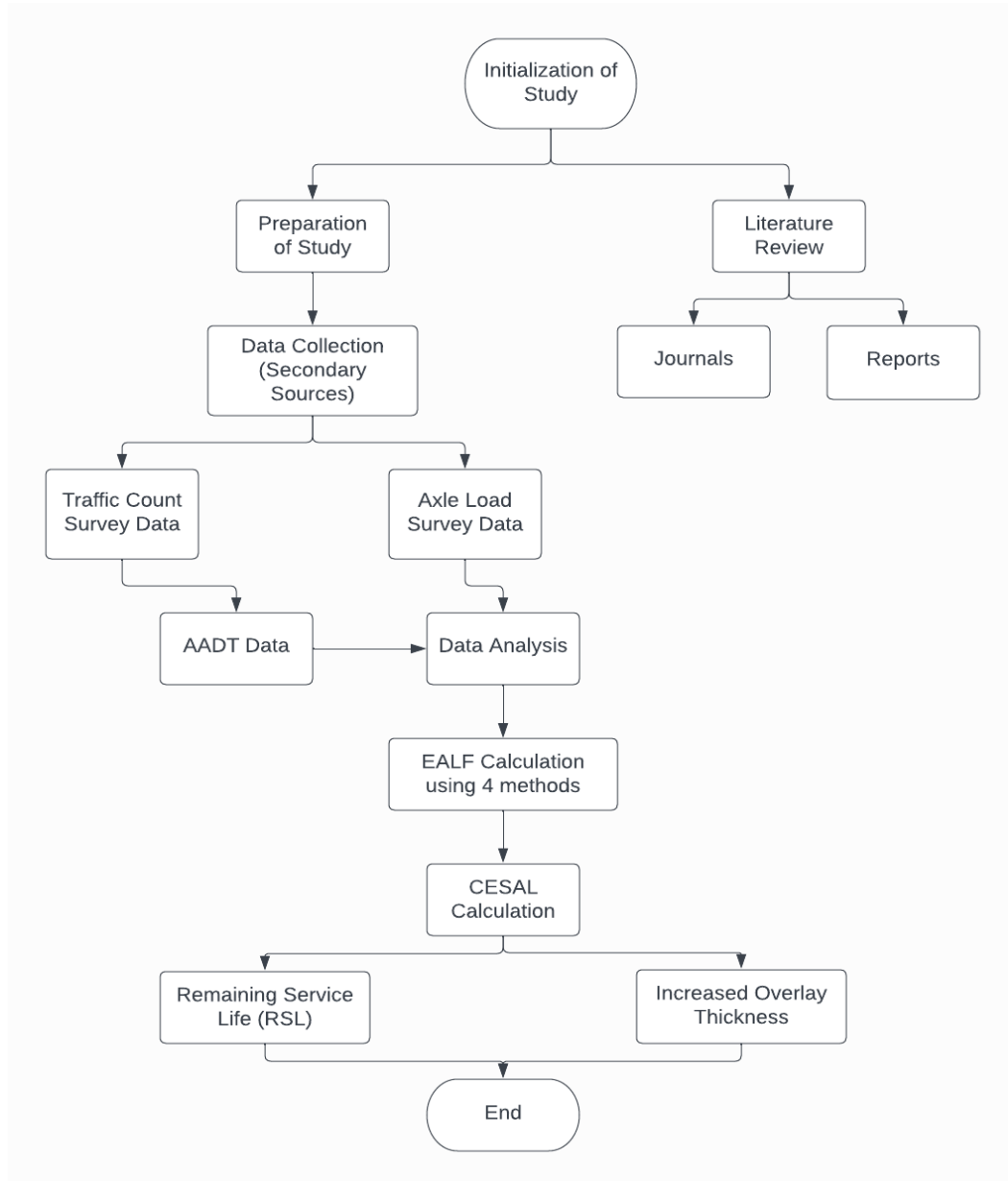


Figure 3.3: Flowchart for Pavement Damage Analysis

4. PAVEMENT DESIGN

4.1 Traffic Study

Accurate traffic data is a crucial element in the design of any pavement. However, due to practical constraints and budget limitations, it was not feasible for us to collect the necessary data regarding vehicle count and axle load survey for our research purposes. Hence, we relied on the traffic data obtained from the traffic survey carried out by the Ministry of Physical Infrastructure and Transport, Government of Nepal, in collaboration with Japanese International Cooperation Agency (JICA), CTI Engineering International CO, Ltd, and others, which was conducted as part of the preparatory survey for Nagdhunga Tunnel Construction.

Upon analysing the traffic data, we discovered that the traffic count at Gurjudhara Station was twice as much as that at Naubise and Nagdhunga Stations. However, a closer examination revealed that the higher traffic count at Gurjudhara Station was primarily due to a larger number of motorcycles, whereas the count of other types of vehicles was almost the same at all three stations. The traffic count of motorcycles was not considered in this study because of the negligible weight. The highest value of the traffic data among all three stations was used for calculation and the highest value is adopted as the design traffic.

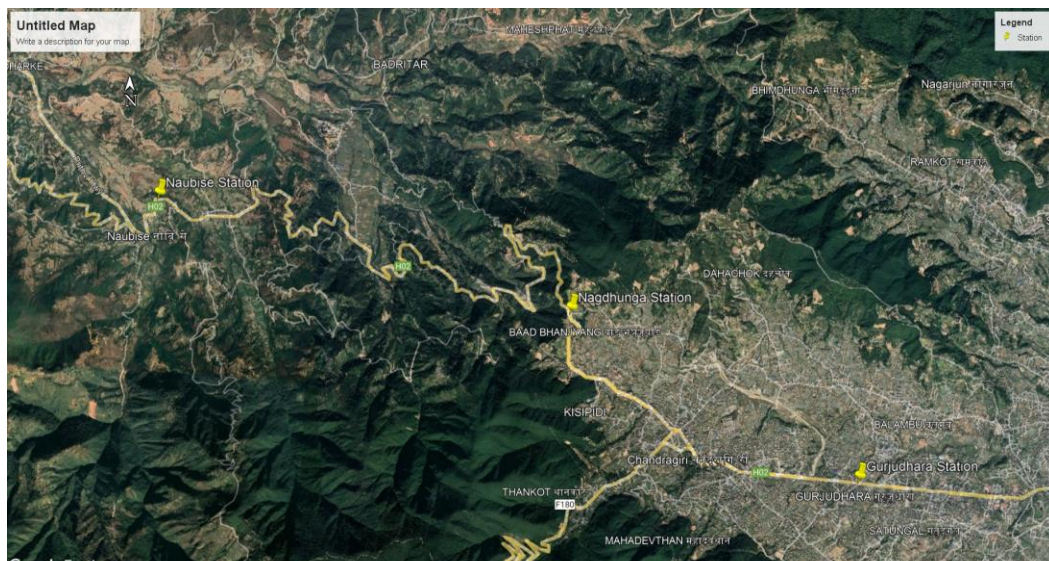


Figure 4.1: Survey stretch

Table 4.1: Vehicle Count

| SN | Vehicle Type | | Naubise Count | Nagdhunga Count | Gurjudhara Count |
|----|-----------------|------------|---------------|-----------------|------------------|
| 1 | Truck | Multi Axle | 894 | 831 | 846 |
| | | Heavy | 1392 | 1097 | 1438 |
| | | Light | 175 | 480 | 212 |
| 2 | Bus | Heavy | 926 | 1138 | 986 |
| | | Mini | 291 | 480 | 1024 |
| | | Micro | 668 | 771 | 1886 |
| 3 | Car | | 1132 | 1347 | 2116 |
| 4 | Utility Vehicle | | 287 | 330 | 752 |
| 5 | Motorcycle | | 1684 | 1416 | 6061 |
| 6 | Others | | 13 | 0 | 133 |
| | Total | | 7462 | 7890 | 15454 |

Source: JICA

4.1.1 Future Traffic

In road construction, it is customary to estimate future traffic by using present traffic as a base. The design life of a pavement typically ranges between 10 to 20 years. For our project, we have chosen 20 years as our design life as the data of the National Highway is being utilized for the design. According to the DoR guideline, in the absence of detailed traffic study, a traffic growth rate of 5% can be assumed. However, the referred report includes a comprehensive study based on the socio-economic framework, and therefore, recommends an average traffic growth rate of 4.1%, which we have opted for.

Table 4.2: Traffic growth rate forecast

| | AGR(2014-2020) |
|---------------|----------------|
| Passenger Car | 3.5% |
| Micro Bus | 3.5% |
| Mini Bus | 3.5% |
| Heavy Bus | 5.0% |
| Light Truck | 4.5% |
| Heavy truck | 4.5% |
| Average | 4.1% |

4.1.2 Axle Loading

The accurate estimation of axle loading is essential for the pavement design which require detail axle load survey. The axle load survey was conducted by JICA in the traffic survey. According to the design guidelines of DoR, the standard axle load can be taken as 80KN (8.16 tonnes) and the legal axle load limit is 10.2 tonnes. The results of axle load survey are mentioned in table 3.3 below.

Table 4.3 Results of Axle load survey

| Direction | Bus (t) | Truck (t) | | |
|------------|---------|--------------|--------------|----------------|
| | | 2 axle Truck | 3 axle Truck | Total of Truck |
| East Bound | 15 | 18 | 32 | 28 |
| West Bound | 15 | 12 | 21 | 17 |
| Average | 15 | 15 | 30 | 25 |

4.1.3 Vehicle Damage Factor

Vehicle Damage Factor (VDF) is a multiplier to convert the given number of commercial vehicles having different configurations and different axle weights into an equivalent number of standard axle load which in the case of Nepal is 80 kN. This conversion is done by using the equations below.

1. Single axle with single wheel on either side

$$VDF = \left[\frac{\text{axle load in kN}}{65} \right]^4 \dots\dots\dots (4.1)$$

2. Single Axle with dual wheel on either side:

$$VDF = \left[\frac{\text{axle load in kN}}{80} \right]^4 \dots\dots\dots (4.2)$$

3. Tandem axle with dual wheel on either side

$$VDF = \left[\frac{\text{axle load in kN}}{148} \right]^4 \dots\dots\dots (4.3)$$

4. Tridem axle with dual wheel on either side

$$VDF = \left[\frac{\text{axle load in kN}}{224} \right]^4 \dots\dots\dots (4.4)$$

These equations can be used for vehicles with different axle configurations. The VDF is derived by carrying out axle load surveys on roads for 24 hours in each direction. From the analysis of axle load survey, the guideline has developed the following values of VDF which is used in our calculations.

Table 4.4: Vehicle damage factor

| Vehicle type | VDF | Remarks |
|----------------------------------|------|---------------------|
| Heavy truck (three axle or more) | 6.50 | |
| Heavy two axle | 4.75 | Hilly Terrain (3.5) |
| Mini truck | 1.0 | |
| Large bus | 0.50 | |
| Bus | 0.35 | |

Source: Guidelines for flexible pavement (DOR)

Sub-grade Rutting criteria, Fatigue criteria of bituminous layers and Fatigue performance of the CTB have been taken into consideration for design analysis of the pavement layers.

4.1.4 Sub-grade Rutting criteria

An average rut depth of 20 mm or more, measured along the wheel paths, is considered in the design guidelines as critical or failure rutting condition. The equivalent number of standard axle load (80 kN) repetitions that can be served by the pavement, before the critical average rut depth of 20 mm or more occurs, is given by 4.5 and 4.6 respectively for 80 % and 90 % reliability levels [1].

For the reliability of 80 % (design traffic of less than 20 msa):

$$N_R = 4.1656 * 10^{-8} \left[\frac{1}{\epsilon_v} \right]^{4.5337} \dots\dots\dots (4.5)$$

For the reliability of 90 % (design traffic of 20 msa or more):

$$N_R = 1.4100 * 10^{-8} \left[\frac{1}{\varepsilon_v} \right]^{4.5337} \dots\dots\dots (4.6)$$

Where,

N_R : *sub-grade rutting life (cumulative equivalent number of 80 kN standard axle loads that can be served by the pavement before the critical rut depth of 20 mm or more occurs.*

ε_v : *vertical compressive strain at the top of the sub-grade calculated using linear elastic layered theory by applying standard axle load at the surface of the selected pavement system.*

The computation of stresses, strains and deflections in the pavement was done for the given values of pavement thicknesses and elastic properties (elastic modulus and Poisson’s ratio) of different layers. IITPAVE software or the Software developed by DoR was taken as the analysis tool for these calculations. All the analysis is done for the traffic loading of 80 kN (single axle with dual wheel). The shape of the contact area of the tyre is assumed in the analysis to be circular. The uniform vertical contact stress shall be considered as 0.56 MPa.

4.1.5 Fatigue cracking criteria for bituminous layers

The appearance of fatigue cracking on the pavement surface, whose total area in the section of the road under consideration is 20 % or more than the paved surface area of the section, is considered to be the critical or failure condition [1]. The equivalent number of standard axle (80 kN) load repetitions that can be served by the pavement, before the critical condition of the cracked surface area of 20 % or more occurs, is given by 4.7 and 4.8 respectively for 80 % and 90 % reliability levels.

For the reliability of 80%

$$N_f = 1.6064 * C * 10^{-4} \left[\frac{1}{\varepsilon_t} \right]^{3.89} \left[\frac{1}{M_{Rm}} \right]^{0.854} \dots\dots\dots (4.7)$$

For the reliability of 90%

$$N_f = 0.5161 * C * 10^{-4} \left[\frac{1}{\varepsilon_t} \right]^{3.89} \left[\frac{1}{M_{Rm}} \right]^{0.854} \dots\dots\dots (4.8)$$

Where,

N_f = fatigue life of bituminous layer (cumulative equivalent number of 80 kN standard axle loads that can be served by the pavement before the critical cracked area of 20 % or more of paved surface area occurs)

ϵ_t = maximum horizontal tensile strain at the bottom of the bottom bituminous layer (DBM) calculated using linear elastic layered theory by applying standard axle load at the surface of the selected pavement system.

M_{Rm} = resilient modulus (MPa) of the bituminous mix used in the bottom bituminous layer, selected as per the recommendations made in these guidelines

The factor 'C' is an adjustment factor used to account for the effect of variation in the mix volumetric parameters (effective binder volume and air void content) on the fatigue life of bituminous mixes and was incorporated in the fatigue models to integrate the mix design considerations in the fatigue performance model.

4.2 Computation of Design Traffic

The design traffic is considered in terms of cumulative number of standard axle loads in the lane carrying maximum traffic. This can be computed as:

$$N = \frac{365 * [(1+r)^n - 1]}{r} * A * D * F \dots\dots\dots (4.9)$$

Where,

N = Cumulative number of standard axles to be catered for the design in terms of msa

A = Initial traffic in the year of completion of construction in terms of CVPD

D = Lane distribution factor

F = Vehicle damage factor (as shown above VDF table)

n = Design life in years = 20 years

r = annual growth rate of commercial vehicle

We have considered the traffic count as the traffic in the year of completion of construction of the road for simplicity.

4.2.1 Calculation of Forecasted Cumulative Number of Standard Axles

The traffic count included various types of vehicles such as trucks (multi, heavy, and light), buses (heavy, mini, and micro), cars, utility vehicles, and motorcycles. However, motorcycles were not taken into account when calculating the standard axle loads. To determine the traffic loading, VDF values were utilized, as per the guidelines. Based on the traffic counts, the forecasted traffic volumes for Naubise, Gurjudhara, and Nagdhunga were 110msa, 115.35msa, and 99.6msa, respectively, as shown in Tables 4.5, 4.6, and 4.7. The highest value among the three, i.e., the forecasted traffic of Gurjudhara (115.35msa), was adopted for the design.

Table 4.5: Traffic Forecast for Naubise

| SN | Vehicle Type | | Vehicle Count (One way) | VDF | Forecasted traffic(msa) | Remarks |
|----|-----------------|------------|-------------------------|-------|-------------------------|-----------|
| 1 | Truck | Multi Axle | 894 | 6.5 | 47864348 | |
| | | Heavy | 1392 | 4.75 | 54462066 | |
| | | Light | 175 | 1 | 1441449 | |
| 2 | Bus | Heavy | 926 | 0.5 | 3813663 | |
| | | Mini | 291 | 0.35 | 838923 | |
| | | Micro | 668 | 0.35 | 1925776 | |
| 3 | Car | | 1132 | 0.001 | 9324 | |
| 4 | Utility Vehicle | | 287 | 0.001 | 2364 | |
| 5 | Motorcycle | | 1684 | | | Neglected |
| | Total | | 7449 | | 110357913 | |

Table 4.6: Traffic Forecast of Nagdunga

| SN | Vehicle Type | | Vehicle Count (One way) | VDF | Forecasted traffic | Remarks |
|----|--------------------|------------|----------------------------|-----------|-----------------------|-----------|
| 1 | Truck | Multi Axle | 846 | 6.5 | 45294450 | |
| | | Heavy | 1438 | 4.75 | 56261819 | |
| | | Light | 212 | 1 | 1746213 | |
| 2 | Bus | Heavy | 986 | 0.5 | 4060768 | |
| | | Mini | 1024 | 0.35 | 2952088 | |
| | | Micro | 1886 | 0.35 | 5437146 | |
| 3 | Car | | 2116 | 0.00 1 | 17429 | |
| 4 | Utility Vehicle | | 752 | 0.00 1 | 6194 | |
| 5 | Motorcycle | | 6061 | | | Neglected |
| | Total | | 15321 | | 115776106 | |

Table.4.7: Traffic forecast for Gurjudhara

| SN | Vehicle Type | | Vehicle Count (One way) | VDF | Forecasted traffic | Remarks |
|----|--------------------|------------|----------------------------|-----------|-----------------------|-----------|
| 1 | Truck | Multi Axle | 831 | 6.5 | 44491357 | |
| | | Heavy | 1097 | 4.75 | 42920177 | |
| | | Light | 480 | 1 | 3953689 | |
| 2 | Bus | Heavy | 1138 | 0.5 | 4686769 | |
| | | Mini | 480 | 0.35 | 1383791 | |
| | | Micro | 771 | 0.35 | 2222715 | |
| 3 | Car | | 1347 | 0.00 1 | 11095 | |
| 4 | Utility Vehicle | | 330 | 0.00 1 | 2718 | |
| 5 | Motorcycle | | 1416 | | | Neglected |
| | Total | | 7890 | | 99672311 | |

4.3 Pavement Design

The thickness for the pavement was assumed as follows and trials were performed. According to the design guidelines 2021, selection of trial thickness is to be done based on experience or the thickness recommended in the guideline and analysis was done by using IITPAVE software. The thickness for which the strains computed by IITPAVE was less than the allowable strains derived

from the performance models was selected. For this, three iterations were necessary in our calculations and the thickness for each iteration is given below.

Table 4.5: Trial thickness for design iterations

| Layer | Resilient Modulus | Poisson's Ratio | Thickness |
|---------------|-------------------|-----------------|-----------|
| Bitumen | 3000 | 0.35 | 110 |
| Granular Base | 450 | 0.35 | 300 |
| GSB | 200 | 0.35 | 300 |
| Subgrade | 62 | 0.35 | |

4.3.1 Properties of Material

The properties of materials used for the designs are all derived from the recommended values provided by the Design Guidelines for Flexible Pavements -2014 (Second Edition) DoR, Nepal.

Effective CBR of Subgrade= 7%

Effective resilient modulus of Sub-grade = $17.6 \times (7.0)^{.64} = 62 \text{ MPa}$

Resilient Modulus of GSB Layer= 200MPa

Poisson Ratio for GSB Layer= 0.35

Resilient Modulus of Granular Base Layer=450MPa

Poisson Ratio for Granular Base Layer= 0.35

Resilient Modulus of Asphalt Layer=3000MPa

Poisson Ratio for Asphalt Layer= 0.35

4.3.2 Analysis of Pavement

The pavement analysis has been done using IITPAVE software as specified by the DoR guidelines for design of flexible pavements. IITPAVE software is based on the analysis of linear elastic layered theory for pavement analysis. IITPAVE is applied for computing the stresses, strains and deflections caused at different locations in a pavement by a uniformly distributed single load applied over a circular contact area at the surface of pavement. The effect of additional loads

(which should also be uniformly distributed loads over circular contact areas) was considered using superposition principle. The single vertical load applied at the surface is described in terms of:

- Contact pressure and radius of contact area,
- Wheel load and contact pressure,
- Wheel load and radius of contact area

Standard Wheel load (20kN) and standard contact pressure (0.56MPa) were given as load inputs. The elastic properties and thickness of all layers except subgrade layers was also entered. IITPAVE can be used to analyse pavements up to 10 layers. The location of any element in the pavement is determined using depth from the surface and the radial distance measured along the centre of circular contact area.

IITPAVE displayed the computed values of identified stresses, strains and deflections for the locations represented by depth and radial distance. The parameters reported are shear stress (τ_z), vertical deflection (u_z), vertical strain (ϵ_z), horizontal tangential strain (ϵ_t), horizontal radial strain (ϵ_r), vertical stress (σ_z), tangential stress (σ_t), radial stress (σ_r),

The critical parameter, horizontal tensile strain was taken as the largest of tangential and radial strains at the bottom of the bituminous layer and the vertical compressive strain was taken as the larger among the two strains values obtained for the interface between subgrade and the granular layer. The absolute values of both strains are taken.

4.3.3 Results

Here, after the third iteration, the strains computed by IITPAVE was less than the calculated allowable strains using the formula provided in the guidelines. So, the thickness assumed in trial 3 was selected as the final design parameters of the road pavement. The results are tabulated in the table 4.9.

Table 4.6: Allowable strain

| Parameter | Allowable (10^{-3}) | Trial 1 | Trial 2 | Trial 3 |
|-----------------------------|-------------------------|---------|---------|---------|
| Horizontal Tensile Strain | 0.145 | 0.179 | 0.146 | 0.136 |
| Vertical Compressive Strain | 0.293 | 0.247 | 0.129 | 0.124 |

Here, after the third iteration, the strains computed by IITPAVE was less than the calculated allowable strains using the formula provided in the guidelines. So, the thickness assumed in trial 3 was selected as the final design parameters of the road pavement,

4.4 Final Design Parameters

The final parameters of road were selected as listed below in Table 4.10.

Table 4.7: Final Design Parameters

| Layer | Resilient Modulus | Poisson Ratio | Thickness |
|----------------------|--------------------------|----------------------|------------------|
| Bitumen | 3000 | 0.35 | 110 |
| Granular Base | 450 | 0.35 | 300 |
| GSB | 200 | 0.35 | 300 |
| Subgrade | 62 | 0.35 | |

5. FEM MODELLING AND ANALYSIS

5.1 General Theory

5.1.1 Finite Element Solution in Time domain

A structure can be analysed using different methods, including static, quasi-static, and dynamic analysis, depending on the loading and natural frequency of the structure. Static analysis is suitable for structures with minimal or no acceleration, while dynamic analysis is used for structures with significant acceleration. Quasi-static analysis assumes the structure is in static equilibrium but considers inertial force as external loading. While this reduces computational time, it also results in some approximation compared to dynamic analysis.

Finite element analysis (FEA) is used to determine the solution since analytical solution is complicated for nonlinear material under some load cases. FEA can be solved in the frequency domain using methods such as the Fourier method or in the time domain using integration methods like implicit and explicit modes. The equation of motion for dynamic analysis of pavement structure using FEM is:

$$[M]\{\ddot{u}\} + [C]\{\dot{u}\} + [K]\{u\} = F(t) \dots\dots\dots (5.1)$$

Where,

[M] represents mass

[C] represents damping

[K] represents stiffness matrices

$\{\ddot{u}\}$, $\{\dot{u}\}$ and $\{u\}$ represents acceleration, velocity and displacement respectively

$\{P\}$ represents external force vectors.

Finite element analysis (FEA) is used to determine the solution since analytical solution is complicated for nonlinear material under some load cases. FEA can be solved in the frequency domain using methods such as the Fourier method or in the time domain using integration methods like implicit and explicit modes.

5.1.2 Material Behaviour of Pavement Layers

The behaviour of pavement materials in real-world conditions is exceedingly intricate, and accurately representing the exact material behaviour in a model can be a challenging task. Mathematical calculations and simulations involve numerous approximations and assumptions to simplify the calculations while maintaining the precision of the material behaviour to the greatest extent possible. In actuality, granular materials possess various properties, such as interlocking, permeability, and others, and exhibit a form of linear elasticity known as Hertzian elasticity. Despite this, granular materials are considered as linearly elastic solid materials in simulations and calculations.

Asphalt layer exhibits viscoplasticity, viscoelasticity and fatigue in addition to other properties. The understanding of these behaviours is essential for design and analysing pavements, but due to the complex nature of these behaviours, asphalt layer is generally modelled as linearly elastic that does not exactly represent the actual behaviour of asphalt. A generalized Maxwell model was used to model the viscoelastic behaviour of asphalt layers. The hereditary integral formulation of isotropic viscoelastic material stress function can be expressed as:

$$\sigma(t) = \int_0^t 2G(t - \tau) d\epsilon \frac{d\epsilon}{dt} + \int_0^t k(t - \tau) \frac{d\Delta}{dt} d\tau \dots\dots\dots(5.2)$$

Where,

σ is the stress tensor,

e and Δ are the deviatoric and volumetric parts of strain tensor respectively,

τ denotes relaxation time

t denotes current time

The Maxwell model was expressed in the form of Prony series as:

$$G(t) = G_\infty + \sum_{i=1}^n G_i e^{-t/\tau} \dots\dots\dots(5.3)$$

$$K(t) = K_\infty + \sum_{i=1}^n K_i e^{-t/\tau} \dots\dots\dots (5.4)$$

Where,

G_{∞} and G_i are the material shear modulus in Pa

K_{∞} and K_i are the material bulk modulus in Pa

τ is the relaxation time

The shear and bulk moduli of asphalt concrete were determined from the elasticity modulus using the following relationship.

$$G(t) = \frac{E(t)}{(1+\mu)} \dots \dots \dots (5.4)$$

$$K(t) = \frac{E(t)}{3(1-3\mu)} \dots \dots \dots (5.5)$$

Where, μ is the poisson ratio

5.1.3 Modelling of Moving Vehicle Load

In an FEM model, there are various methods for representing a moving vehicle load, ranging from basic load representation to modelling the tyre and load representation. The loading distribution is non-uniform and is influenced by numerous factors, including pavement stiffness, tyre pressure, vehicle velocity, and friction factors. In our model, we have chosen to represent wheel stress as a uniform and rectangular distribution, disregarding friction factors.

Huang (2004) proposed a rectangular equivalent area to estimate the contact area of a tyre. The rectangular area is a simplification of the elliptical contact area of a tyre model. The size of contact area depends on the contact pressure. It is assumed that the contact area for each tyre is composed of a rectangle with two semi circles to the side. Huang assumed length L and width 0.6L to find the total area to be $0.5227L^2$. So, the length of rectangle was found to be:

$$L = \sqrt{\frac{A_c}{0.5227}} \dots \dots \dots (5.6)$$

Where, A_c is the contact area calculated by dividing the load on each tyre-by-tyre pressure.

The equivalent rectangular area has a length of 0.87L and a width of 0.6L.

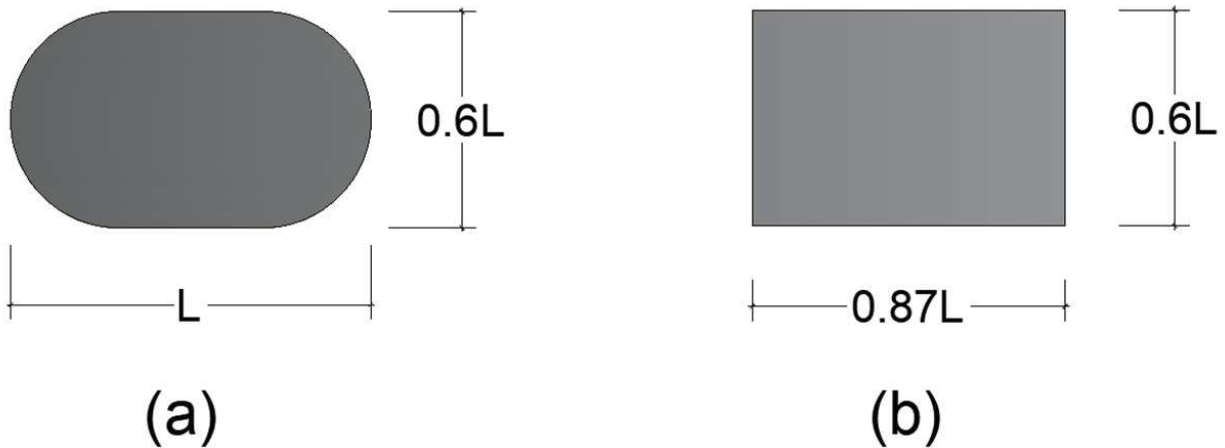


Figure 5.1: Area of contact for wheel

The movement of a vehicle's tyre can be simulated by discretizing the loading and speed of the tyre. The vehicle load is distributed uniformly over the contact area, and the movement speed is divided into discrete time intervals. At a given time t , the tyre is located at a specific point "i". As the tyre moves to the next node "j" at time $t+1$, the load is applied to node "j". This process is repeated until the load is applied throughout the entire length of the tyre. Once the load reaches the end of the tyre length at the node "I", the load at the previous node "i" is unloaded, and the load is then applied to node "I+1" to simulate the movement of the vehicle load over a length. The speed of the load is represented by the time for which the load is in contact with the pavement surface

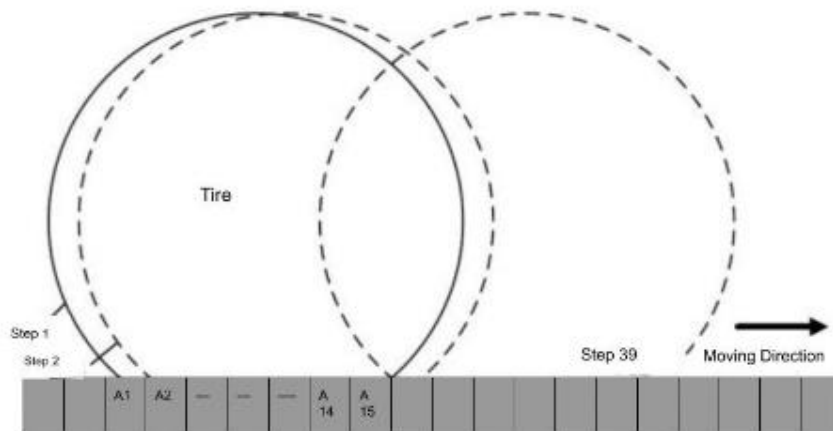


Figure 5.2: Different Steps for FE Discretization

5.2 Model Validation

Before conducting any analysis in ABAQUS, it is important to validate the model to ensure accuracy of the method and results. Since the final model used involved viscoelastic material properties and moving load conditions, it was not possible to validate it based on other analytical methods such as Bousinesq equation, IIT PAVE, and KENPAVE, which assume linearly elastic material behaviour under static load. Therefore, a similar model was created using static load and linear material behaviour for validation purposes. The validation was conducted by comparing the results with those obtained from IIT PAVE.

IIT PAVE is a software developed by Civil Engineering Department of IIT Bombay that is used for modelling and analysing behaviour of flexible pavements. The accuracy of IITPAVE has been evaluated and validated by using many field and experimental studies and it has shown good agreement in predicting the behaviour of flexible pavements. This software has also been recommended and used by the Guidelines for Flexible pavement design, DoR so the results obtained from this software can be used to validate our model.

5.2.1 Validated Model Description

The model used for validation was similar to the final model. It consists of three layers, Asphalt, Base and Subbase on top of a subgrade layer. The dimensions of the model are 1.2mx1.5m with a total depth of 1.41m. The properties of the material are as follows:

Table 5.1: Layer properties

| Layer | Resilient Modulus | Poisson Ratio | Thickness |
|---------------|-------------------|---------------|-----------|
| Bitumen | 3000 | 0.35 | 110 |
| Granular Base | 450 | 0.35 | 300 |
| GSB | 200 | 0.35 | 300 |
| Subgrade | 62 | 0.35 | |

The loading is applied as stationary load of 0.758 MPa over an area of 0.600mx0.416m.

5.2.2 Validation

Validation of the model is done by comparing the results obtained from IITPAVE and ABAQUS. The discrepancies between the values are between 2% and 6% which is within an acceptable range.

The data shows that the values obtained by ABAQUS are smaller than that of IITPAVE. The discrepancy in displacement can be due to the differences between the boundary conditions considered by the two software. Furthermore, due to the use of different methods, specifically the layer elastic analysis method in IITPAVE and the FEM modelling method in ABAQUS, there was a minor discrepancy in the obtained values.

Table 5.2: Comparison of values obtained by IITPAVE and ABAQUS

| Parameter | IITPAVE | ABAQUS | Error |
|--------------------------------------------|---------|--------|--------|
| Depth of 0.110m | | | |
| Displacement (u_y) | 1.559 | 1.596 | -2.37% |
| Vertical Compressive Stress (σ_y) | 0.6151 | 0.651 | -5.84% |
| Horizontal Tensile Strain (ϵ_z) | 0.3739 | 0.39 | -4.31% |

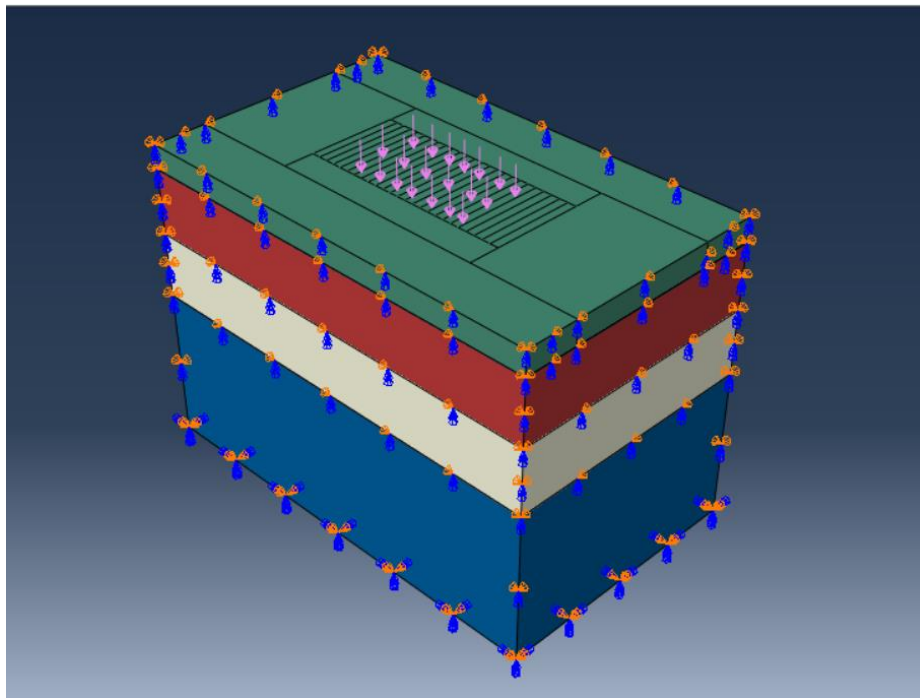


Figure 5.3: Model Used for Validation

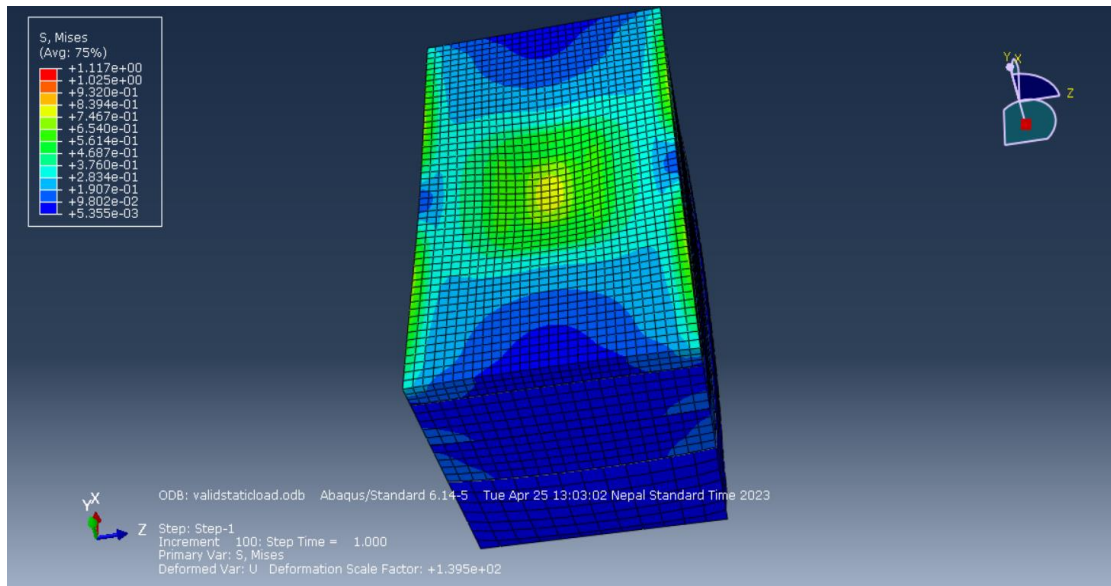


Figure 5.4: Stress distribution in Model used for Validation

5.3 Final Model Description

5.3.1 General Description

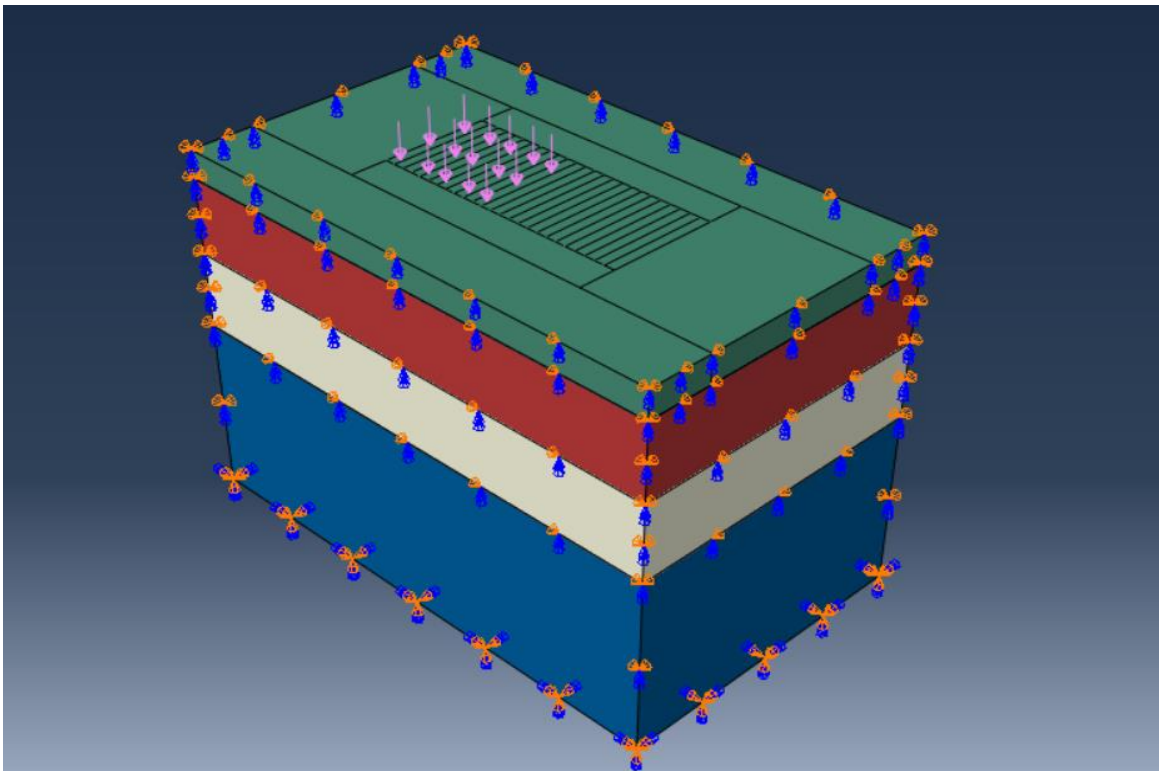


Figure 5.5: General Model with Loading

A 3D finite element model was simulated in ABAQUS 6.14-5. The model has the dimensions of 1.5x1.2x1.410m. The pavement consists of four layers, namely asphalt, base, subbase and subgrade layer. The asphalt layer is considered to be viscoelastic while other layers are linearly elastic. The vehicle load was simulated in a rectangular area of 0.420x0.295m area. TATA motor (LPK 2518) was taken as the representative vehicle to analyse the pavement response. The pavement was discretized into a finite number of 8-noded 3-D solid brick element (C3D8R) with a total of 12,765 elements.

5.3.2 Boundary Condition

The boundary condition allows rotation about x axis and z axis. The bottom layer has rigid i.e., fixed boundary condition not allowing any translation and rotation.

Boundary conditions play an important role in FEM analysis. The reactions and forces due to the boundary condition may change the resultants of the model. By various trials, the thickness of subgrade was selected to be of 0.7 m such that the effect of loading does not reach the bottom of the layer and the analysis is completed within a reasonable time.

The bottom of the layer was constrained in vertical direction.

5.3.3 Vehicle Modelling

TATA Motors LPK 2518 was taken as the representative vehicle to analyse loading response. The vehicle was observed to be the most commonly used truck in Nepal. The vehicle specification is shown in the table 5.3 below.

Table 5.3: TATA LPK 2518 Specifications

| | | |
|--------------------------------|----------------------|-----------|
| Wheel Base | 3880mm | |
| Width | 2400mm | |
| Overall Weight | 25000kg | |
| | Front Axle | Back Axle |
| Wheel Configuration | Single | Tandem |
| Gross Weight | 6000kg | 1900kg |
| Tyres | 10.00x20-16PR | |
| Width | 10 inches (25.4 cm) | |
| Tyre Inflation Pressure | 110psi (758.424 kPa) | |

The stress distribution of tyre is considered to be uniform and rectangular for simplicity. Huang (2004) found that the tyre footprint is in fact elliptical and converted it into an equivalent rectangle of length $0.87L$ and width $0.6L$, where L is the length of elliptical footprint. (Figure 5.6). For the modelling purpose the tyre pressure was considered to be 110psi (0.758 MPa) as recommended by the specifications of vehicle. Using the pressure of 110psi and the load 190kN of the vehicle, the footprint of front tyre was found to be 0.240m and 0.165m and the rear tyre was found to be 0.425m and 0.295m. In the final model, uniform pressure of 0.758Mpa was spread over the area of 0.425×0.295 m to simulate the load of 190KN acting at the rear axle which is for the critical condition.

Table 5.4: Calculation of equivalent tyre dimensions

| | FRONT | REAR |
|------------------------------------|-------|-------|
| Contact Area(m ²) | 0.079 | 0.25 |
| Length of Elliptical Footprint (m) | 0.389 | 0.692 |
| Length of Equivalent Area(m) | 0.338 | 0.600 |
| Width of Equivalent Area(m) | 0.233 | 0.416 |

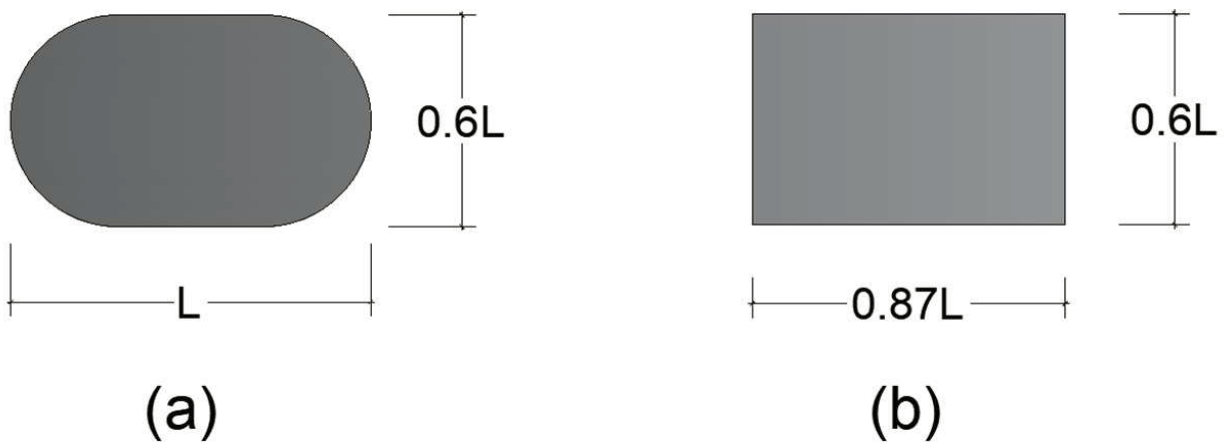


Figure 5.6: Area of contact of wheel

5.3.4 Material Characterization

The materials used in the pavement design are taken according to the Design Guidelines for Flexible Pavements -2014 (Second edition 2021) DoR, Nepal considering these are the representative materials used for road design in Nepal. The layers were assumed to be perfectly bonded. The layers except the top asphalt layer are considered to be linearly elastic while the asphalt layer is considered to be viscoelastic.

Table 5.5: Layer properties

| Layer | Resilient Modulus(MPa) | Poisson Ratio | Thickness(m) |
|---------------|------------------------|---------------|--------------|
| Bitumen | 3000 | 0.35 | 0.110 |
| Granular Base | 450 | 0.35 | 0.300 |
| GSB | 200 | 0.35 | 0.300 |
| Subgrade | 62 | 0.35 | |

Most of the analysis of pavement layers consider the layers to be linearly elastic. This assumption makes the analysis simpler even though it is not an exact representation of real-world conditions. The research of Beskou et al (2016) recommended the use of viscoelasticity in asphalt layer for practical applications as it is simple and requires lowest computation time and produces similar results compared to when other layers were considered non-linearly elastic while being the simplest and requiring lowest computational time.

Table 5.6 Prony Series for Generalized Maxwell Model

| n | τ | G_i | K_i |
|---|--------|----------|----------|
| | | 3.89E+02 | 7.71E+02 |
| 1 | 20 | 5.88E+01 | 9.10E+01 |
| 2 | 2 | 1.85E+02 | 3.70E+02 |
| 3 | 1 | 1.80E+01 | 5.71E+01 |
| 4 | 0.2 | 4.57E+02 | 1.10E+03 |

For the analysis, only asphalt layer is assumed to exhibit the viscoelastic behaviour. The viscoelasticity of asphalt layer was expressed by generalized Maxwell equation using a four term prony series. The value of material constant G_i was taken from the experimental results of Bertholot et. al (2003) which is scaled from $G(0)= 817$ to $G(0)= 1111.11$ to be compatible with the elastic properties of our asphalt layer which has an elasticity modulus of 3000MPa.

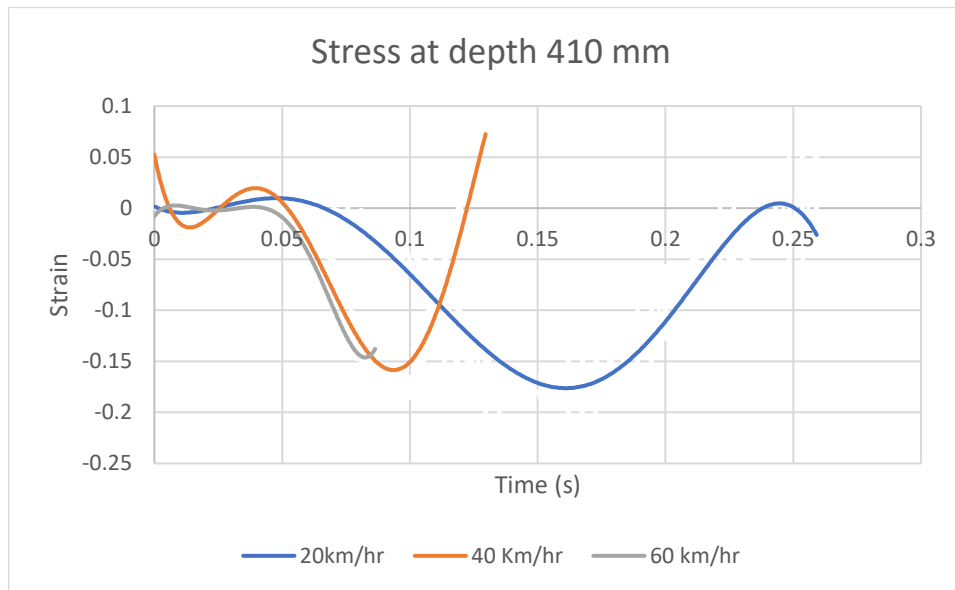
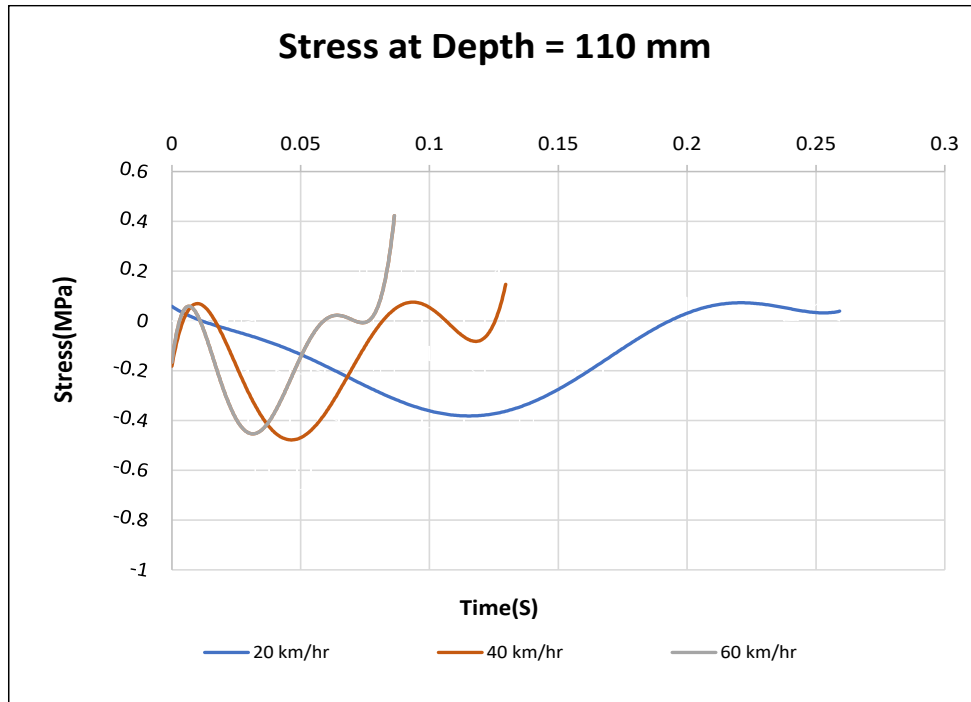
5.4 Response Analysis of Linear Model

To analyse the structural behaviour of flexible pavements under traffic loading, the linear elastic pavement model was used. Layers in this model behave elastically under applied load, meaning they deform and recover elastically. To comprehend the response of various vehicle speeds in a linear elastic model, a FEM model with 39 loading steps is utilized, with each step having a time period proportional to the model's speed. This replicates the vehicle's speed in the model, generating stress and strain. A separate modelling of pavement is done for vehicular speed 20 km/hr, 40 km/hr and 60 km/hr. The response of the different pavement layers is determined by using ABAQUS and they are analysed. Stress, strains and vertical displacement of the pavement was analysed on moving vehicle on the pavement similar to linear model. The summary of the response of pavement layers on passing vehicle through it is as shown in the table 5.8 below:

Table 5.7: Response of Viscoelastic pavement model on various speed

| Speed (kmph) | Y (mm) | Strain (x) | Strain (y) | Strain (z) | Stress (x) | Stress (y) | Stress (z) | Displacement (Uy) |
|---------------|---------|------------|------------|------------|------------|------------|------------|-------------------|
| 20 | 110 | 0.000194 | -0.000200 | 0.000198 | 2.05456 | -0.80891 | 1.952272 | -0.2350 |
| | 410 | 0.000022 | -0.000388 | 0.000106 | -0.0174 | -0.24608 | 0.021597 | -0.05548 |
| | 710 | -1.30E-07 | -7.055E-06 | 1.95E-07 | -3.68E-04 | -3.34E-03 | -3.59E-04 | -6.67E-05 |
| 40 | 110 | 0.000115 | -0.000161 | 0.000165 | 1.28927 | -0.74014 | 1.545145 | -0.14008 |
| | 410 | -0.000055 | -0.000327 | 0.000162 | 0.14220 | -0.11509 | -0.10261 | -0.06511 |
| | 710 | -7.79E-07 | -1.023E-05 | 4.31E-07 | -1.94E-03 | -6.57E-06 | -1.76E-03 | -1.07E-04 |
| 60 | 110 | 0.000073 | -0.000120 | 0.000147 | 0.98834 | -0.43217 | 1.402286 | -0.09505 |
| | 410 | -0.000018 | -0.000252 | 0.000017 | 0.06810 | -0.03797 | -0.05737 | -0.00450 |
| | 710 | -1.74E-09 | -1.986E-08 | 6.29E-10 | -3.88E-06 | -6.92E-04 | -3.53E-06 | -6.25E-08 |

.4.1 Stress (σ_y) on the pavement:



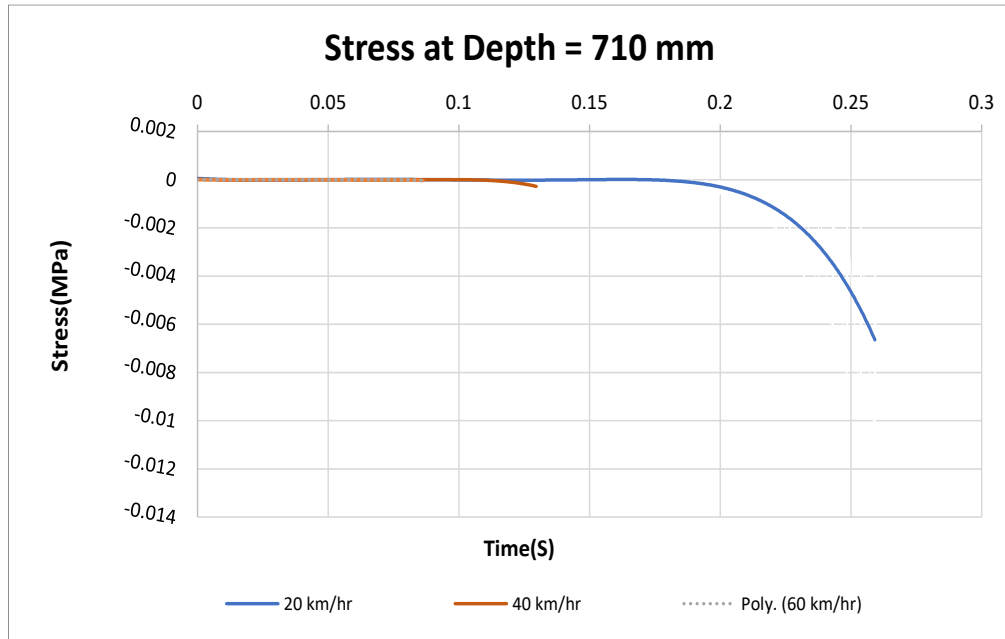


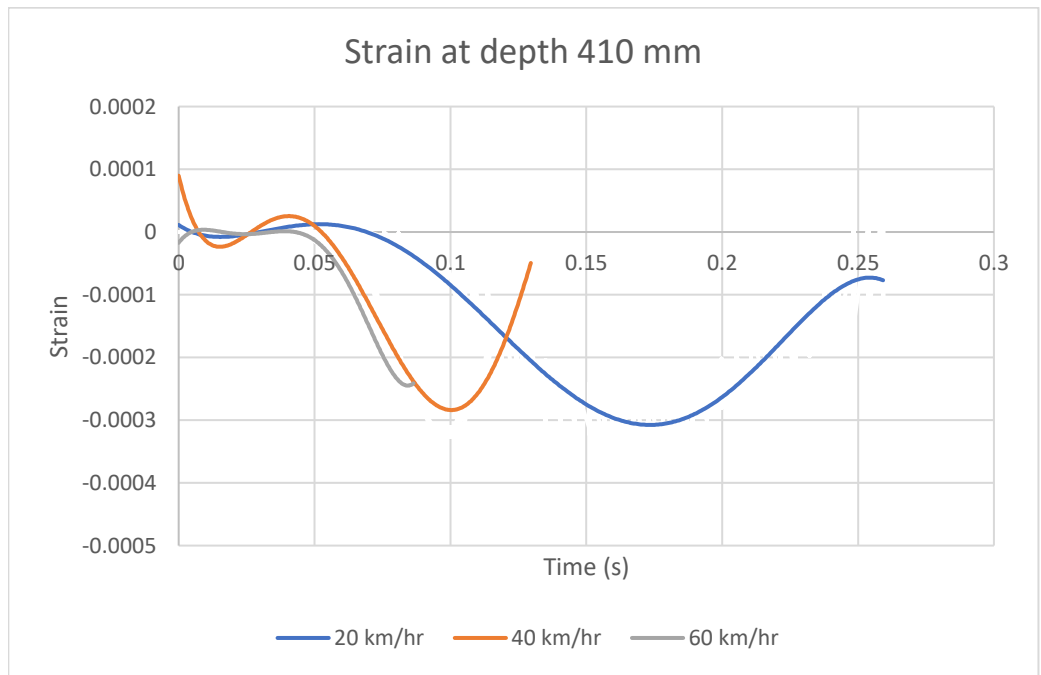
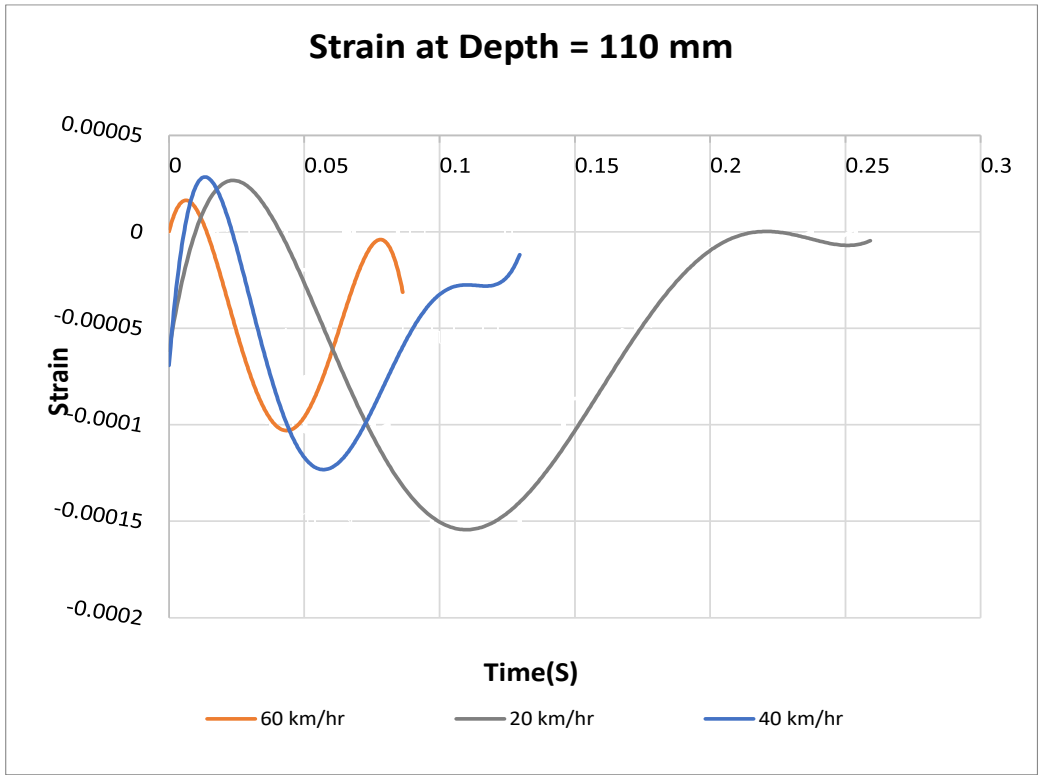
Figure 5.7: Stress at various positions of viscoelastic pavement under different velocities

We can observe a correlation between the decrease in vertical stress and an increase in speed, albeit a slight one. Specifically, the stress reduction is approximately 35% and 57% on average for speeds of 40kmph and 60kmph, respectively, compared to the stress experienced at 20kmph. Notably, this decrease in stress is more pronounced at higher speeds than at lower speeds. Furthermore, higher speeds result in peak stress values occurring for shorter durations.

Analysing Table 5.7, we can note a consistent decline in stress levels with increasing depth. At the interface between the asphalt-base layer and the base-sub base layer, there is an average stress reduction of 70%. Additionally, between the sub base-subgrade layer interfaces, the stress diminishes by an average of 95%. These reductions in stress can be attributed to the load being distributed over a wider area as depth increases, along with the fact that the upper layers exhibit greater stiffness compared to the lower layers.

Both the longitudinal and transverse stresses exhibit a similar pattern to the vertical stress, decreasing with higher speeds and greater layer depth. The lateral stresses experienced at speeds of 40kmph and 60kmph are, on average, 37% and 51% lower, respectively, compared to those at 20kmph

5.4.2 Strain (ϵ) on the pavement



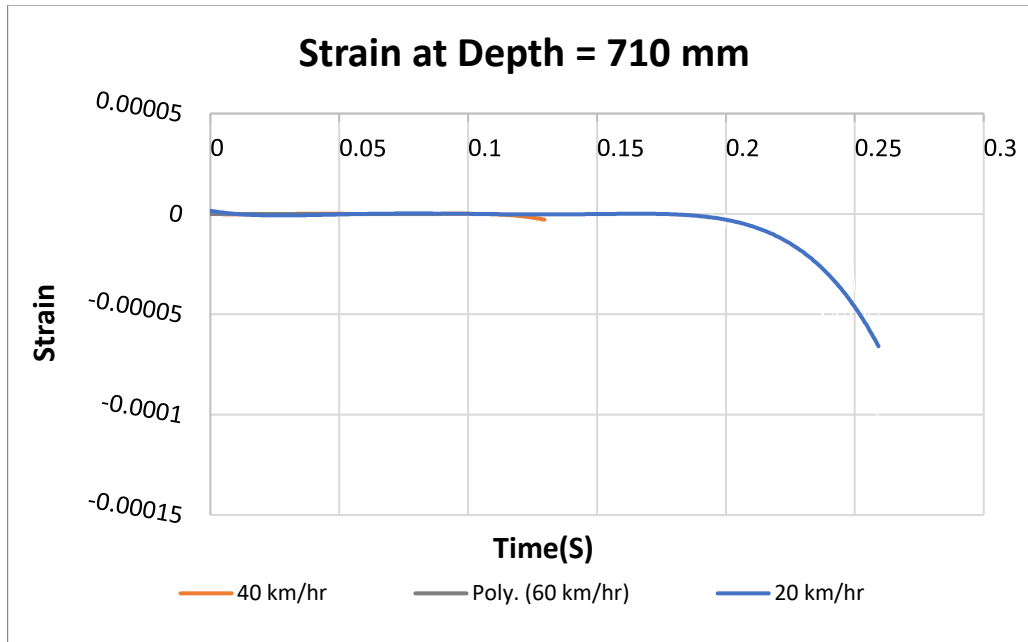


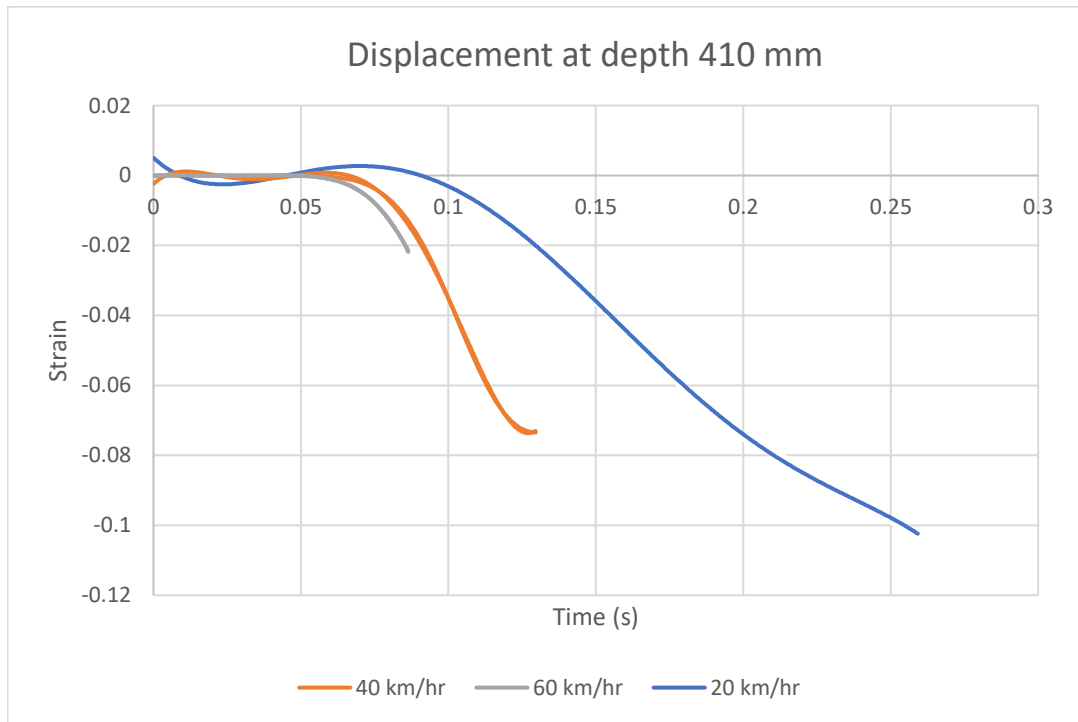
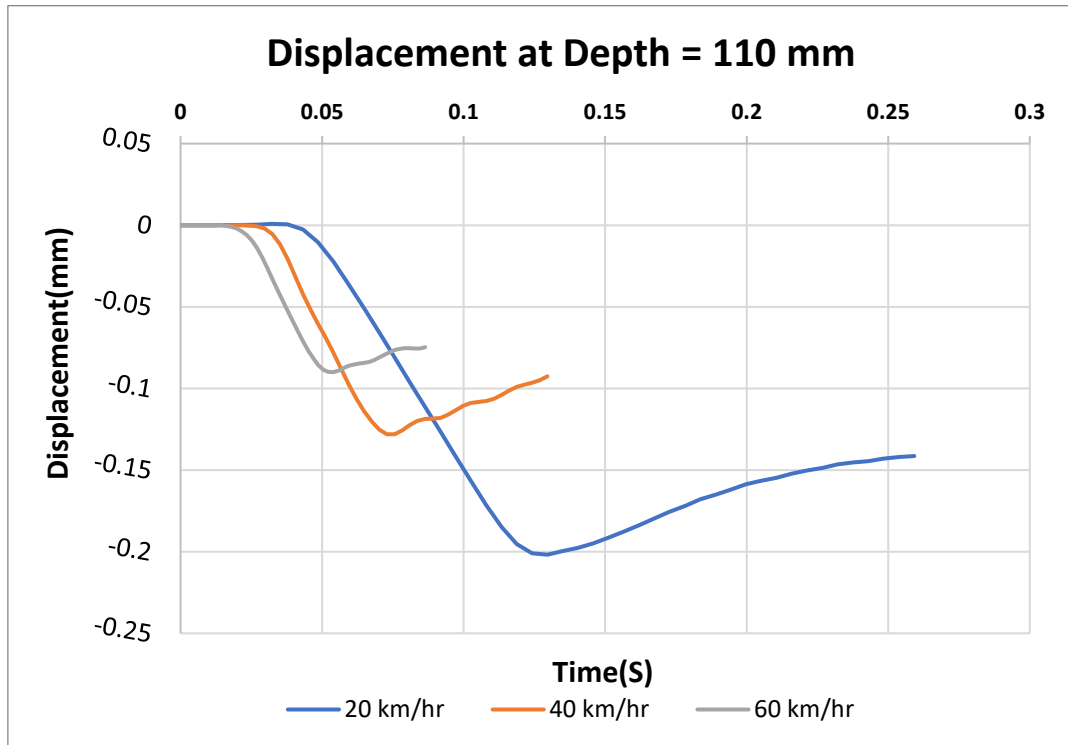
Figure 5.8: Strain at various positions of viscoelastic pavement under different velocities

The time history trend curve for vertical strain (ϵ_y) showed that for the same depth, the strains are decreasing along with the increase in speed. The peak values of strain occur faster in higher speeds and the peak values are lower in higher speeds. We can see a decrease of 18% and 25% on average when comparing the strain values of 20kmph with 40kmph and 60kmph respectively.

Also, from table 5.7 we can observe that the strains were increasing along with increase in depth of the layers. The average vertical strain increases by approximately 80% from one layer to the next. This increase can be attributed to a reduction in the elasticity modulus between the layers. As the elasticity modulus decreases, the same stress values lead to higher strains. On comparing the time it takes to reach peak value for the various speeds, we can observe that there is a slight delay to reach the peak values for higher depth due to the time required for propagation.

The strains in transverse as well as longitudinal directions (X and Z directions) follow similar patterns as the strain in vertical direction. The strains in these directions are nearly equal for all depths for a single speed. At the same depths for different speeds, the strain values are decreasing as the speed increases. On average there is an decrease of 40% and 65% in lateral strains comparing the values of 40kmph and 60kmph with 20kmph.

5.4.3 Displacement (U_y) on the pavement:



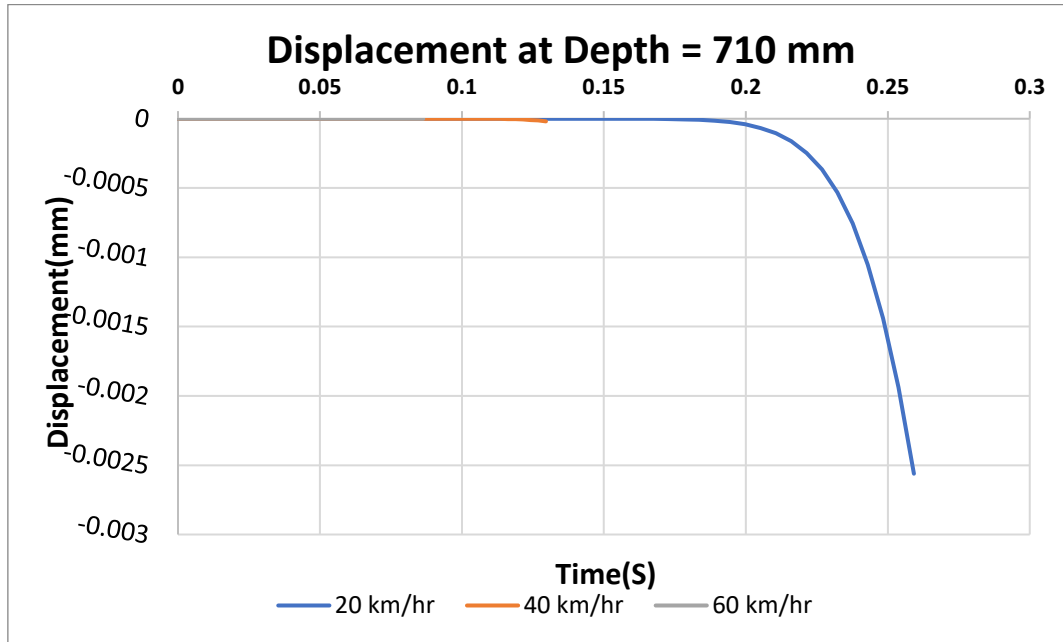


Figure 5.9: Displacement at various positions of viscoelastic pavement under different velocities

Based on the displacement trend lines, we can observe that the displacements values are decreasing as the speed increases for the same depth. There is an average reduction of 36% and 60% in displacement of 40kmph and 60kmph when compared with the displacement at 20kmph for the same depth. Similar to the stress and strain graphs, the peak values of displacements are experienced later and for a longer duration in higher speeds. The peak values are experienced as the load passes the point where the response is measured for the upper layers with slight delays for lower layers. From the table 5.7 we can observe that the displacements are decreasing along with increase in depth. For 20kmph, there is a reduction of 75% in the displacement at 410mm compared to 110mm depth and for 40kmph, there is a reduction of 50%.

5.4 Response Analysis of Viscoelastic FEM Model

Viscoelasticity is the property of materials that exhibit both viscous and elastic properties when it undergoes deformation. It is observed that the asphalt concrete layer of pavement exhibits the behaviour of viscoelasticity when vehicular load is applied on it. So, to analyse the viscoelastic behaviour of the pavement, a FE modelling of pavement is done in ABAQUS software for different vehicular speeds. A pavement model is made in ABAQUS to analyse different response (stress, strain and deflection) developed at the interactions between different pavement layers and is

compared with the response due to elastic behaviour of asphalt concrete under similar conditions and same properties of other pavement layers.

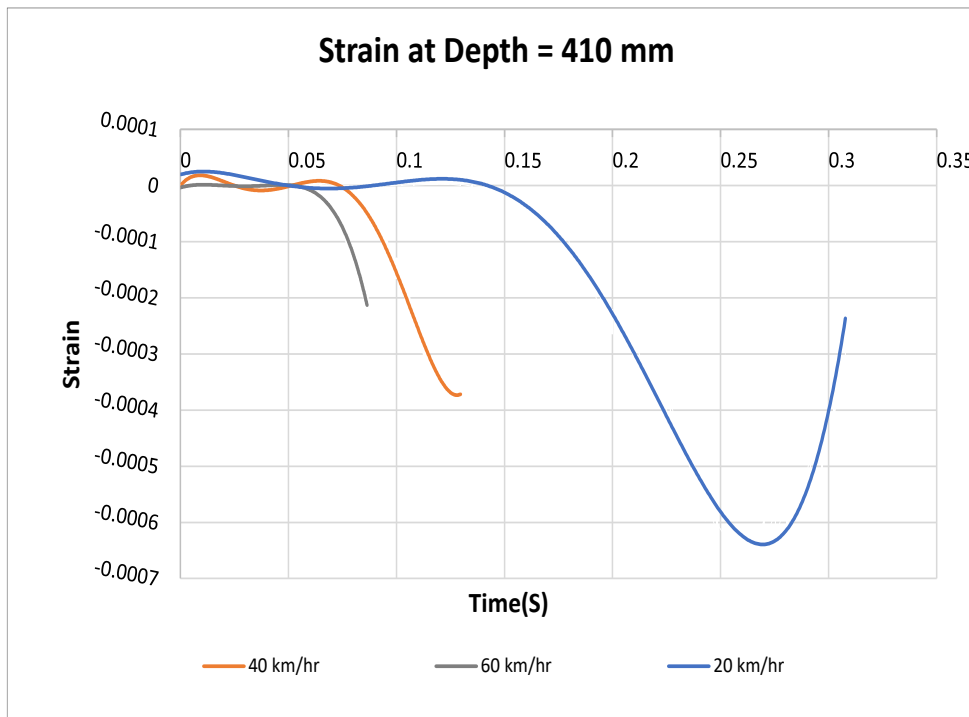
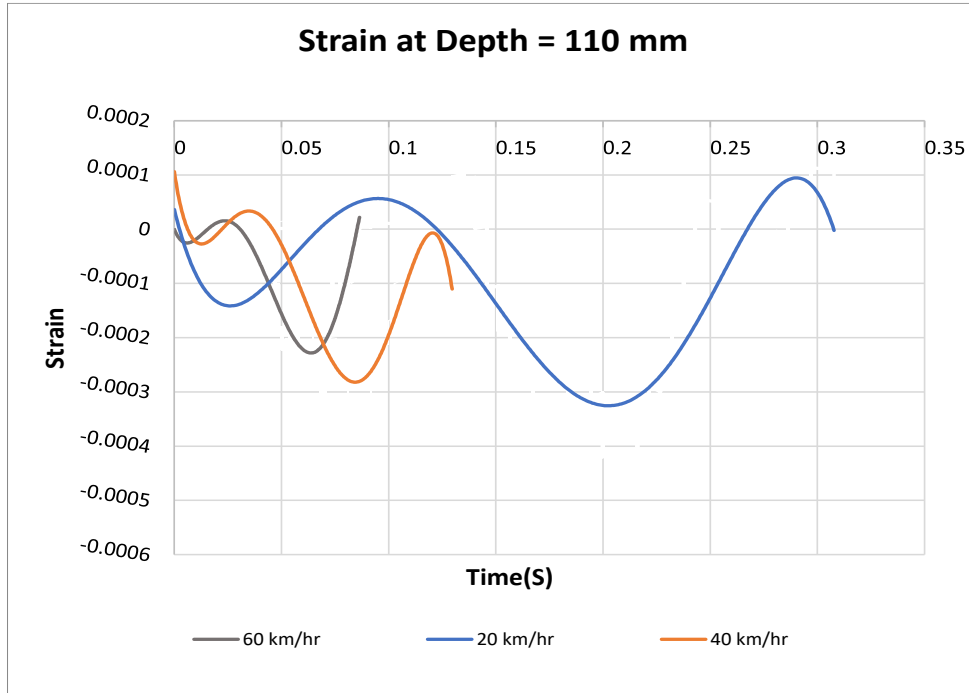
Response of the pavement model due to varying speed is analysed by recording stress, strain and displacement value in different section and different depth of the FEM model. The maximum stress, strain and displacement of the response for speed of 20, 40 and 60 km/hr at the depth of 110mm, 410mm, and 710 mm which are the interface points between asphalt-granular base, granular base-sub base and sub base- sub grade layers were recorded was tabulated in table 5.7.

Table 5.8: Response of Viscoelastic pavement model on various speed

| Speed (kmph) | Y (mm) | Strain (x) | Strain (y) | Strain (z) | Stress (x) | Stress (y) | Stress (z) | (Uy) |
|--------------|--------|------------|------------|------------|------------|------------|------------|-----------|
| 20 | 110 | 0.000394 | -0.000473 | 0.000322 | 1.63157 | -0.76262 | 1.39200 | -0.323693 |
| | 410 | 0.000488 | -0.000653 | 0.000401 | 0.25915 | -0.2020 | 0.22535 | -0.221306 |
| | 710 | 5.61E-05 | -2.91E-04 | 6.14E-05 | -0.01461 | -0.0274 | -0.01233 | -0.034808 |
| 40 | 110 | 0.000174 | -0.000337 | 0.000281 | 0.85336 | -0.7493 | 1.04411 | -0.168134 |
| | 410 | 0.000164 | -0.000370 | 0.000177 | -0.14401 | -0.2385 | -0.09815 | -0.060731 |
| | 710 | 4.28E-09 | -2.85E-08 | 4.98E-10 | -2E-07 | -3E-07 | -2E-07 | -7.07E-08 |
| 60 | 110 | 0.000218 | -0.000302 | 0.000238 | 0.64266 | -0.84529 | 0.90838 | -0.112294 |
| | 410 | 0.000019 | -0.000220 | 0.000025 | -0.08722 | -0.15524 | -0.07398 | -0.007647 |
| | 710 | 1.80E-10 | -4.97E-09 | 1.53E-10 | -2.4E-07 | -4.7E-07 | -2.4E-07 | -4.12E-09 |

5.5.1 Strain (ϵ) on the pavement

The time history for vertical strain (ϵ_y) at different depth and section of the pavement model in comparison to the various vehicular speed are given in trend lines below.



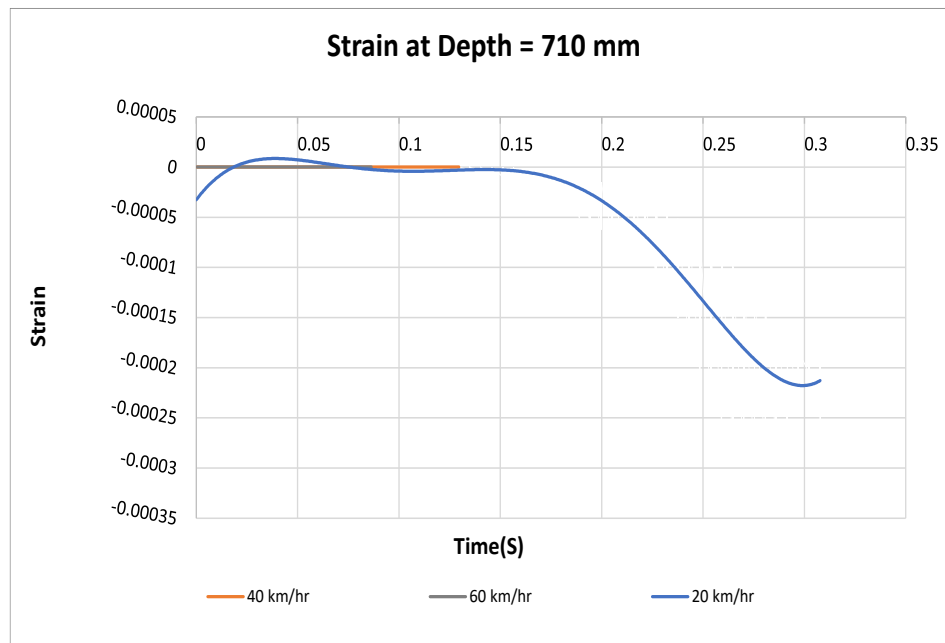


Figure 5.10: Strain at various position of viscoelastic pavement under different velocities

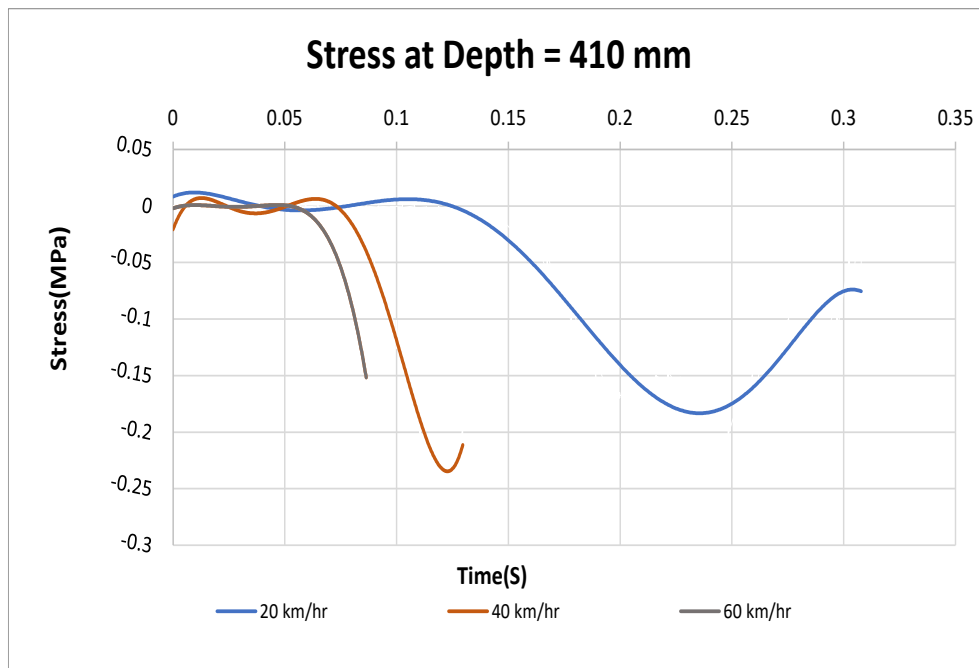
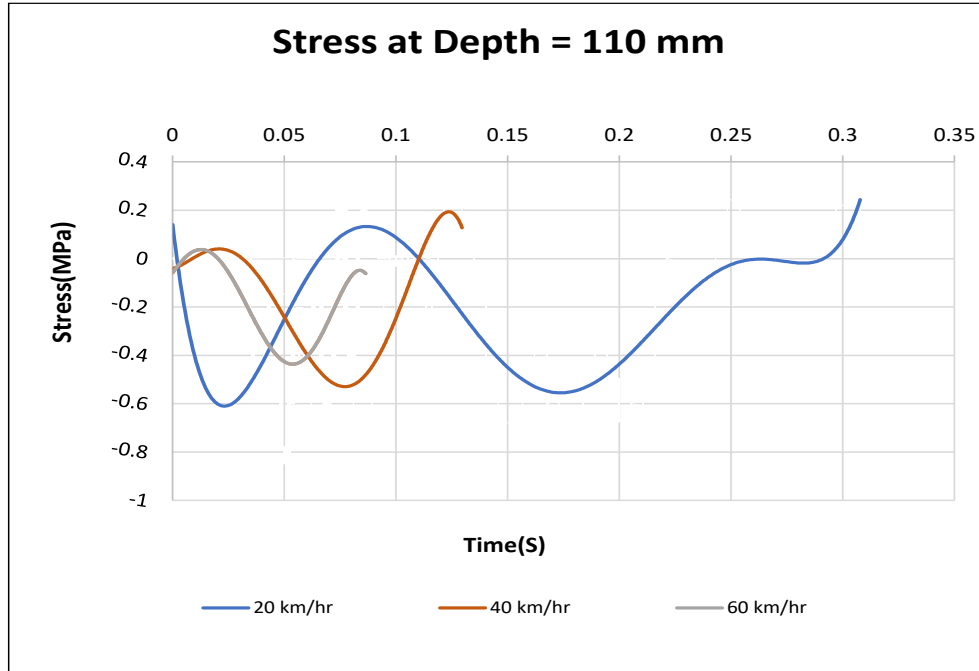
The time history trend curve depicting vertical strain (ϵ_y) reveals that, at a given depth, strains decrease with increasing speed. Higher speeds result in faster attainment of peak strain values, albeit at lower magnitudes. On average, there is a reduction of 35% and 55% in strain values when comparing speeds of 20kmph to 40kmph and 60kmph, respectively. Notably, reaching peak values at greater depths is slightly delayed due to propagation time.

Furthermore, as indicated by Table 5.7, strains increase with greater layer depths. Each subsequent layer exhibits an average increase of approximately 30% in vertical strain compared to the preceding layer. This can be attributed to a reduction in the elasticity modulus between the layers. With a decrease in elasticity modulus, the same stress values result in higher strains.

The strains observed in the transverse and longitudinal directions (X and Z directions) follow a similar pattern to the vertical strains. These strains are comparable to each other and, on average, are approximately 105% lower than the strains observed in the vertical direction.

5.5.2 Stress (σ_y) on the pavement:

The time history for vertical stress (σ_y) at different depth and section of the pavement model in comparison to the various vehicular speed are given in figure 5.8 below.



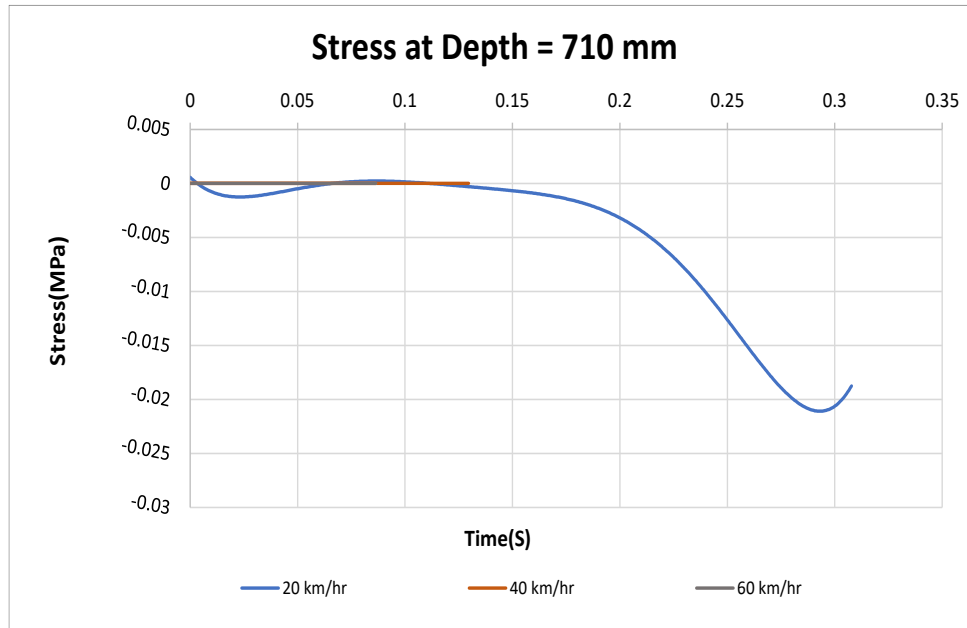


Figure 5.11: Stress at various positions of elastic pavement under different velocities

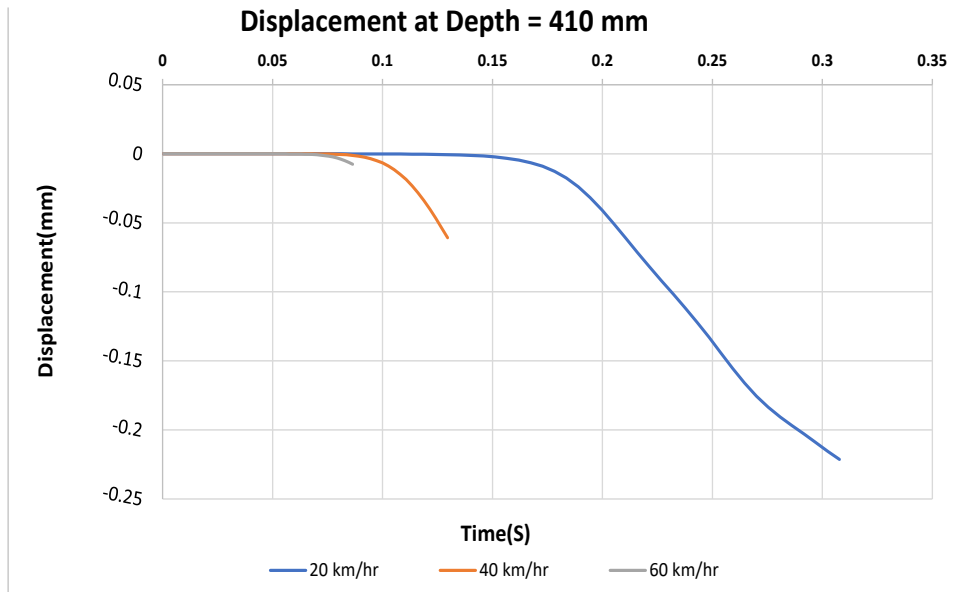
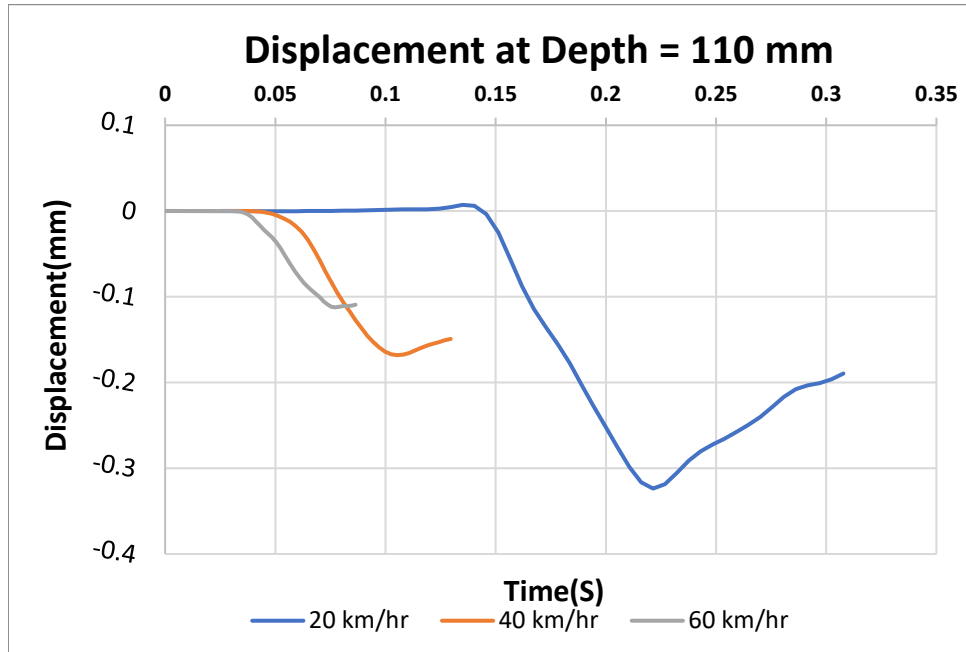
We can observe a similar trend in the vertical stress response as we did for the strain response. There is a slight decrease in stress with an increase in speed. On average, the stress reduction is approximately 10% and 23% for speeds of 40kmph and 60kmph, respectively, compared to the stress experienced at 20kmph. The trend lines indicate that the decrease in stress levels is more pronounced at higher speeds than at lower speeds. Additionally, peak stress values occur for a shorter duration at higher speeds.

Analysing Table 5.7, we can see a consistent decrease in stress levels with increasing depth. At the interface between the asphalt-base layer and the base-sub base layer, there is an average stress reduction of 70%. Furthermore, between the sub base-subgrade layer interfaces, the stress decreases by an average of 95%. This reduction in stress can be attributed to the spreading of the load across a wider area as depth increases and the stiffness of the upper layers being greater than that of the lower layers.

The stress in the longitudinal and transverse directions follows the same pattern as the vertical stress and is comparable to each other. They decrease with increasing speed as well as with increasing depth of the layers.

5.5.3 Displacement (U_y) on the pavement:

The time history for displacement (U_y) at different depth and section of the pavement model in comparison to the various vehicular speed are given in figure 5.9 below.



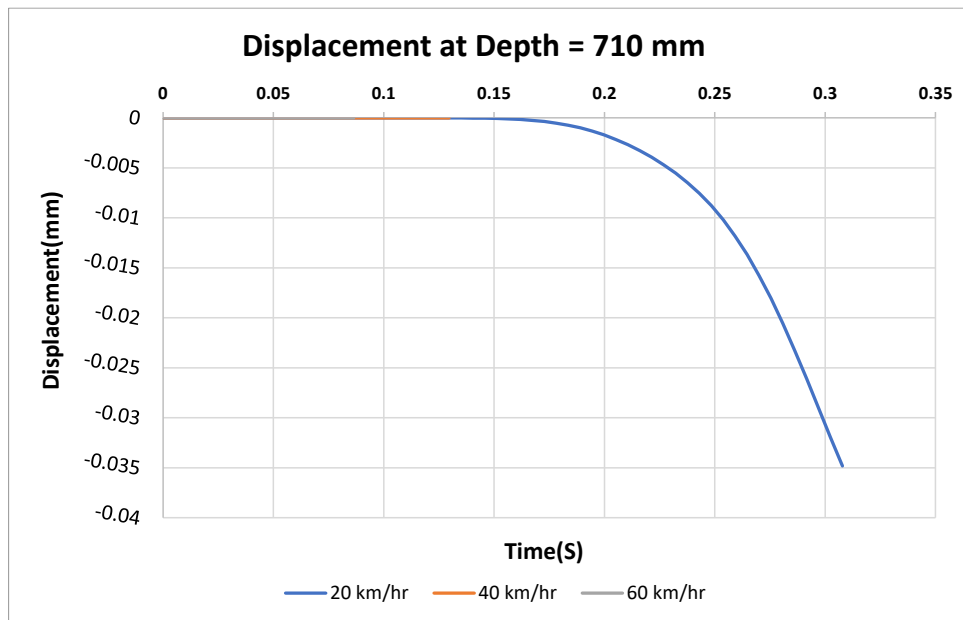


Figure 5.12: Displacement at various positions of elastic pavement under different velocities

Based on the displacement trend lines, we can observe that the displacements values are increasing as the speed decreases. There is an average reduction of 42% and 75% in displacement of 40kmph and 60kmph when compared with the displacement at 20kmph for the same depth. Similar to the stress and strain graphs, the peak values of displacements are experienced later and for a longer duration in higher speeds. The peak values are experienced as the load passes the point where the response is measured for the upper layers with slight delays for lower layers. From the table 5.7 we can observe that the displacements are decreasing along with increase in depth.

5.6 Comparison between Linear and Viscoelastic Model

The pavement response was analysed by using linear characteristics as well as viscoelastic characteristic for only the asphalt layer. On comparison of linear and viscoelastic model we can observe that the viscoelastic model produced a higher response than linear model for all parameters except the stress in lateral directions. Also, we can observe the peak values occurring slightly earlier in linear model as compared to viscoelastic model. The graphs depicting comparison between Linear and Viscoelastic models for 40km/hr at 110mm and 410mm depths are presented in figure 5.13 and 5.14 below. The vertical stress for viscoelastic model was found to be on average 35% greater than that of linearly elastic model whereas the vertical strain was found to be on average 45% greater in viscoelastic model. The displacement was on average 30% greater in viscoelastic model than that of linear model.

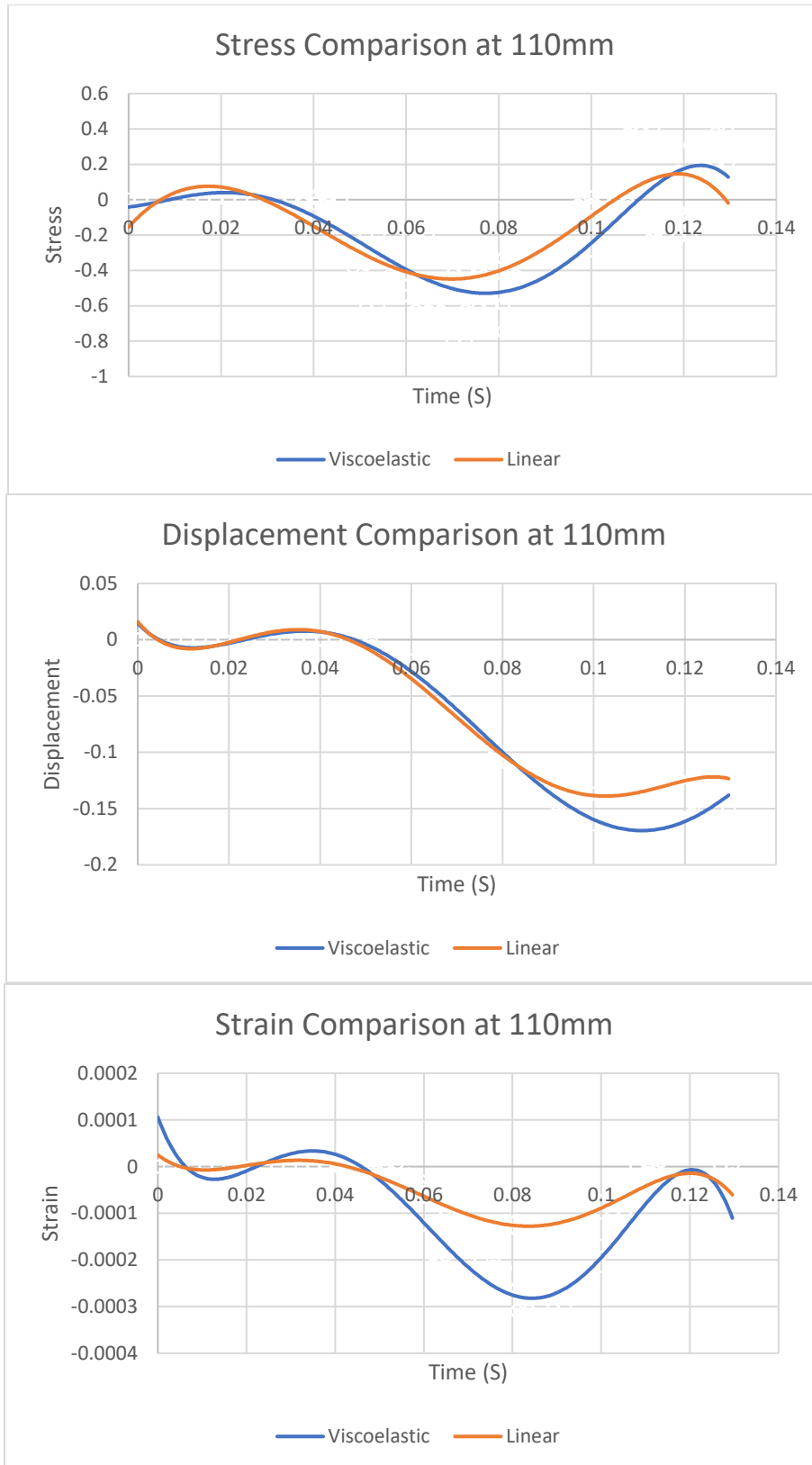


Figure 5.13: Response comparison for 110mm

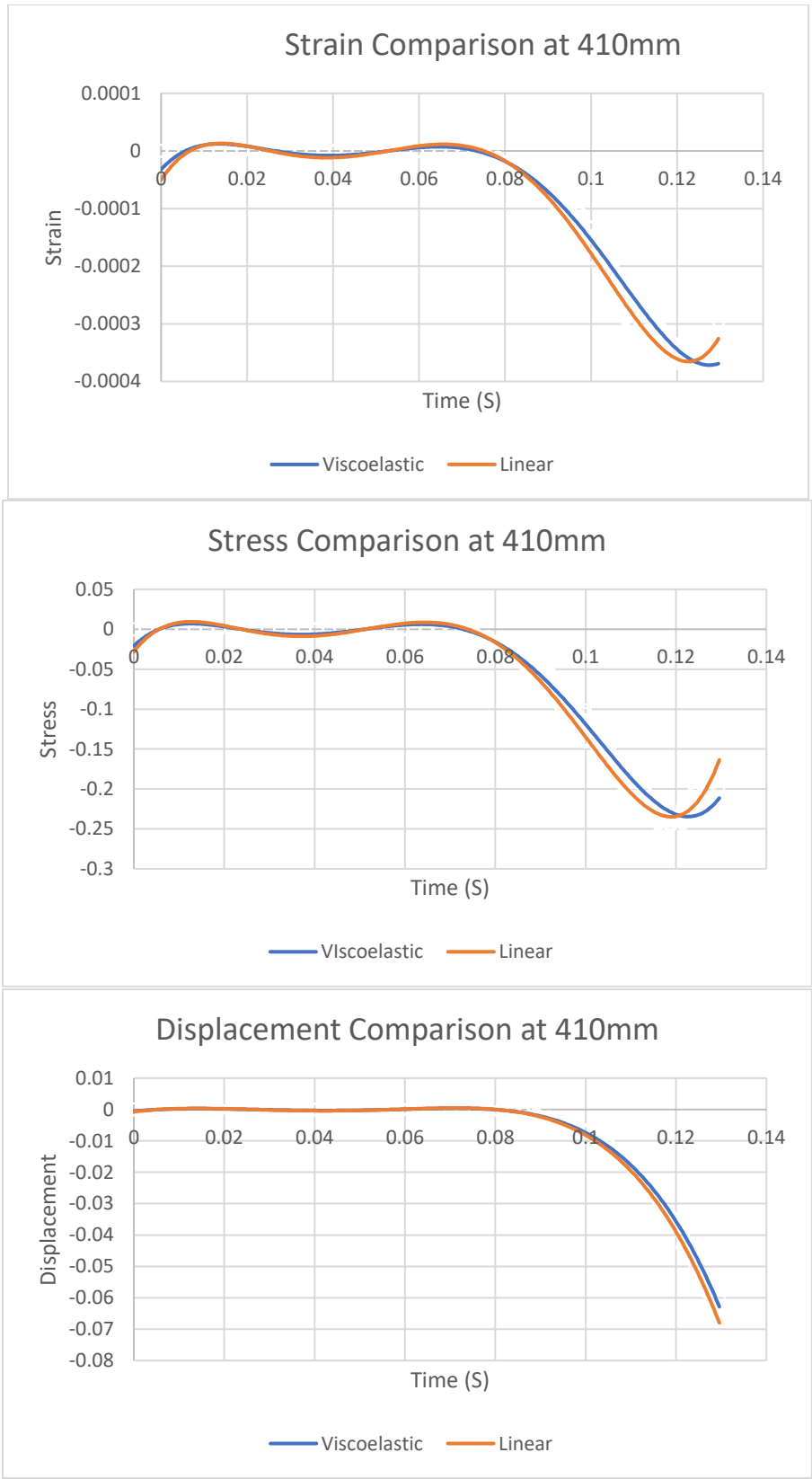


Figure 5.14: Comparison of Responses at 410mm

6. PAVEMENT DAMAGE ANALYSIS

6.1 Introduction

Up until now, we have found out the various stresses and strains in a pavement structure due to overloading in the pavement over hundreds of cycles, which has provided us an insight into various damage parameters relating to fatigue cracking, rutting, etc. Pavement distress is primarily caused by traffic, as the loads exerted by various axle vehicles can lead to structural damage. While legally loaded traffic typically does not result in pavement failure, heavy traffic is a major contributor to significant distresses such as fatigue cracking and rutting, which often require costly pavement rehabilitation measures.

Vehicle overloading is a widespread issue that affects countries of all scales and severities. However, this problem is especially serious in poor and developing countries, such as Nepal. Nepal often struggles to maintain its road infrastructure due to limited financial resources and technical expertise, not to mention rampant corruption. Therefore, the pavement is more prone to damage from overloading, leading to faster deterioration and higher maintenance costs. In countries like Nepal where the economy relies heavily on the land transport of goods, overloading is a major issue. The damage caused by overloaded vehicles can increase transport costs and delay delivery times, negatively affecting the country's economic development.

Naubise-Nagdhunga stretch of highway is the most common entry point to the Kathmandu valley for cargo and people, as it is a part of Tribhuvan Highway and connects Kathmandu with Terai region and India. Therefore, it is probably the most important stretch of road in all of Nepal for social and economic purposes. In this section, we are going to be analysing the vehicle weight database in this stretch to calculate load factors for various vehicles with the potential to damage pavement structures.

6.2 Survey Data

All the traffic data used in this study has been derived from the final report on “Preparatory Survey for Nagdhunga Tunnel Construction in Nepal” conducted by the Department of Roads (DoR) in collaboration with Japan International Cooperation Agency (JICA) in 2014/15.

In the study, a number of tests were carried out including Traffic Count Survey, Axle load Survey and Vehicle Emission Test. For our study, Traffic Count and Axle Load Surveys are relevant.

6.2.1 Traffic Data

Traffic data was collected in 3 stations, namely Naubise, Nagdhunga and Gurjadhara. As per the report, the study was a 24-hour study done on the weekend day of Saturday, July 19, 2014. Manual count was performed by direction per vehicle type and tallying of hourly and daily traffic volume. Vehicles were classified into 10 classifications. Further detail on the classifications is provided later in the chapter. A map showing the 3 stations has been shown below:

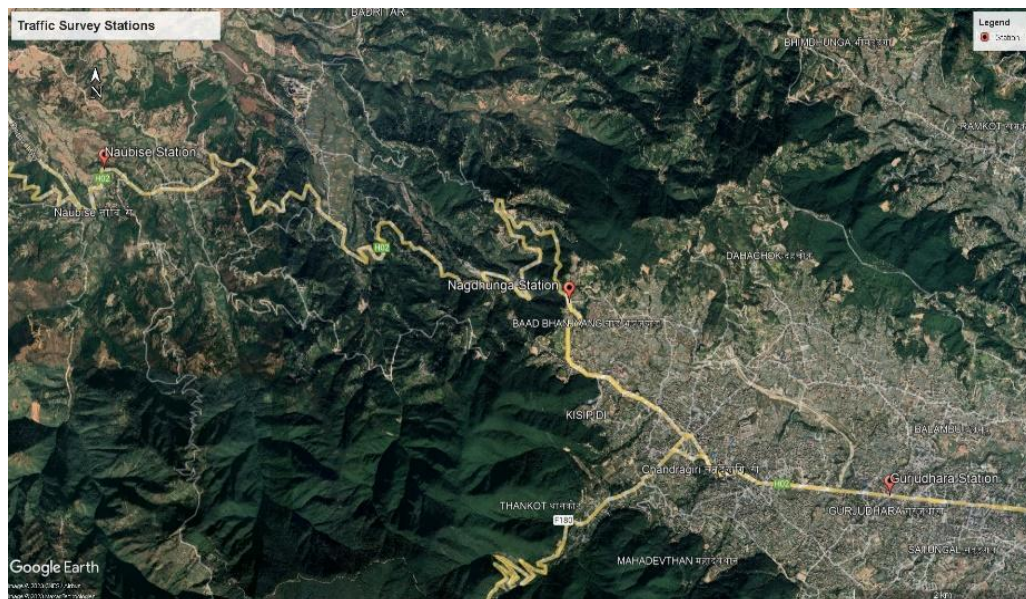


Figure 6.1: Traffic Survey Stations Map

6.2.1.1 Traffic Count Survey

The result of the traffic count survey at 3 stations is shown in Table 5.1. According to this survey result, total traffic volume including motorcycles is 7,462 vehicles at Station 1 (Naubise), 7,890

vehicles at Station 2 (Nagdhunga) and 15,454 vehicles at Station 3 (Gurjudhara). Similarly, total traffic volume without motorcycles is 5,778 vehicles at Station 1 (Naubise), 6,474 vehicles at Station 2 (Nagdhunga) and 9,393 vehicles at Station 3 (Gurjudhara).

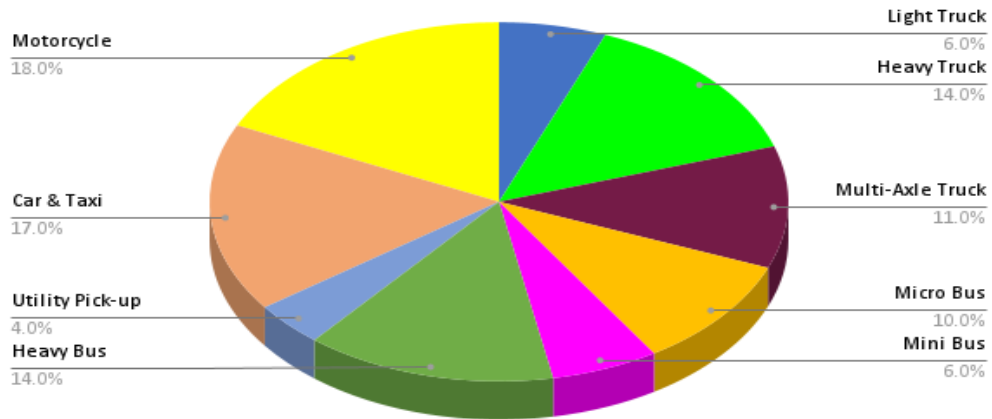


Figure 6.2: A Pie Chart Showing Vehicle Composition at Gurjudhara

Table 6.1: Traffic Count Survey

| TRAFFIC COUNT SURVEY | | Trucks | | | Buses | | | Utility Pick-up | Car & Taxi | MC | Others | Total | % of Heavy Vehicle | % of Heavy Trucks | AADT |
|----------------------|----------------------|-------------|-------------|------------------|-----------|----------|-----------|-----------------|------------|-------|--------|-------|--------------------|-------------------|-------|
| | | Light Truck | Heavy Truck | Multi-Axle Truck | Micro Bus | Mini Bus | Heavy Bus | | | | | | | | |
| Naubise | Number | 175 | 1,392 | 894 | 668 | 291 | 926 | 287 | 1,132 | 1,684 | 13 | | | | |
| | % of Total | 2% | 19% | 12% | 9% | 4% | 12% | 4% | 15% | 23% | 0% | 7462 | 43% | 31% | 8880 |
| | % of Total excl. MCs | 3% | 24% | 15% | 12% | 5% | 16% | 5% | 20% | | 0% | 5778 | 56% | 40% | 6876 |
| Nagdhu nga | Number | 480 | 1,097 | 831 | 771 | 480 | 1,138 | 330 | 1,347 | 1,416 | 0 | | | | |
| | % of Total | 6% | 14% | 11% | 10% | 6% | 14% | 4% | 17% | 18% | 0% | 7890 | 39% | 24% | 9389 |
| | % of Total excl. MCs | 7% | 17% | 13% | 12% | 7% | 18% | 5% | 21% | | 0% | 6474 | 47% | 30% | 7704 |
| Gurjudhara | Number | 212 | 1,438 | 846 | 1886 | 1024 | 986 | 752 | 2,116 | 6,061 | 133 | | | | |
| | % of Total | 1% | 9% | 5% | 12% | 7% | 6% | 5% | 14% | 39% | 1% | 15454 | 21% | 15% | 16485 |
| | % of Total excl. MCs | 2% | 15% | 9% | 20% | 11% | 10% | 8% | 23% | | 1% | 9393 | 35% | 24% | 10238 |

6.2.1.2 Hourly Variation of Traffic Volume

According to the survey conducted, the highest traffic volume was observed at Gurjudhara Station, followed by Nagdhunga and Naubise Stations in that order. The traffic volume increases steadily from 7:00 in the morning, peaks around 11:00, and then somewhat plateaus until around 19:00 in the evening. After that, the traffic volume starts to decrease, reaching its minimum value at approximately 2:00 in the night.

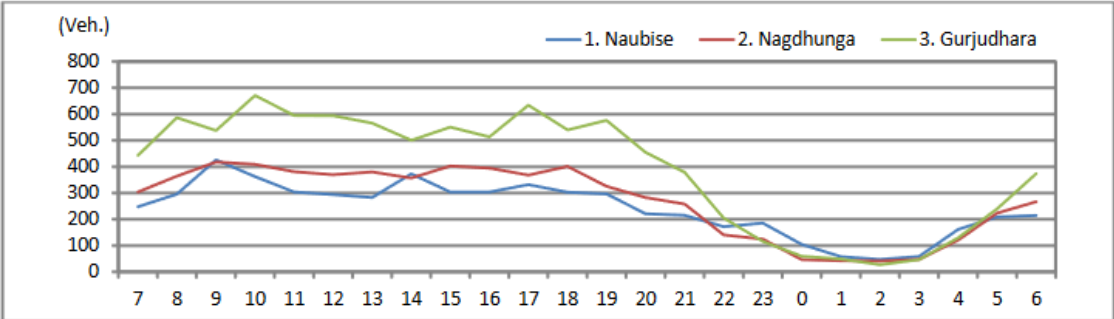


Figure 6.3: Hourly Variation of Traffic Volume (Excluding Motorcycles)

6.2.2 Axle Load Survey

6.2.2.1 Purpose and Survey Method

The Axle load survey was carried out to collect the actual loading data of heavy vehicles and for the basic information of pavement design. The survey equipment used was a manual weight scale.



Figure 6.4: Axle Load Survey

6.2.2.2 Ratio of loading truck and empty truck

97% of Heavy trucks eastbound, which is into Kathmandu, are loaded. In contrast, the empty truck accounts 87 % in the direction out of Kathmandu i.e., westbound.

Kathmandu is the capital city of Nepal and a hub for business and industry. This means that a lot of goods are brought into the city from different parts of Nepal and neighbouring countries like India and China. These goods are then distributed within the city. In contrast, the trucks leaving Kathmandu may have less cargo because they may be empty, going to other parts of Nepal or neighbouring countries to get more supplies.

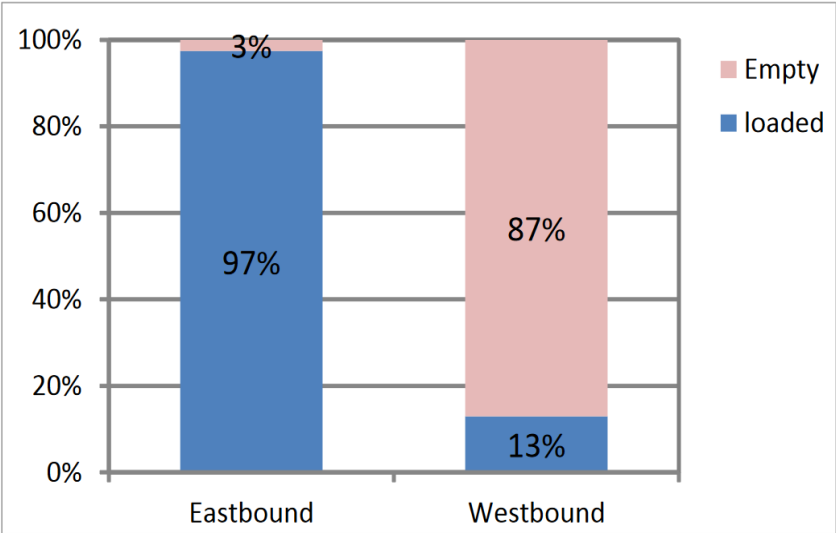


Figure 6.5: A bar graph comparing Eastbound to Westbound Loading Conditions

6.2.2.3 Average loading weight of heavy truck

It was observed that the majority of the commodities entering the Kathmandu valley is construction material i.e., Cement, Aggregates, Timber, etc. These are inherently dense objects and therefore, they may be the reason for the high overload of freight vehicles entering the valley. They are then followed by agricultural products, fuel and other consumables.

Table 6.2: Loading Weight of Each Commodity Type

| Commodity Type | Loading Weight (Tonnes) |
|----------------------------------------|-------------------------|
| Construction material | 14 |
| Agricultural product | 14 |
| Fuel (Diesel, Petrol, Gas) | 13 |
| Other Consumables, Daily Commodities | 9 |
| Other than above | 10 |
| Food Product | 11 |
| Machinery, Equipment, Motorcycles etc. | 9 |
| Chemicals, Industrial Raw Materials | 15 |
| Average | 13 |

6.2.2.4 Gross Vehicle Load (GVW)

The table below depicts the results of gross vehicle loads. Notably, the bus weighed 15 tons in both directions, indicating consistency. However, a noticeable disparity exists between the gross weight of 2-axle and 3-axle trucks in eastward and westward directions. On average, the 2-axle truck weighed 18 tonnes when moving eastbound and 12 tonnes when moving westbound, while the 3-axle truck weighed 32 tonnes when moving eastbound and 21 tonnes when moving westbound, which can be attributed to the proportion of empty trucks as mentioned previously. It's worth noting that in this particular section, a 2-axle truck weighed 15 tonnes, while a 3-axle truck weighed 30 tonnes.

Table 6.3: Total Weight Recorded

| Direction | Total Weight (Tonnes) | | |
|-----------|-----------------------|--------|--------|
| | Bus | Truck | |
| | | 2-Axle | 3-Axle |
| Eastwards | 15 | 18 | 32 |
| Westwards | 15 | 12 | 21 |
| Average | 15 | 15 | 30 |

The overload results of this survey are fairly consistent with other axle-load surveys, notably the survey done under the *Road Transport Safety and Axle Load Control Study in Nepal* for determining *Freight Flow Pattern and Location of Axle Load Control Stations* at a number of locations in 2015 as shown in table 6.4.

Table 6.4: Results of Axle Load Surveys Done in Other Studies

| SN | Particulars | Heavy Truck | | Multi Axle Truck | | Remarks |
|------------------------------------------------------------|-------------------------------|-------------|-------|------------------|-------|--------------------------------------------------------|
| | | Average | Max. | Average | Max. | |
| Dharke (Naubise) Station: Prithivi Highway | | | | | | |
| 1. | Gross Vehicle Weight (Tonnes) | 17.41 | 20.3 | 32.44 | 35.5 | Survey Date: 20 15.3.9 Source: The Study Team |
| 2. | Legal Load Limit (Tonnes) | 16.2 | | 25 | | |
| 3. | % of Overloading Trucks | 39 | | 66 | | |
| 4. | Freight Weight (Tonnes) | 8.38 | 11 | 21.21 | 24.27 | |
| 5. | Overloaded Weight (Tonnes) | 1.21 | 4.1 | 7.44 | 10.5 | |
| 6. | % of Overload | 7.46 | 25.3 | 4.16 | 42 | |
| Gaindakot (Nawalparasi) Station: East-West Highway | | | | | | |
| 1. | Gross Vehicle Weight (Tonnes) | 16.43 | 19.5 | 28.12 | 33.9 | Survey Date: 20 15.3.9 Source: The Study Team |
| 2. | Legal Load Limit (Tonnes) | 16.2 | | 25 | | |
| 3. | % of Overloading Trucks | 50 | | 62 | | |
| 4. | Freight Weight (Tonnes) | 7.4 | 10.47 | 16.89 | 22.67 | |
| 5. | Overloaded Weight (Tonnes) | 0.23 | 3.3 | 3.12 | 8.9 | |
| 6. | % of Overload | 1.43 | zo | 12.48 | 35.6 | |
| Thanabhanjyang (Hetauda) Station: East-West Highway | | | | | | |
| 1. | Gross Vehicle Weight (Tonnes) | 16.58 | 21.6 | 29.61 | 37.2 | Survey Date: |
| 2. | Legal Load Limit (Tonnes) | 16.2 | | 25 | | |
| 3. | % of Overloading Trucks | 51 | | 77 | | |

| SN | Particulars | Heavy Truck | | Multi Axle Truck | | Remarks |
|-------------------------------------------------------------|-------------------------------|-------------|-------|------------------|-------|---------------------------------------------|
| | | Average | Max. | Average | Max. | |
| 4. | Freight Weight (Tonnes) | 2.45 | 12.57 | 18.31 | 25.97 | 20 15.3.9 Source: The Study Team |
| 5. | Overloaded Weight (Tonnes) | 0.38 | 5.4 | 4.61 | 12.2 | |
| 6. | % of Overload | 2..3 | 33.75 | 18.44 | 48.8 | |
| Aaptari (Narayanghat) Station: Narayanghat -Mugling Highway | | | | | | |
| I. | Gross Vehicle Weight (Tonnes) | 16.28 | 23.80 | 29.85 | 51.9 | Source: Axle Load Survey Data 2010, RSDP II |
| 2. | Legal Load Limit (Tonnes) | 16.2 | | 25 | | |
| 3. | % of Overloading Trucks | 51/83(61%) | | 101/113(89%) | | |
| 4. | Freight Weight (Tonnes) | 11.58 | 19.10 | 23.14 | 45.4 | |
| 5. | Overloaded Weight (Tonnes) | 2.15 | 7.6 | 5.9 | 26.90 | |
| 6. | % of Overload | 12.76 | 46.91 | 22.09 | 107.6 | |

6.3 Regulatory Standards in Nepal

- Maximum allowable axle load is the axle load as specified by the manufacturer within safe axle load as specified below and described thereafter (Heavy Vehicle Management Policy 2005 AD, Nepal):
 - a. Single axle fitted with 2 tyres: 6 tonnes
 - b. Single axle fitted with 4 tyres: 10.2 tonnes
 - c. Tandem axle fitted with 8 tyres: 19 tonnes

With this information, a table for each axle group has been developed as shown in table 6.5.

Table 6.5: Loading Limit for Different Axles

| SN | Axle Type | Max. GVW (Tonnes) | Total GVW (Tonnes) |
|----|----------------------------|-------------------|--------------------|
| 1 | Two Axles (4 Tyres) | | |
| | Front Axle (2 Tyres) | 6 | 12 |
| | Rear Axle (2 Tyres) | 6 | |









| SN | Axle Type | Max. GVW (Tonnes) | Total GVW (Tonnes) |
|----|------------------------------------|-------------------|--------------------|
| 2 | Two Axles (6 Tyres) | | |
| | Front Axle (2 Tyres) | 6 | 16.2 |
| | Rear Axle (4 Tyres) | 10.2 | |
| 3 | Three Axle Trucks | | |
| | Front Axle (2 Tyres) | 6 | 25 |
| | Rear Axle (8 Tyres: Tandem) | 19 | |
| 4 | Four Axle Trucks (12 Tyres) | | |
| | Front Axle (2 Tyres) | 6 | 31 |
| | Lift Axle (2 Tyres) | 6 | |
| | Rear Axle (8 Tyres: Tandem) | 19 | |
| 5 | Four Axle (14 Tyres) | | |
| | Front Axle (2 Tyres) | 6 | 30 |
| | Rear Axle (12 Tyres: Tandem) | 24 | |
| 6 | Five Axle (18 Tyres) | | |
| | Front Axle (2 Tyres) | 6 | 40.2 |
| | Mid Axle (4 Tyres) | 10.2 | |
| | Rear Axle (12 Tyres: Tandem) | 24 | |





6.4 Study Process

6.4.1 Vehicle Classification

The Road Transport Safety and Axle Load Control Study in Nepal has outlined the categorization of vehicles in Nepal in the following manner:

Table 6.6: Vehicle Classification

| Vehicle Type | Vehicle Characteristics | Typical Vehicle |
|-------------------|-------------------------------------------------------------------------|---------------------------------------------------------------------------------------|
| Multi-Axle Truck | Standard / heavy trucks, trailers/articulated. (≥ 3 axles) |  |
| Heavy Truck | Standard / heavy trucks, trailers/articulated. (2 axles) |  |
| Mini Truck | Mid-sized trucks with single rear-axle (usually 4-wheeled, <8 tons GVW) |  |
| Standard Bus | Buses having seating capacity of 35-50 seats |  |
| Mini-bus | Medium size buses having seating capacity of 20-35 seats. |  |
| Motorcycle | Motorised two wheelers such as scooters and motorcycles |  |
| Bullock/Hand cart | Bullock, horse or manually driven vehicles (Non-motorised) |  |
| Rickshaws | Non-motorised cycle rickshaws |  |

| Vehicle Type | Vehicle Characteristics | Typical Vehicle |
|------------------|-----------------------------------------------------------------------------------------------------------------|---------------------------------------------------------------------------------------|
| Micro-bus | Small buses and vans having seating capacity of 10-15 seats. |  |
| Car | Passenger car taxis and vans (≤ 5 seats). |  |
| Utility Vehicles | Pickups or 4-wheeled vehicles with single/twin cabin and load compartment (open/hooded), Light freight vehicles |  |
| Tractor | Farm tractors |  |
| Four Wheel Drive | Vehicles strictly having four wheel gears (seating approximately 10) such as Mitsubishi Pajero, Prado etc. |  |
| Three Wheeler | Electrical or gasoline/LPG fuelled 3-wheeled vehicles (excluding power tillers, farm tractors) |  |
| Power Tiller | Motorised four wheel vehicles used for carrying goods and mainly driven by hands and not steering. |  |

Our study focuses on overloaded vehicles travelling on a specific stretch of highway. During our axle load survey, we found that the vehicles causing the most pavement damage were Multi-Axle Trucks, Heavy Trucks, and Heavy Buses. Therefore, we will be primarily analysing these vehicle types.

To ensure that our selection of vehicles adequately covers the required spectrum of loads, we referred to *the Guidelines for the Design of Flexible Pavements-2014* by DoR. According to this guide, our selected vehicles have high VDF (Vehicle Damage Factor) values, confirming their significance in pavement damage.

Regarding Multi-Axle Trucks, we have identified 12-tyred trucks as the dominant ones in the category. They are generally seen in Nepali roads with a hydraulic lift on one of the axles when the load on ordinary axles exceeds the permissible limit as the most significant. The provision of a lifted axle in a truck can significantly reduce the extent of damage on the road pavement and structures because the load is distributed among more tyres when the lifted axle comes into effect.

In terms of Heavy Trucks, we have identified 10-tyred trucks with dual, tandem axles at the rear end, and for Heavy Buses, we have identified buses with dual tyres in the rear end.

6.5 Equivalent Single Axle Load (ESAL)

6.5.1 Introduction

In transport engineering, ESAL stands for **Equivalent Single Axle Load**. To analyse the impact of vehicles, especially overloads, on pavement performance, we convert all axle loads and vehicles into a standard representative axle. This conversion allows us to compare the effect of different vehicles on the pavement.

According to the AASHTO Guide of Pavement Structure (1993), ESAL is the ratio between the damage of the passage of an axle on pavement and the damage of a standard axle, usually the 80 KN single axle loads, passing on the same pavement.

It is a standardized measure used to convert damage from wheel loads of various magnitudes and repetitions to damage from an equivalent number of “standard” or “equivalent” loads. The most commonly used equivalent load is the **18,000 lb (80 kN or 8.16 tonne)** equivalent single axle load.

For practical scenarios where a number of vehicles with different axle loads are moving in a certain section of road for a certain period of time, we need further parameters. In those scenarios, we use parameters like the Vehicle Distribution Factor (VDF) to represent the type of vehicle or Equivalent Axle Load Factor (EALF) to represent the types of axle in each vehicle.

6.5.2 Methods of Calculation

The equivalent axle load factor (EALF) defines the ratio between the damage caused by the passage of an axle on a pavement and the damage caused by the passage of a standard axle on the same pavement. This EALF is used in pavement design to convert the spectrum of vehicles with different types of axles (i.e., single, tandem and tridem) into single axles with dual tires, i.e., the ESAL, by using Equation (1), where n is the number of axle load groups, i is the number

of the axle load group, $EALF_i$ is the EALF for i^{th} axle load group and n_i is the number of passes of the i^{th} axle load group.

$$ESAL_i = \sum_{i=1}^n EALF_i * n_i \dots\dots\dots (6.1)$$

For flexible pavements, the EALF, which is defined based on experience and on the results of the AASHTO Road Test (1962), is defined as

$$EALF = W_{18} / W_x \dots\dots\dots (6.2)$$

where W_{18} is the number of standard 18-kip axle applications, W_x is the number of x-axle applications, L_x is the axle load (kip), L_2 is the axle code (1 for single axle, 2 for tandem axles and 3 for tridem axles), p_t is the terminal serviceability, SN is the structural number (in) and b_{18} is the value of b, when L_x is equal to 18 and L_2 is equal to 1.

$$\begin{aligned} \text{Log} \left(\frac{W_x}{W_{18}} \right) &= 4.79 \log (18 + 1) - 4.79 \log (L_x + L_2) \\ &+ 4.33 \log L_2 + \frac{G_t}{\beta_x} - \frac{G_t}{\beta_{18}} \\ G_t &= \log \left(\frac{4.2 - p_t}{4.2 - 1.5} \right) \\ \beta_x &= 0.40 + \frac{0.081(L_x - L_2)^{3.23}}{(SN + 1)^{5.19} L_2^{3.23}} \dots\dots\dots (6.3) \end{aligned}$$

Many studies have been conducted since to compute the EALF values, which use alternative ways to calculate its value.

Many methods today calculate EALF using a relationship resembling equation (6.4).

$$EALF = k \left[\frac{P_x}{P_{80}} \right]^\alpha \dots\dots\dots (6.4)$$

Where, P_x = actual axle load and P_{ref} = load of the standard axle (usually 80 KN.)

These relations typically use a power value of 4 (i.e. $\alpha=4$), but this value can vary depending on pavement type, distress, failure level, and contact stresses. For tandem or tridem axles, the above equation is applied for all individual axles of the axle group, meaning that for a tandem axle, it is applied two times whereas for tridem axles it is applied three times.

Some methods for EALF calculation as prescribed by various studies and guidelines have been described below

a. Suggestion by Laboratoire Central des Ponts et Chaussées (LCPC)

To consider the axle type - single, tandem, or tridem – LCPC (Laboratoire Central des Ponts et Chaussées), France (1994) proposed the equation below in the French pavement design guide for calculating ESAL (dubbed as axle aggressiveness in the guide itself). This equation further includes a coefficient (k) based on the type of axle and α coefficient based on pavement type and pavement stiffness.

$$EALF = k \left[\frac{P_x}{P_{80}} \right]^\alpha \dots\dots\dots (6.5)$$

The k coefficient, which depends upon the various axle types, is listed in the Table below:

Table 6.7: Values of k as suggested by LCPC

| Pavement Type | k | | | |
|-------------------------------|----------|-------------|-------------|-------------|
| | α | Single axle | Tandem axle | Tridem axle |
| Flexible pavement | 5 | 1 | 0.75 | 1.1 |
| Rigid and semi-rigid pavement | 12 | 1 | 12 | 113 |

b. Suggestion by the Slovenian Design Guide

The SPENS project report (Kokot and Gaspar 2009) provides an overview of load equivalency factor models utilized in multiple European countries. Out of all the models, only the Slovenian approach, as presented in the Equation, takes into account the impact of the wheel type.

$$EALF = 10^{-8} * f_0 * (f_k * L_{stat})^4 \dots\dots\dots (6.9)$$

$$\text{Say, } 10^{-8} * f_0 * f_k^4 = k \dots\dots\dots (6.10)$$

$$\text{Then } EALF = k * L_{stat}^4 \dots\dots\dots (6.11)$$

Where f_0 is the factor of axle distribution (single = 2.212, tandem = 1.583), f_k is the factor of wheel distribution (single = 1.0, double = 0.9) and L_{stat} is the static axle load of an individual vehicle (kN).

c. Recommendation by DoR

The *Flexible Pavement Design Guideline* by DoR recommends the following values of individual-axle VDF (EALF) values.

a) Single axle with single wheel on either side:

$$VDF = \left[\frac{\text{axle load in kN}}{65} \right]^4$$

b) Single axle with dual wheel on either side:

$$VDF = \left[\frac{\text{axle load in kN}}{80} \right]^4$$

c) Tandem axle with dual wheel on either side:

$$VDF = \left[\frac{\text{axle load in kN}}{148} \right]^4$$

d) Tridem axle with dual wheel on either side:

$$VDF = \left[\frac{\text{axle load in kN}}{224} \right]^4$$

d. Suggestion by Amorim et al. (2015)

In a paper titled *A model for equivalent axle load factors*, Amorim et al. (2015) proposed an equation to model the k coefficient.

$$EALF = k \left[\frac{P_x}{P_{80}} \right]^\alpha \dots\dots\dots (6.6)$$

Where,

$$k = a_1 * (H_{asp})^2 * (H_{gra})^3 * (E_{asp})^4 * (E_{subg})^5 * e^{(a_6 ALP)} \dots\dots\dots (6.7)$$

$$ET = \sqrt[3]{\frac{(H_{asp})^3 * E_{asp} + (H_{gra})^3 * E_{gra}}{E_{subg}}} \dots\dots\dots (6.8)$$

Where *Hasp*, *Hgra*, *Easp*, *Egra* and *Esubg* represent the thickness of the asphalt layer, the thickness of the granular layer (both in m), the stiffness of the asphalt layer and the stiffness of the sub-grade (both in MPa) respectively. ET refers to extra thickness while ALP is the Axle Load Parameter as defined below in Table 6.9.

Values of *a*₁ through *a*₆ have been shown in Table 6.8.

Table 6.8: Values of ALP

| <i>α</i> | ET(m) | <i>α</i> ₁ | <i>α</i> ₂ | <i>α</i> ₃ | <i>α</i> ₄ | <i>α</i> ₅ | <i>α</i> ₆ | R ² |
|----------|-------|-----------------------|-----------------------|-----------------------|-----------------------|-----------------------|-----------------------|----------------|
| 4 | ≤1.2 | 1.08E+01 | -9.41E-01 | 6.69E-02 | -2.85E-01 | 3.04E-01 | -1.41E+00 | 0.992 |
| | ≥1.2 | 5.20E+00 | 3.33E-02 | 1.82E-03 | 1.15E-01 | -1.17E-01 | -1.33E+00 | 0.975 |

Table 6.9: Values of 1 through *a*₆

| Single Axle Single wheel | Single Axle Dual Wheel | Tandem Axle Single Wheel | Tandem Axle Dual Wheel | Tridem Axle Single Wheel | Tridem Axle Double Wheel |
|-----------------------------|---------------------------|-----------------------------|---------------------------|-----------------------------|-----------------------------|
| 1.0 | 2.0 | 2.7 | 4.1 | 3.8 | 5.2 |

6.5.3 Recommendation by DoR

Due to the unavailability of the exact pavement design data for the selected road section, we have created an approximate equivalent pavement design for that exact stretch of road by considering the traffic and vehicle load conditions. All the values of ESAL calculated through the method (d) - Suggestion by Amorim et al. (2015) have been based on this hypothetical design. Details regarding the pavement design have been presented in Chapter 4.

6.5.4 ESAL Formula

When we require a cumulative ESAL value that accumulates over a span of 'n' years, we use the term Cumulative Equivalent Standard Axle Load (CESAL) and it is calculated by the following formula:

$$CESAL = 365 * AADT * DD * DL * GR * VDF \dots\dots\dots (6.13)$$

Where, Directional distribution factor (DD) is 0.5 in the case of the assumed stretch of road. Lane distribution factor (DL) is 75%. Annual growth factor (GR) was calculated using the formula $GR = \{(1 + g)^n\} / \{g\}$ where, g = the traffic growth rate in percentage. For finding the cumulative ESAL of each axle, we can substitute the VDF for EALF i.e.

$$CESAL = 365 * AADT * DD * DL * GR * EALF \dots\dots\dots (6.14)$$

The growth rate is adopted as 4.1 percent as done previously in the pavement design process

6.5.5 Pavement Overlay Thickness

Several studies have quantified the relationship between vehicle load and pavement damage effects. A study by Alavi et al. (2018) investigated the equivalent axle load on pavement deterioration of forest roads. The results showed that vehicles with lower values of equivalent axle load should be used alongside with lower volume of timber with enough time in between two trips to reduce damage in pavement.

In 2018, Pais and Pereira delved into the effects of overloaded vehicles using a database of vehicle weights. They examined truck factors across various vehicle categories and found that

overloaded vehicles contribute to a 30% increase in pavement damage and life-cycle costs compared to those with permissible axle loads. By utilizing fatigue equations established through the Shell method and factoring in a 20 cm granular layer, the researchers were able to determine the appropriate thickness of the asphalt layer (h) as outlined in the following equation:

$$\text{Log}(h) = a + b(\text{log}(N))^2 + \frac{c}{\text{Log}(N)} \dots\dots\dots (6.15)$$

Where, N is the cumulative number of standard axles.

The constants a, b, and c are factors depending on the stiffness of the subgrade and asphalt layer as given in Table ... The value of stiffness of the asphalt layer E_{asp} is the stiffness of the asphalt layer and E_{subg} is the stiffness of the subgrade.

Table 6.10: Values of a, b, c for thickness

| Easp (MPa) | Esubg (MPa) | a | b | c |
|------------|-------------|-----------|----------|-----------|
| 5000 | 20 | -4.94E-01 | 6.63E-03 | -2.79E+00 |
| | 40 | -2.66E-01 | 5.32E-03 | -4.49E+00 |
| | 60 | -8.48E-02 | 4.53E-03 | -5.91E+00 |
| | 80 | 1.22E-01 | 3.67E-03 | -7.44E+00 |
| | 100 | 2.80E-01 | 3.12E-03 | -8.71E+00 |
| | 120 | 3.10E-01 | 3.18E-03 | -9.23E+00 |
| | 140 | 3.99E-01 | 2.95E-03 | -1.01E+00 |

The cost of laying pavement on a road is affected by various factors, including the vehicle load. As the vehicle load increases, the damage inflicted on the pavement also increases, leading to the need for more frequent repairs and maintenance, which increases the cost of laying pavement.

In our study, we will utilize the aforementioned equation to determine the additional thickness of asphalt layer needed for overloading conditions. Whilst the granular layer in our pavement section is thicker than the 20 cm used in the original study, this equation will help us arrive at a generalized estimate of increased pavement costs.

6.5.6 Remaining Service Life

As per Gedafa et al. (2010), remaining service life (RSL) has been defined as the estimation of total years that a pavement will be functionally and structurally in a normal condition only with regular, routine preservation attempts.

Jihanny et al. (2018) devised a formula to calculate the impact of overloaded vehicles on pavement structure:

$$RSL = (CESAL\ standard / CESAL\ Overload) * DL \dots\dots\dots (6.16)$$

Where RSL is the remaining service life of pavement (years) and DL is design life and CESAL is Cumulative Equivalent Single Axle Load at the end of design life years.

6.5.7 Reduction in Service Life

In a study by Ojha (2018), a simple method for determining the remaining service life of a road under overloaded conditions was used. The approach involved comparing the cumulative equivalent standard axle load (CESAL) value at the end of the service life in standard loading conditions to the year that produces the same CESAL value in overloaded conditions.

The actual service life of the road due to vehicle overloading was then determined based on the year that produces the same CESAL value in overloaded conditions (say, year x). By using CESAL values, the method takes into account the cumulative damage caused by all the vehicles that have passed over the road during its lifespan.

The difference between the service life years and year x is considered as the reduction in service life due to overloading. This method offers a straightforward way of evaluating the effect of overloading on the remaining service life of a road.

6.6 Methodology

The concepts mentioned above have been utilized for our study calculation. The study started out through a thorough study of related literature. After gaining all the required knowledge, we started looking for available data.

Once we had gathered all the necessary data, we proceeded to analyse it. Initially, we determined the main types of vehicles that were responsible for causing damage to the pavement. Then, we calculated the values of EALF and CESAL for each of the 4 cases/methods previously described. These values were further evaluated to determine the Remaining Service Life (RSL) and the increase in overlay thickness. We have provided a concise flowchart to explain the process of our study below. Each step of the analysis process will be discussed in more detail in the following sections.

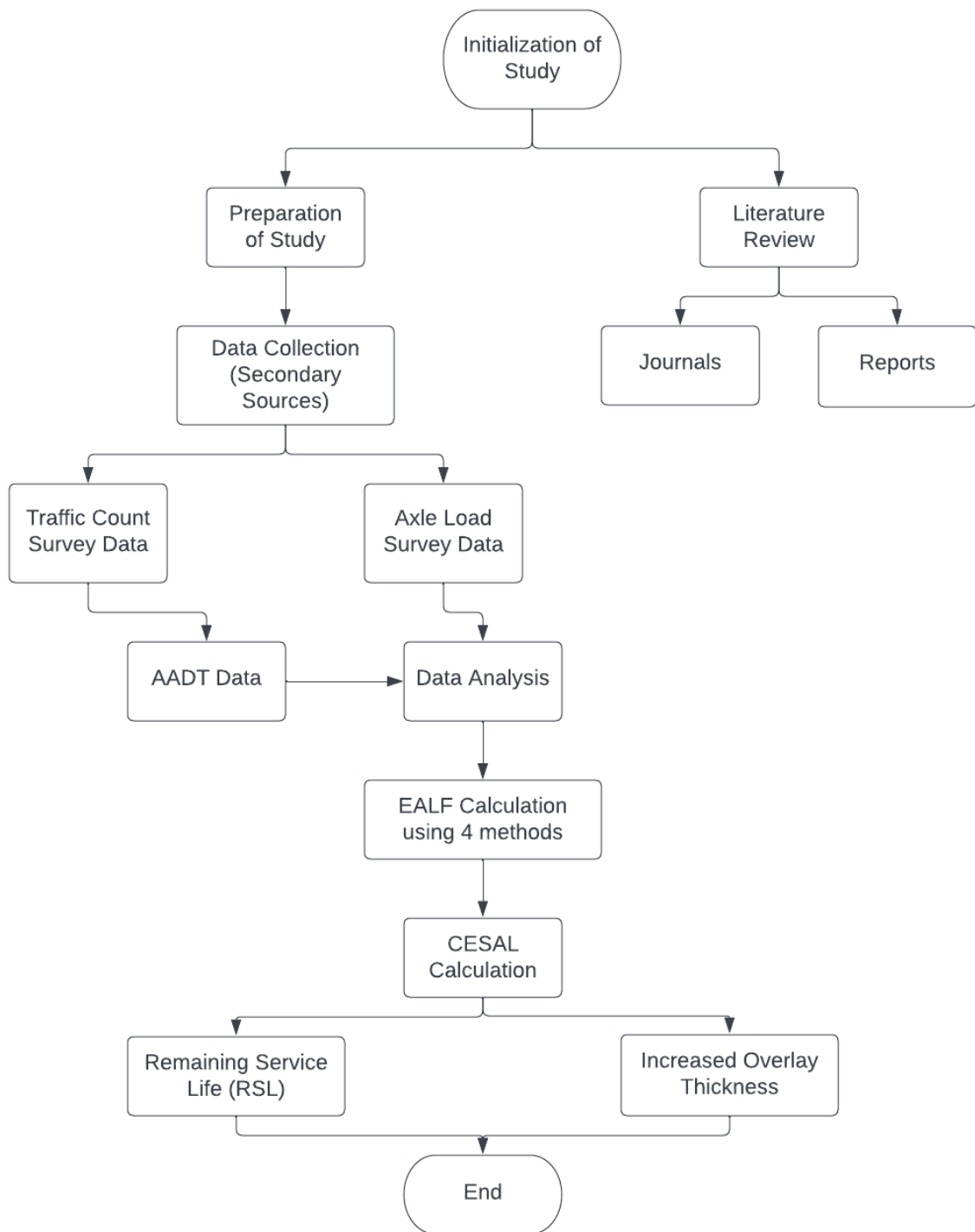


Figure 6.6: Flowchart for Statistical Analysis

6.7 Calculation

6.7.1 EALF Calculation

The calculation of EALF has been done as per the concepts in 6.5.2 (a), (b), (c) and (d), The obtained values are shown in Tables 6.11, 6.12 and 6.13. It is to be noted that the value provided using method (d) is based on a hypothetical pavement design specifically tailored to accommodate the vehicular data within the selected stretch.

Table 6.11: EALF for Heavy Bus


| Axle load (Tonne) – Eastbound | | | | |
|-------------------------------|-----------------------------------------------------------------------------------|--------------|--------------------|--------|
| Heavy Bus |  | 1st axle | 2nd axle | VDF |
| Type of axle/wheel | | Single Axle | Single axle | |
| | | Single Wheel | Double Wheel | |
| Legal limits | | 6.000 | 10.2 for each axle | |
| Actual load (Average) | | 6.180 | 11.82*2 | |
| Actual load (Maximum) | | 8.000 | 15*2 | |
| EALF | | | | |
| A | Legal | 0.215 | 3.052 | 3.267 |
| | Average | 0.249 | 6.377 | 6.626 |
| | Maximum | 0.906 | 20.990 | 21.895 |
| B | Legal | 0.266 | 1.455 | 1.720 |
| | Average | 0.299 | 2.623 | 2.922 |
| | Maximum | 0.839 | 6.803 | 7.642 |
| C | Legal | 0.292 | 2.441 | 2.734 |
| | Average | 0.329 | 4.403 | 4.732 |
| | Maximum | 0.924 | 11.418 | 12.342 |
| D | Legal | 2.121 | 4.324 | 6.445 |
| | Average | 1.116 | 3.930 | 5.046 |
| | Maximum | 16.366 | 20.222 | 36.588 |

Table 6.12: EALF for Heavy Truck



| Axle load (Tonne) - Eastbound | | | | | |
|-------------------------------|-----------------------------------------------------------------------------------|--------------|--------------------|----------|--------|
| Heavy Truck |  | 1st axle | 2nd axle | 3rd axle | VDF |
| Type of axle/wheel | | Single Axle | Tandem axle | | |
| | | Single Wheel | Double Wheel | | |
| Legal limits | | 6.000 | 10.2 for each axle | | |
| Actual load (Average) | | 6.180 | 11.82*2 | | |
| Actual load (Maximum) | | 8.000 | 15*2 | | |
| EALF | | | | | |
| A | Legal | 0.215 | 4.578 | | 4.793 |
| | Average | 0.249 | 9.566 | | 9.815 |
| | Maximum | 0.906 | 31.484 | | 32.390 |
| B | Legal | 0.266 | 2.082 | | 2.348 |
| | Average | 0.299 | 3.755 | | 4.054 |
| | Maximum | 0.839 | 9.739 | | 10.578 |
| C | Legal | 0.671 | 0.418 | | 1.088 |
| | Average | 0.755 | 0.753 | | 1.508 |
| | Maximum | 2.120 | 1.953 | | 4.073 |
| D | Legal | 2.121 | 0.445 | | 2.566 |
| | Average | 2.388 | 0.802 | | 3.190 |
| | Maximum | 6.701 | 2.080 | | 8.782 |

Table 6.13: EALF for Multi Axle Truck

| Axle load (Tonne) - Eastbound | | | | | | |
|-------------------------------|-----------------------------------------------------------------------------------|--------------|--------------|--------------------|----------|---------|
| Multi-Axle Truck |  | 1st axle | 2nd axle | 3rd axle | 4th axle | VDF |
| Type of axle/wheel | | Single Axle | Single Axle | Tandem axle | | |
| | | Single Wheel | Single Wheel | Double Wheel | | |
| Legal limits | | 6.000 | 6.000 | 10.2 for each axle | | |
| Actual load (Average) | | 7.110 | 12.260 | 12.41*2 | | |
| Actual load (Maximum) | | 10.000 | 15.000 | 15*2 | | |
| EALF | | | | | | |
| A | Legal | 0.215 | 0.215 | 4.578 | | 5.008 |
| | Average | 0.502 | 7.656 | 12.204 | | 20.362 |
| | Maximum | 2.764 | 20.990 | 31.484 | | 55.238 |
| B | Legal | 0.266 | 0.266 | 2.082 | | 2.613 |
| | Average | 0.524 | 4.628 | 4.563 | | 9.715 |
| | Maximum | 2.049 | 10.371 | 9.739 | | 22.159 |
| C | Legal | 0.671 | 0.292 | 0.418 | | 1.381 |
| | Average | 1.323 | 5.096 | 0.915 | | 7.333 |
| | Maximum | 5.175 | 11.418 | 1.953 | | 18.547 |
| D | Legal | 2.121 | 2.121 | 0.445 | | 4.686 |
| | Average | 4.183 | 36.970 | 0.975 | | 42.128 |
| | Maximum | 16.366 | 82.842 | 2.080 | | 101.288 |

For tandem or tridem axles, the equation for EALF Calculation is applied for all individual axles of the axle group, meaning that for a tandem axle, it is applied two times whereas for tridem axles it is applied three times.

6.7.2 CESAL Calculation throughout the Design Life

Table 6.14: CESAL calculation throughout the design life

| Year | TOTAL CESAL (msa) | | | | | | | | | | | |
|------|-------------------|---------|---------|--------|---------|---------|--------|---------|---------|--------|---------|---------|
| | A | | | B | | | C | | | D | | |
| | Legal | Average | Maximum | Legal | Average | Maximum | Legal | Average | Maximum | Legal | Average | Maximum |
| 1 | 1.981 | 5.187 | 15.774 | 1.004 | 2.315 | 5.683 | 0.747 | 1.774 | 4.590 | 1.922 | 6.084 | 18.164 |
| 2 | 4.042 | 10.588 | 32.194 | 2.050 | 4.725 | 11.598 | 1.524 | 3.621 | 9.369 | 3.923 | 12.417 | 37.073 |
| 3 | 6.189 | 16.209 | 49.288 | 3.139 | 7.233 | 17.757 | 2.334 | 5.544 | 14.344 | 6.007 | 19.010 | 56.757 |
| 4 | 8.423 | 22.061 | 67.082 | 4.272 | 9.845 | 24.167 | 3.176 | 7.545 | 19.522 | 8.175 | 25.873 | 77.248 |
| 5 | 10.749 | 28.153 | 85.606 | 5.451 | 12.563 | 30.841 | 4.053 | 9.629 | 24.913 | 10.433 | 33.018 | 98.579 |
| 6 | 13.171 | 34.495 | 104.890 | 6.679 | 15.393 | 37.788 | 4.967 | 11.798 | 30.525 | 12.783 | 40.455 | 120.785 |
| 7 | 15.691 | 41.097 | 124.964 | 7.958 | 18.339 | 45.020 | 5.917 | 14.056 | 36.367 | 15.229 | 48.198 | 143.901 |
| 8 | 18.315 | 47.969 | 145.861 | 9.288 | 21.406 | 52.548 | 6.907 | 16.406 | 42.449 | 17.776 | 56.258 | 167.965 |
| 9 | 21.047 | 55.123 | 167.615 | 10.674 | 24.599 | 60.386 | 7.937 | 18.853 | 48.780 | 20.427 | 64.648 | 193.016 |
| 10 | 23.890 | 62.571 | 190.261 | 12.116 | 27.922 | 68.544 | 9.009 | 21.400 | 55.370 | 23.187 | 73.382 | 219.093 |
| 11 | 26.850 | 70.324 | 213.836 | 13.617 | 31.382 | 77.037 | 10.125 | 24.052 | 62.231 | 26.060 | 82.475 | 246.240 |
| 12 | 29.932 | 78.394 | 238.377 | 15.180 | 34.983 | 85.878 | 11.287 | 26.812 | 69.373 | 29.050 | 91.940 | 274.500 |
| 13 | 33.140 | 86.796 | 263.924 | 16.807 | 38.733 | 95.082 | 12.497 | 29.685 | 76.807 | 32.164 | 101.793 | 303.919 |
| 14 | 36.479 | 95.542 | 290.518 | 18.500 | 42.635 | 104.663 | 13.756 | 32.677 | 84.547 | 35.405 | 112.051 | 334.543 |
| 15 | 39.955 | 104.647 | 318.203 | 20.263 | 46.698 | 114.637 | 15.067 | 35.790 | 92.604 | 38.779 | 122.729 | 366.424 |
| 16 | 43.574 | 114.125 | 347.023 | 22.099 | 50.928 | 125.020 | 16.432 | 39.032 | 100.991 | 42.291 | 133.844 | 399.611 |
| 17 | 47.341 | 123.991 | 377.025 | 24.009 | 55.331 | 135.828 | 17.852 | 42.406 | 109.722 | 45.947 | 145.416 | 434.159 |
| 18 | 51.263 | 134.262 | 408.257 | 25.998 | 59.914 | 147.080 | 19.331 | 45.919 | 118.811 | 49.753 | 157.462 | 470.124 |
| 19 | 55.345 | 144.954 | 440.769 | 28.068 | 64.686 | 158.793 | 20.870 | 49.576 | 128.273 | 53.715 | 170.001 | 507.563 |
| 20 | 59.595 | 156.085 | 474.614 | 30.224 | 69.653 | 170.986 | 22.473 | 53.383 | 138.123 | 57.840 | 183.055 | 546.537 |

The values of EALF as obtained in Tables 6.11, 6.12 and 6.13 are then utilized in the calculation of CESAL of multi-axle trucks, heavy trucks and buses for each case. These are then substituted into equation (6.13) to calculate the CESAL value for each individual year of the 20-year service life of the pavement.

The values presented in Table 6.14 were derived by performing calculations of the CESAL values for each vehicle that was taken into consideration. The calculations for each vehicle are provided in the Appendix. A general trend was observed of the CESAL values being the highest for Case D, followed by A, C, and B respectively.

The graphs showing the increase in CESAL for each of the considered vehicles throughout the design life considering all values of k have been provided below.

a. Yearly CESAL for Bus

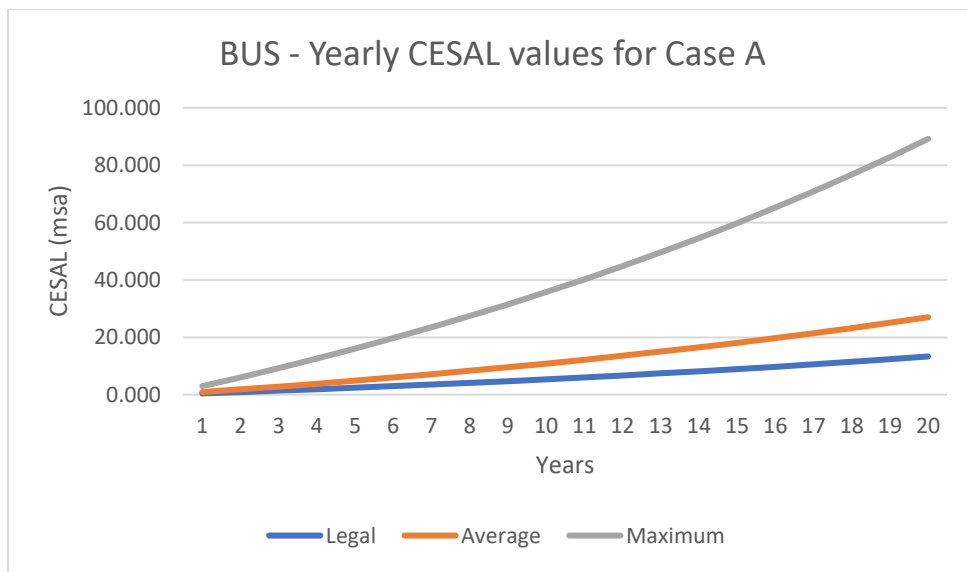


Figure 6.7: Yearly CESAL for Bus (Case A)

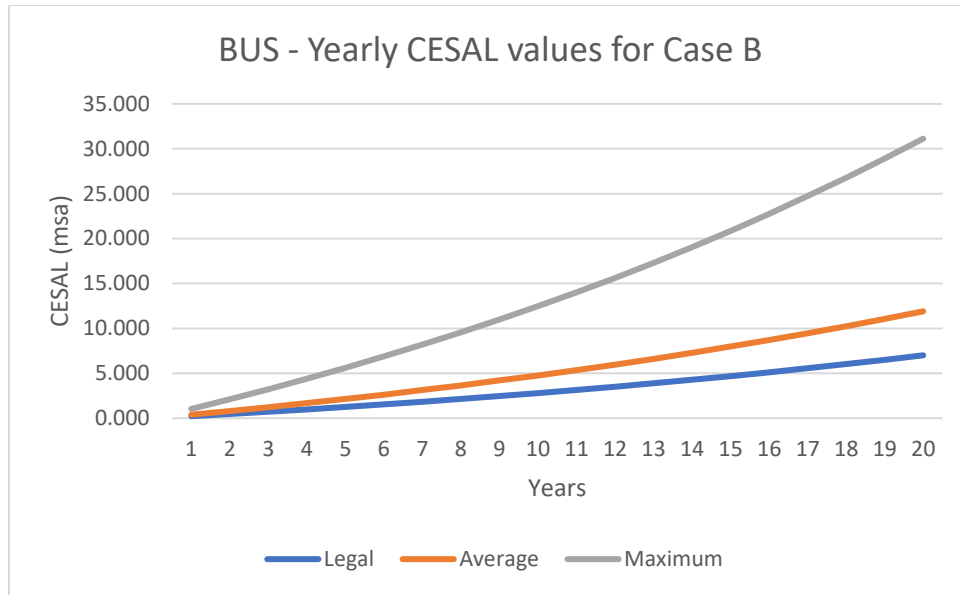


Figure 6.8: Yearly CESAL for Bus (Case B)

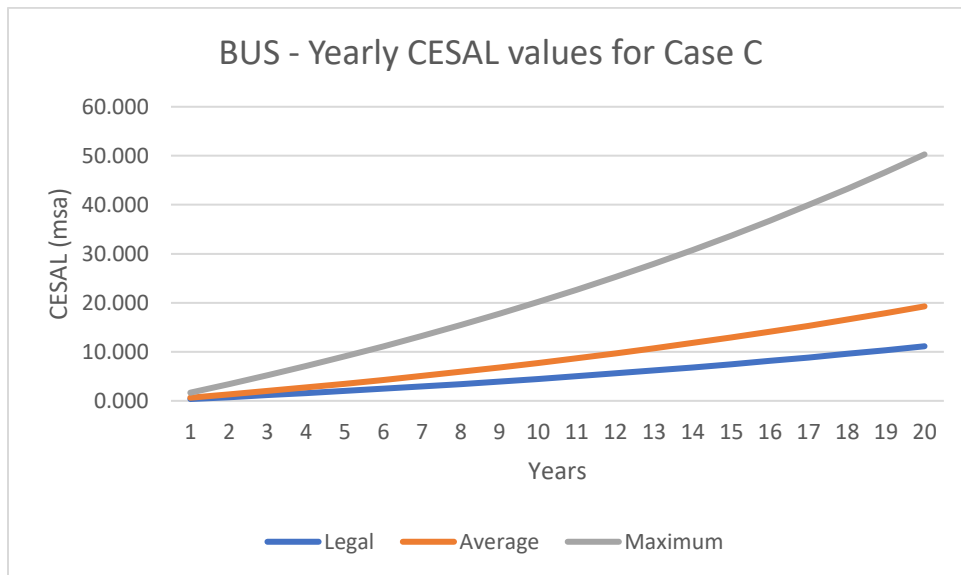


Figure 6.9: Yearly CESAL for Bus (Case C)

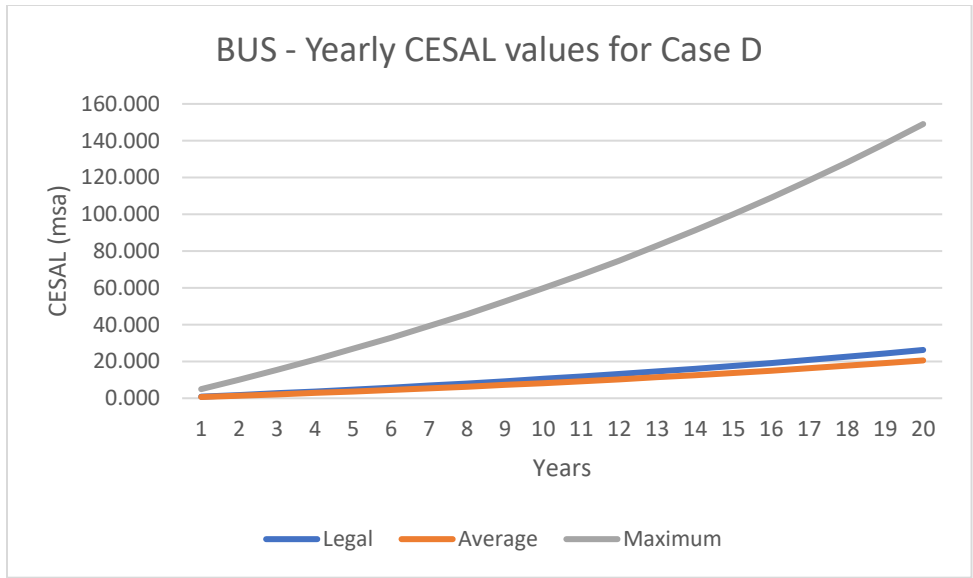


Figure 10 Yearly CESAL Values for Case D

b. Yearly CESAL for Heavy Truck

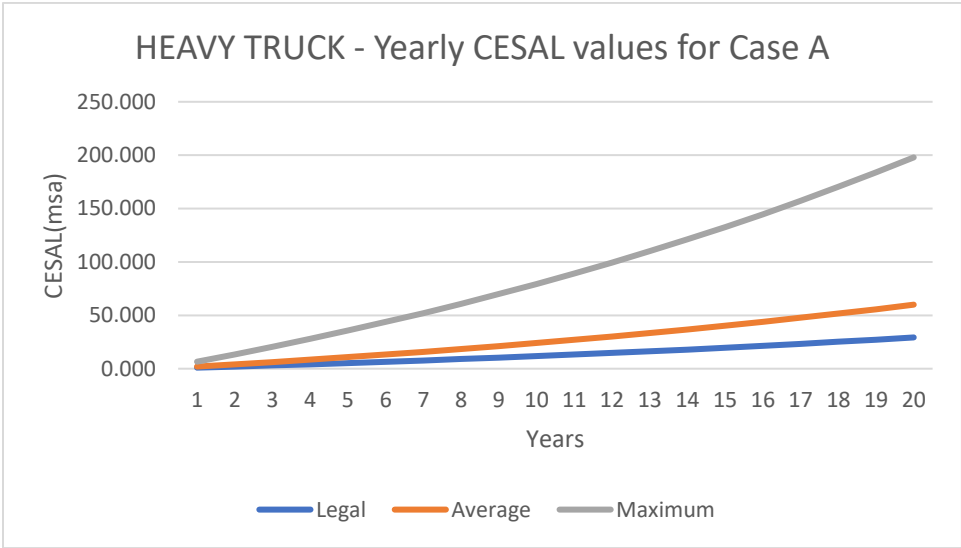


Figure 6.11: Yearly CESAL for heavy truck (Case A)

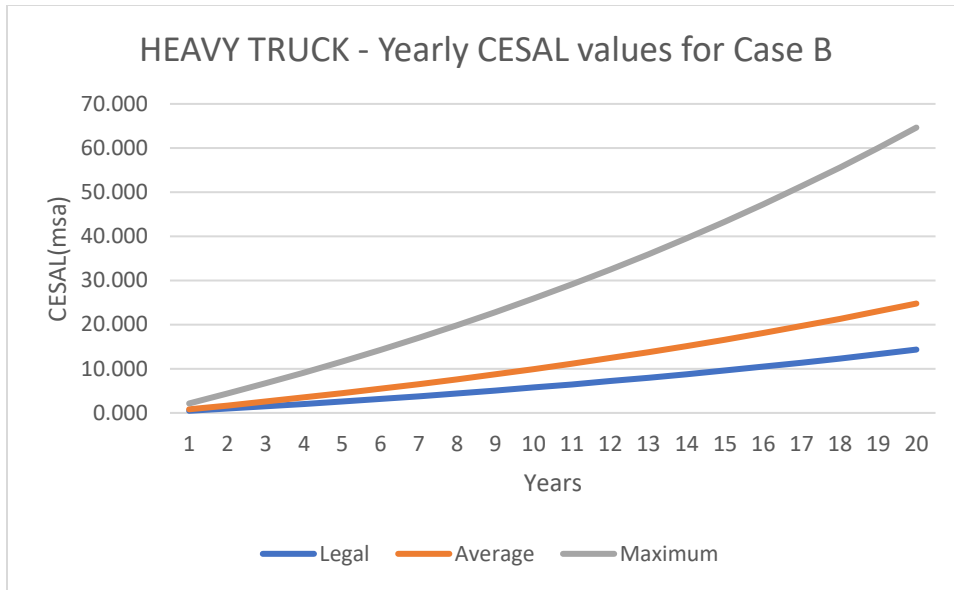


Figure 6.12: Yearly CESAL for Heavy Truck (Case B)

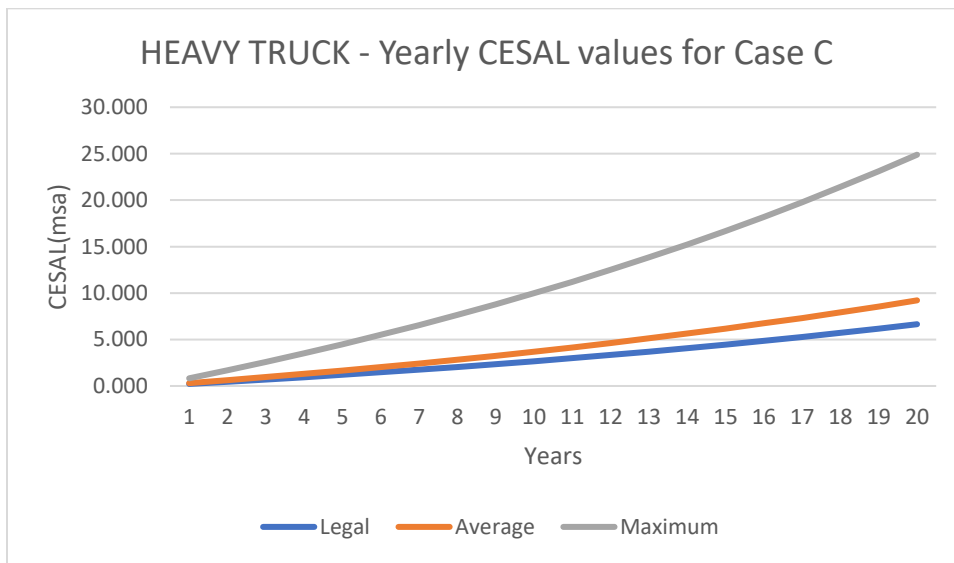


Figure 6.13: Yearly CESAL for Heavy Truck (Case C)

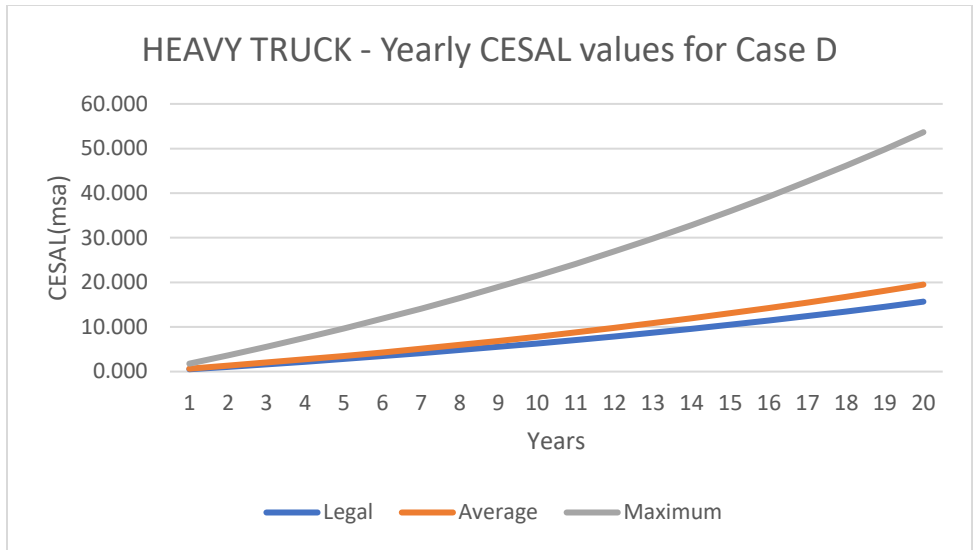


Figure 14: Yearly CESAL for Heavy Truck (Case D)

c. Yearly CESAL for Multi- Axle Truck

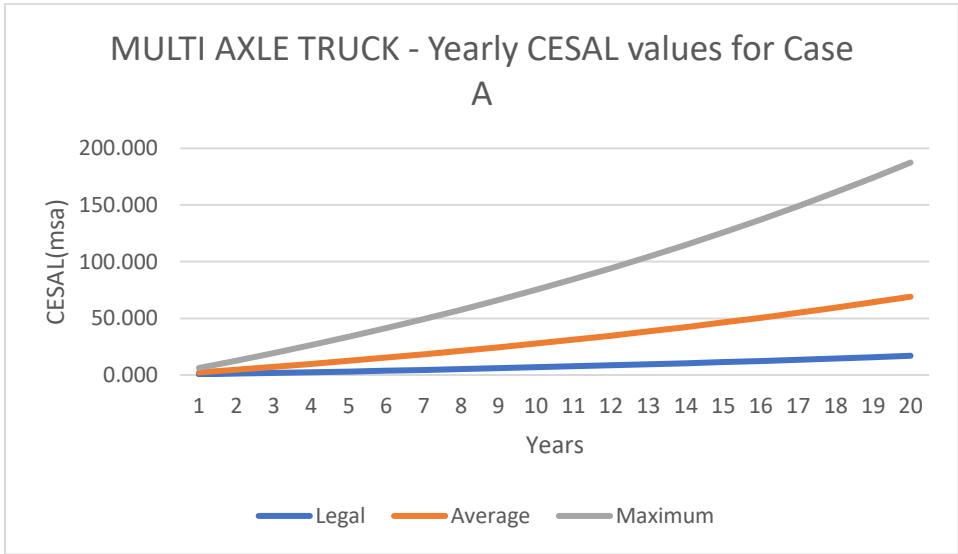


Figure 6.15: Yearly CESAL for Multi-Axle Truck (Case A)

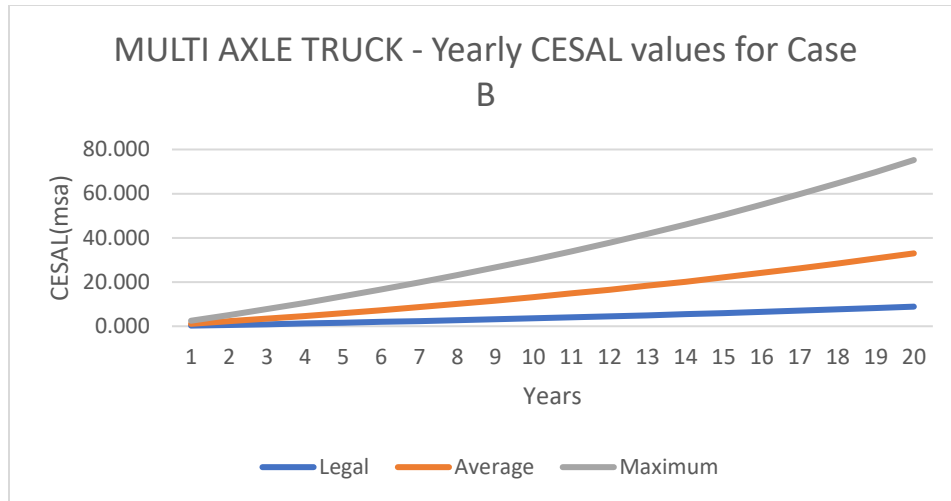


Figure 6.16 Yearly CESAL for Multi-Axle Truck (Case B)

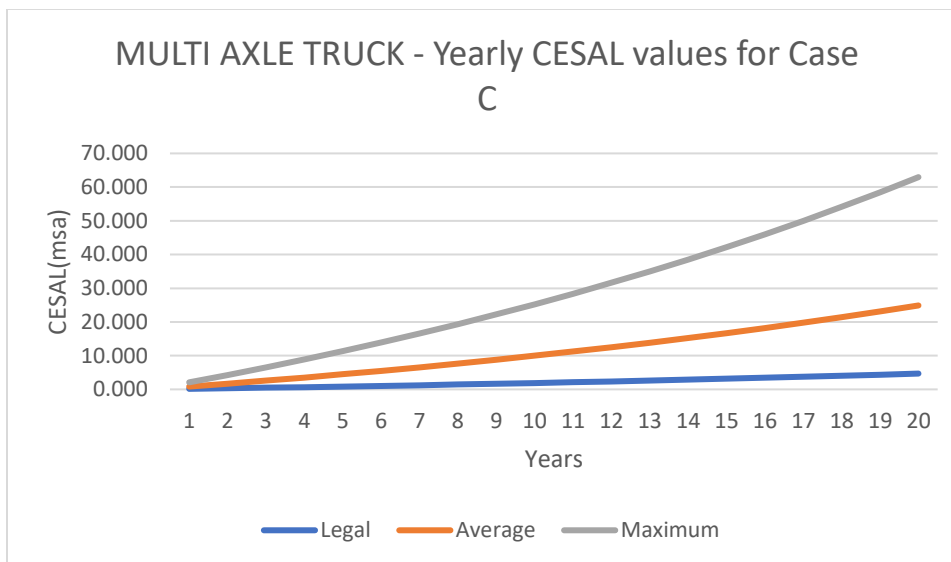


Figure 6.17: Yearly CESAL for Multi-Axle Truck (Case C)

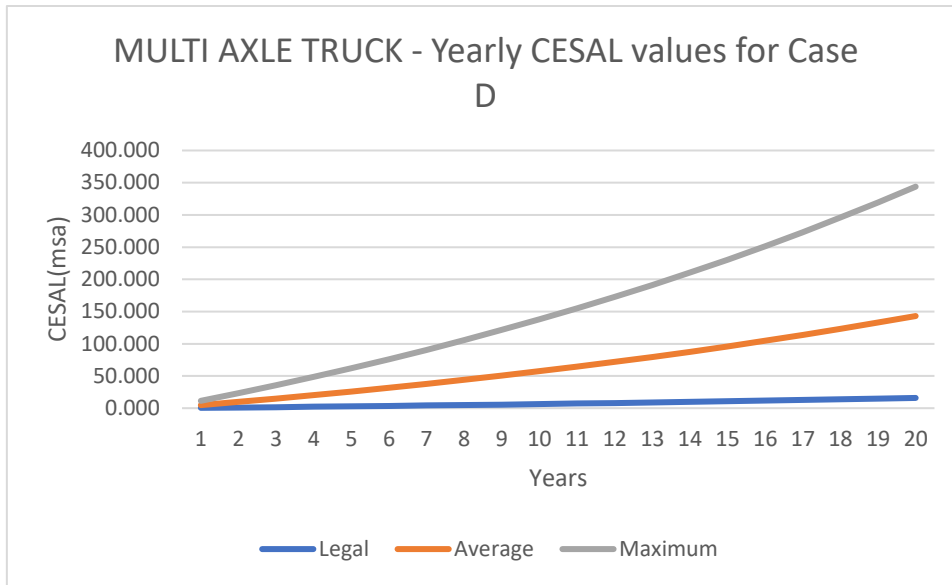


Figure 18: Yearly CESAL for Multi Axle Truck (Case D)

d. Total Yearly CESAL for Considered Vehicles

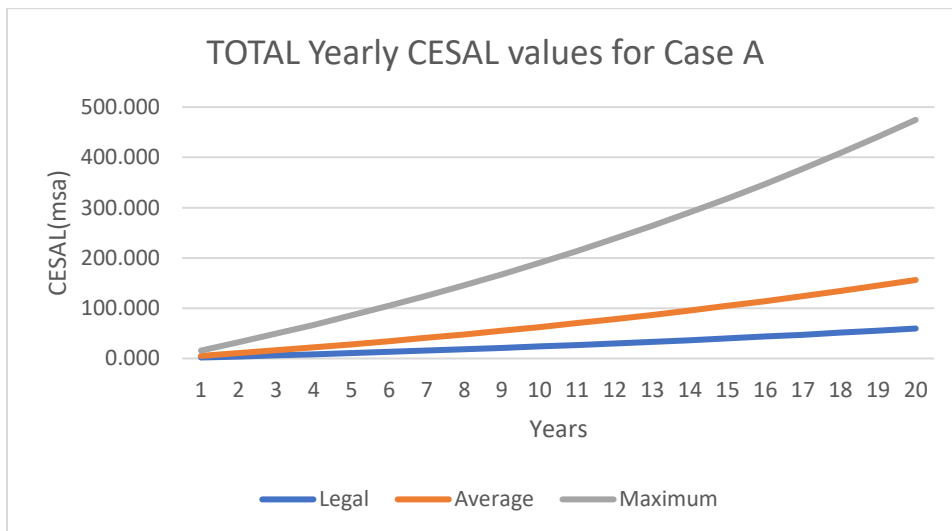


Figure 6.19: Yearly CESAL (Case A)

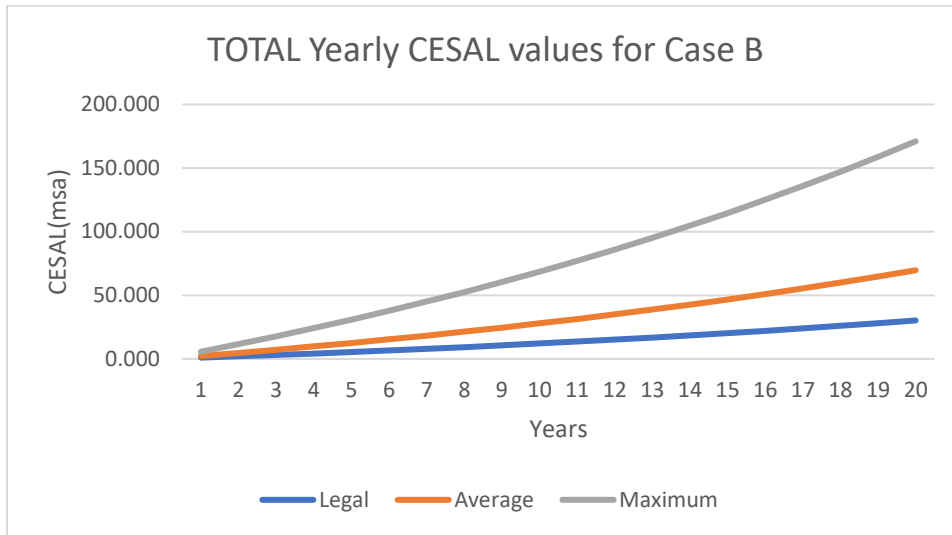


Figure 6.20: Yearly CESAL (Case B)

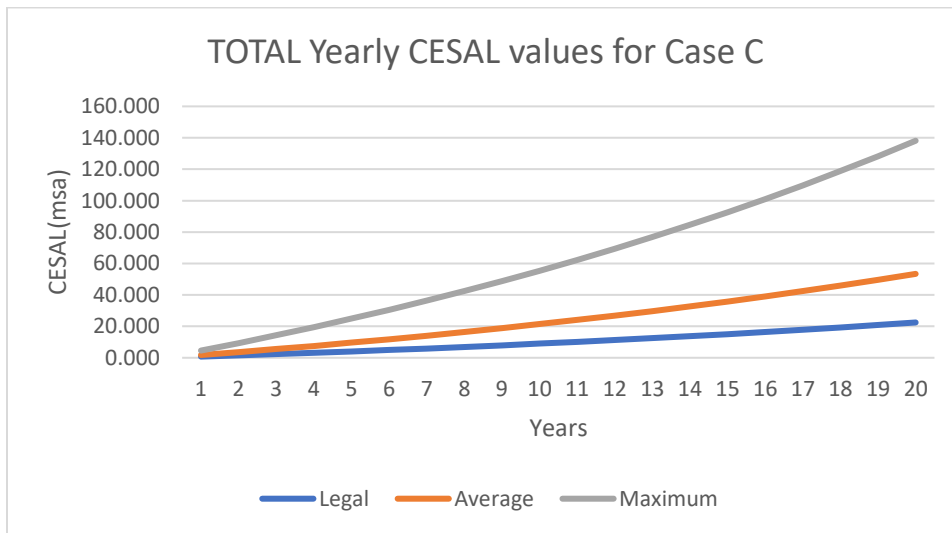


Figure 6.21: Yearly CESAL (Case C)

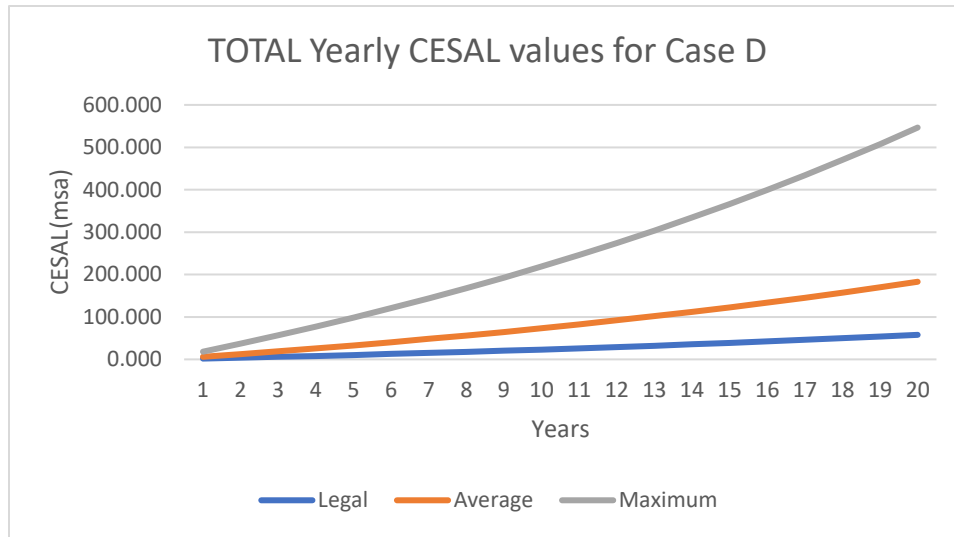


Figure 22: Yearly CESAL (case D)

6.7 Results from Calculation

a. Remaining Service Life

(i) Using the Relation proposed by Jihanny et al. (2018)

Using equation 6.16, the Remaining Service Life in Average and Maximum Loading conditions have been calculated below considering all values of EALF.

(ii) Through Interpolation

The values of CESAL for each year in the design life period has been analysed from Table 6.14 and through linear interpolation, the exact year where the overloaded CESAL values (both average and maximum) reach the standard CESAL value at the end of the design life have been determined and presented below. In many cases, the maximum values do not accurately reflect the typical loadings. As a result, the average overload conditions are considered to be more representative values.

Table 6.15: Reduction in Service life

| Remaining Service Life (RSL) | | | | | | | | |
|--------------------------------------|--------|--------|--------|--------|--------|--------|--------|--------|
| | A | | B | | C | | D | |
| | Avg | Max | Avg | Max | Avg | Max | Avg | Max |
| As per Jihanny et.al. | 7.636 | 2.511 | 8.678 | 3.535 | 8.420 | 3.254 | 6.319 | 2.117 |
| Interpolation | 9.600 | 3.579 | 10.665 | 4.959 | 10.404 | 4.547 | 8.188 | 3.052 |
| Percentage Reduction in Service Life | | | | | | | | |
| As per Jihanny et. al. | 61.819 | 87.443 | 56.608 | 82.324 | 57.902 | 83.730 | 68.403 | 89.417 |
| Interpolation | 52.000 | 82.105 | 46.675 | 75.205 | 47.980 | 77.265 | 59.060 | 84.740 |

b. Change in Asphalt Thickness

For the change in asphalt thickness, we have applied the relationship in equation (6.11), which has also been mentioned below.

The values of a, b, c for various values of stiffness of subgrade have been shown in Table (6.10), our design, however, had a subgrade stiffness value of 62MPa, which hasn't been shown in the table. So, we have interpolated their values for 62 MPa, which are as follows:

$$a = 64.12E-03$$

$$b = 4.451E-03$$

$$c = -6.052$$

These values have been applied for cases A, B and C.

The reason we didn't apply this relationship for case D is to avoid further compounding of errors. Further details have been provided in section 6.5.5.

$$\text{Log}(h) = a + b(\text{log}(N))^2 + \frac{c}{\text{Log}(N)}$$

Using this formula, we can calculate the additional amount of asphalt needed to strengthen the road surface against overloading, which can, in some cases, correspond to an increase in the cost of the road surface due to overloading.

i. For A

Table 6.16: Increased Asphalt thickness for method A

| Year | ASPHALT THICKNESS (in metres) | | | PERCENTAGE INCREASE | |
|------|-------------------------------|---------|---------|---------------------|---------|
| | Legal | Average | Maximum | Average | Maximum |
| 1 | 0.191 | 0.232 | 0.286 | 21.448 | 49.682 |
| 2 | 0.221 | 0.266 | 0.325 | 20.291 | 46.998 |
| 3 | 0.240 | 0.288 | 0.350 | 19.698 | 45.630 |
| 4 | 0.255 | 0.304 | 0.369 | 19.308 | 44.733 |
| 5 | 0.267 | 0.318 | 0.385 | 19.020 | 44.076 |
| 6 | 0.277 | 0.329 | 0.398 | 18.795 | 43.560 |
| 7 | 0.286 | 0.339 | 0.410 | 18.610 | 43.138 |
| 8 | 0.294 | 0.349 | 0.420 | 18.453 | 42.782 |
| 9 | 0.302 | 0.357 | 0.430 | 18.317 | 42.474 |
| 10 | 0.309 | 0.365 | 0.439 | 18.198 | 42.204 |
| 11 | 0.315 | 0.372 | 0.447 | 18.092 | 41.962 |
| 12 | 0.321 | 0.379 | 0.455 | 17.995 | 41.745 |
| 13 | 0.327 | 0.385 | 0.463 | 17.908 | 41.547 |
| 14 | 0.332 | 0.392 | 0.470 | 17.827 | 41.365 |
| 15 | 0.338 | 0.398 | 0.477 | 17.753 | 41.197 |
| 16 | 0.343 | 0.403 | 0.484 | 17.683 | 41.041 |
| 17 | 0.348 | 0.409 | 0.490 | 17.619 | 40.896 |
| 18 | 0.353 | 0.414 | 0.496 | 17.558 | 40.759 |
| 19 | 0.357 | 0.420 | 0.502 | 17.500 | 40.630 |
| 20 | 0.362 | 0.425 | 0.508 | 17.446 | 40.509 |

ii. For B

Table 6.17: Increased Asphalt thickness for Method B

| Year | ASPHALT THICKNESS (in metres) | | | PERCENTAGE INCREASE | |
|------|-------------------------------|---------|---------|---------------------|---------|
| | Legal | Average | Maximum | Average | Maximum |
| 1 | 0.165 | 0.198 | 0.237 | 19.583 | 43.104 |
| 2 | 0.193 | 0.228 | 0.271 | 18.393 | 40.460 |
| 3 | 0.210 | 0.248 | 0.293 | 17.783 | 39.114 |
| 4 | 0.224 | 0.263 | 0.309 | 17.383 | 38.232 |
| 5 | 0.235 | 0.275 | 0.323 | 17.088 | 37.584 |
| 6 | 0.244 | 0.285 | 0.334 | 16.856 | 37.076 |
| 7 | 0.252 | 0.294 | 0.345 | 16.666 | 36.660 |

| Year | ASPHALT THICKNESS (in metres) | | | PERCENTAGE INCREASE | |
|------|-------------------------------|---------|---------|---------------------|---------|
| | Legal | Average | Maximum | Average | Maximum |
| 8 | 0.260 | 0.303 | 0.354 | 16.505 | 36.309 |
| 9 | 0.267 | 0.310 | 0.363 | 16.365 | 36.005 |
| 10 | 0.273 | 0.317 | 0.370 | 16.243 | 35.738 |
| 11 | 0.279 | 0.324 | 0.378 | 16.133 | 35.500 |
| 12 | 0.284 | 0.330 | 0.385 | 16.034 | 35.285 |
| 13 | 0.290 | 0.336 | 0.391 | 15.944 | 35.089 |
| 14 | 0.295 | 0.342 | 0.398 | 15.861 | 34.909 |
| 15 | 0.300 | 0.347 | 0.404 | 15.784 | 34.743 |
| 16 | 0.304 | 0.352 | 0.410 | 15.713 | 34.588 |
| 17 | 0.309 | 0.357 | 0.415 | 15.646 | 34.443 |
| 18 | 0.313 | 0.362 | 0.421 | 15.583 | 34.308 |
| 19 | 0.318 | 0.367 | 0.426 | 15.524 | 34.180 |
| 20 | 0.322 | 0.371 | 0.431 | 15.468 | 34.059 |

(iii) For C

Table 6.18: Increased Asphalt thickness for method C

| Year | ASPHALT THICKNESS (in metres) | | | PERCENTAGE INCREASE | |
|------|-------------------------------|---------|---------|---------------------|---------|
| | Legal | Average | Maximum | Average | Maximum |
| 1 | 0.155 | 0.187 | 0.227 | 20.921 | 46.744 |
| 2 | 0.181 | 0.216 | 0.260 | 19.582 | 43.715 |
| 3 | 0.198 | 0.235 | 0.281 | 18.897 | 42.175 |
| 4 | 0.211 | 0.250 | 0.298 | 18.447 | 41.168 |
| 5 | 0.221 | 0.261 | 0.311 | 18.116 | 40.430 |
| 6 | 0.230 | 0.272 | 0.322 | 17.856 | 39.850 |
| 7 | 0.238 | 0.280 | 0.332 | 17.643 | 39.376 |
| 8 | 0.246 | 0.288 | 0.341 | 17.463 | 38.975 |
| 9 | 0.252 | 0.296 | 0.350 | 17.306 | 38.629 |
| 10 | 0.258 | 0.303 | 0.357 | 17.169 | 38.325 |
| 11 | 0.264 | 0.309 | 0.364 | 17.046 | 38.053 |
| 12 | 0.269 | 0.315 | 0.371 | 16.935 | 37.808 |
| 13 | 0.274 | 0.321 | 0.378 | 16.834 | 37.585 |
| 14 | 0.279 | 0.326 | 0.384 | 16.741 | 37.380 |
| 15 | 0.284 | 0.331 | 0.390 | 16.655 | 37.190 |
| 16 | 0.289 | 0.336 | 0.395 | 16.575 | 37.014 |
| 17 | 0.293 | 0.341 | 0.401 | 16.500 | 36.849 |
| 18 | 0.297 | 0.346 | 0.406 | 16.430 | 36.695 |

| Year | ASPHALT THICKNESS (in metres) | | | PERCENTAGE INCREASE | |
|------|-------------------------------|---------|---------|---------------------|---------|
| | Legal | Average | Maximum | Average | Maximum |
| 19 | 0.301 | 0.351 | 0.411 | 16.363 | 36.549 |
| 20 | 0.305 | 0.355 | 0.416 | 16.300 | 36.411 |

Here we can observe an increase in pavement thickness by 15.428 to 21.448 percent in each of the cases for average overload conditions.

Graphs corresponding to these pavement cost increase have been provided below.

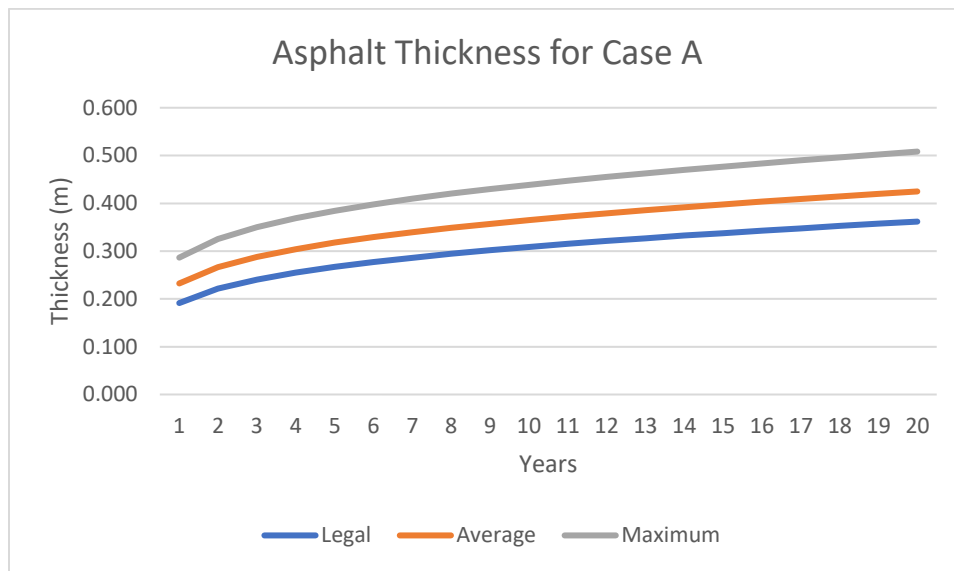


Figure 6.23: Increasing asphalt thickness as increasing year (Case A)

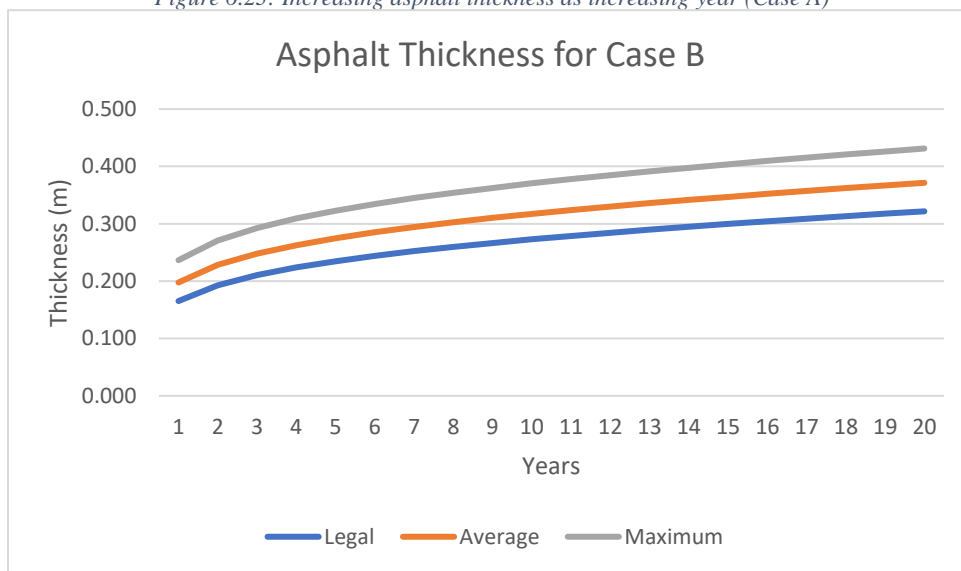


Figure 6.24: Increasing asphalt thickness as increasing year (Case B)

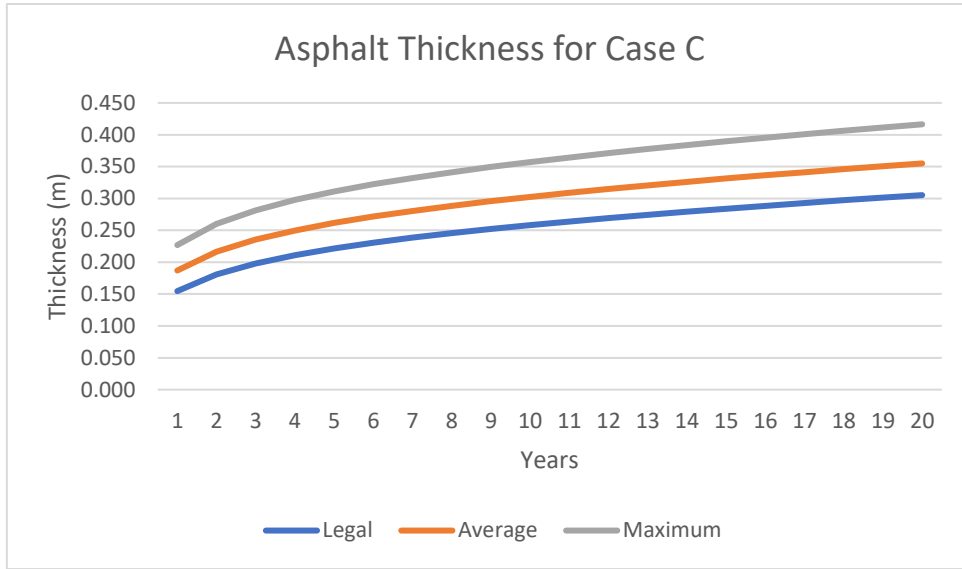


Figure 6.25: Increasing asphalt thickness as increasing year (Case C)

7. CONCLUSION

The quantification of pavement damage with the help of statistical analysis and the study of pavement responses by modelling the pavement in ABAQUS 6.14-5 was done. The pavement used to determine the responses was designed by following the Design Guidelines for Flexible Pavement, DoR, Nepal. The finite element model was validated with the help of IITPAVE. This validated model was then further developed to simulate and obtain the various responses of pavement subjected to vehicular loading under various speeds. The comparison between the linear and viscoelastic material behaviour was also done.

Based on the results obtained from the FE Modelling, the following conclusions can be made;

1. Pavement responses were found to be generally decreasing as the speed increases for the same depth.
2. For the same speed, strain was found to be increasing as the depth increases whereas stresses and displacements were found to be decreasing. Also, the peak values at bottom layers depths were slightly delayed than at upper layers for both models.
3. The response of viscoelastic model is generally found to be higher than that of the linear model except the stresses in lateral directions. The vertical stress was 35% , strain was 45% and displacement was 45% greater in viscoelastic model when compared to linearly elastic.

From our statistical study of pavement damage, we have concluded the following:

1. Due to vehicle overload, the service life of the pavement decreases by approximately 46.675% to 52.000% through interpolation, and by about 56.608% to 61.819% as per the method suggested by Jihanny et. al.
2. For our designed pavement, service life decreases by 59.060% through interpolation and 68.403% as per Jihanny et. al.
3. Due to vehicle overload, we can observe than an extra 15.468% to 21.448% thickness of asphalt overlay is required to sustain the oncoming vehicular loads.
4. While the values of CESAL obtained from various methods vary by a lot, they return similar values in terms of remaining service life and extra overlay thickness.

8. RECOMMENDATION

This study can be seen as a basis for further works in this field. The recommendations for future works based on this project are as follows:

1. To update this study, primary data should be collected and experiments should be conducted to represent the pavement more accurately.
2. To analyse and design the pavement for different traffic conditions, this study should be compared with other methods such which include mechanistic, AASTHO, Road Note 29, CBR, and empirical methods.

To reduce vehicle overloading in Nepal, the following measures should be implemented:

- Weight limits need to be enforced and overloaded vehicles should be fined.
- Awareness should be raised among vehicle owners, drivers, and the public about the negative impacts of overloading.
- Vehicle maintenance and regular inspections should be encouraged.
- Technology-based solutions such as WIM and ANPR should be used to identify and act against overloaded vehicles.
- Road infrastructure should be upgraded to enhance quality and safety.

REFERENCES

- Al-Qadi, I. L., Ozer, H., & Demir, F. (2008). Pavement response and performance evaluation using advanced modeling approaches. *International Journal of Pavement Engineering*, 9(3), 159-173. doi:10.1080/10298430802066603
- Amorim, S. I. R., et al. (2015). A model for equivalent axle load factors. *International Journal of Pavement Engineering*, 16(10), 881–893.
- Ban, B., Shrestha, J.K., Pradhananga, R., & Shrestha, K. C. (2021). Three-Dimensional Elastic Analysis of Flexible Pavement under Static Vehicular Load. *Proceedings of 10th IOE Graduate Conference*
- Beskyroun, S., & Masson, J. F. (2005). Dynamic analysis and in situ validation of perpetual pavement response to vehicular loading. *Journal of Transportation Engineering*, 131(7), 532-541. doi:10.1061/(ASCE)0733-947X(2005)131:7(532)
- Daba, E. M., & Wakshum, D. T. (2017). Analysis of Stress, Strain, and Deflection of Flexible Pavements Using Finite Element Method: Case Study on Bako-Nekemte Road. *Journal of Traffic and Transportation Engineering (English Edition)*, 4(3), 226-234. doi:10.1016/j.jtte.2017.04.002
- Department of Roads (DOR), Ministry of Physical Infrastructure and Transport, Government of Nepal. (2019). Design Guidelines for Flexible Pavements in Nepal. Retrieved from <http://www.dor.gov.np/uploads/document/1603377985.pdf>
- Department of Roads (DOR). (2015). Preparatory survey for Nagdhunga tunnel construction in Nepal final report March 2015.
- Ghadimi, B. (2015). Dynamic simulation of a flexible pavement layers considering shakedown effects and soil-asphalt interaction. *International Journal of Pavement Research and Technology*, 8(5), 364-374. doi: 10.1016/j.ijprt.2015.08.001
- Gungor, A., Ozer, H., & Akin, M.(2016). Development of a finite element model for three-dimensional analysis of flexible pavement responses. *Journal of Materials in Civil Engineering*, 28(2),04015143. doi: 10
- Huang, Y. H. (1993). *Pavement Analysis and Design* (2nd ed.). Prentice Hall.

Jihanny, J., Subagio, B. S., & Hariyadi, E. S. (2018). The analysis of overloaded trucks in Indonesia based on weight in motion data (East of Sumatera National Road Case Study). Department of Civil Engineering Institute Technology Bandung.

Khan, R., Khan, A., Khan, M. T., Ali, I., Alam, B., & Wali, B. (2018). Impact of axle overload, asphalt pavement thickness and subgrade modulus on load equivalency factor using modified ESALs equation. National Institute of Technology, Jamshedpur, India.

Li, S., Zhang, C., Chen, S., & Shen, S. (2016). Analysis of temperature and load characteristics of asphalt pavement structure using finite element method. *Advances in Materials Science and Engineering*, 2016, 3203172. doi: 10.1155/2016/3203172

Liu, Y., Luo, X., & Zhang, W. (2017). Evaluation of Tire-Pavement Contact Stress Distribution of Pavement Response and Some Effects on the Flexible Pavements. *Journal of Applied Mathematics*, 2017, 1-10. doi: 10.1155/2017/8462918

Looney, J. L., & Lytton, R. L. (1981). A finite element model for analysis of flexible pavements. *Transportation Research Record*, (829), 68-76.

Mohammadi and Shah (1992). Statistical evaluation of truck overloads.

Ojha, K.N. (2019). Flexible pavement thickness: A comparative study between standard and overloading condition.

Pais, J.C., & Pereira, P. (2016). The Effect of Traffic Overloads on Road Pavements. In *Proceedings of the Eighth International Conference on Maintenance and Rehabilitation of Pavements* (pp. 456-465). doi: 10.3850/978-981-11-0449-7-046-cd.

Pais, J. C., Figueiras, H., Pereira, P., & Kaloush, K. (2018). The pavements cost due to traffic overloads. *International Journal of Pavement Engineering*, 1(10), 1-11.

Podborochynski, D. (2001). Quantifying incremental pavement damage caused by overweight trucks. PSI Technologies Inc., Canada.

Rashid, M., Li, H., & Yu, J. (2011). Effect of aggregate gradation on rutting of asphalt pavements. *Road Materials and Pavement Design*, 12(3), 613-624. doi: 10.1080/14680629.2011.565767

Wang, H., Zhao, J., & Wang, Z. (2014). Impact of overweight traffic on pavement life using weigh in motion data and mechanistic empirical pavement analysis. Department of Transportation, New Jersey.

Wang, X., Zhang, S., & Xue, Y. (2014). Laboratory evaluation of moisture damage resistance of asphalt mixtures containing cementitious fillers. *Road Materials and Pavement Design*, 15(sup1), 260-273. doi: 10.1080/14680629.2014.990402

Wang, Y., Lu, Y. J., Si, C. D., & Sun, T. C. (2009). Finite element analysis for rutting prediction of asphalt concrete pavement under moving wheel load. *Journal of Zhejiang University SCIENCE A*, 10(6), 836-843. doi: 10.1631/jzus.A0820401

You, L., Wu, S., Xiao, F., & Wei, P. (2014). Effect of compaction temperature on volumetric and mechanical properties of asphalt mixtures with high RAP content. *Road Materials and Pavement Design*, 15(sup2), 338-350. doi:10.1080/14680629.2014.993195

Zaghloul, S., & White, T. (1994). Use of a three-dimensional, dynamic finite element program for analysis of flexible pavement. *Transportation Research Record*, (1432), 8-16.

ANNEX

A. Values of Axle Load Axle for Different Vehicles from Axle Load Survey

1. For Heavy Bus

| 1ST AXLE WESTWARDS | | |
|--------------------|--------------|--------------|
| Weight (x) | Frequency(f) | fx |
| 5 | 34 | 170 |
| 7 | 1 | 7 |
| | 35 | 177 |
| MEAN | 5.06 | 47.17 |
| MAXIMUM | 8 | 78.45 |

| 1ST AXLE EASTWARDS | | |
|--------------------|--------------|--------------|
| Weight (x) | Frequency(f) | fx |
| 5 | 44 | 220 |
| 6 | 1 | 6 |
| 7 | 2 | 14 |
| | 47 | 240 |
| MEAN | 5.11 | 50.11 |
| MAXIMUM | 10 | 98.07 |

| 2ND AXLE WESTWARDS | | |
|--------------------|--------------|---------------|
| Weight (x) | Frequency(f) | fx |
| 8 | 1 | 8 |
| 9 | 4 | 36 |
| 10 | 29 | 290 |
| 14 | 1 | 14 |
| | 35 | 348 |
| MEAN | 9.94 | 80.32 |
| MAXIMUM | 14 | 137.29 |

| 2ND AXLE EASTWARDS | | |
|--------------------|--------------|--------------|
| Weight (x) | Frequency(f) | fx |
| 8 | 1 | 8 |
| 9 | 6 | 54 |
| 10 | 38 | 380 |
| 12 | 1 | 12 |
| 14 | 1 | 14 |
| | 47 | 468 |
| MEAN | 9.96 | 97.67 |
| MAXIMUM | 15 | 147.1 |

2. For Heavy Truck

| 1ST AXLE WESTWARDS | | |
|--------------------|--------------|--------------|
| Weight (x) | Frequency(f) | fx |
| 1 | 27 | 27 |
| 2 | 6 | 12 |
| 3 | 12 | 36 |
| 4 | 9 | 36 |
| 5 | 2 | 10 |
| 6 | 1 | 6 |
| 7 | 11 | 77 |
| | 68 | 204 |
| MEAN | 3 | 29.42 |
| MAXIMUM | 7 | 68.65 |

| 2ND AXLE EASTWARDS | | |
|--------------------|--------------|--------------|
| Weight (x) | Frequency(f) | fx |
| 4 | 2 | 8 |
| 5 | 16 | 80 |
| 6 | 4 | 24 |
| 7 | 25 | 175 |
| 8 | 2 | 16 |
| | 49 | 303 |
| MEAN | 6.18 | 60.61 |
| MAXIMUM | 8 | 78.45 |

| TANDEM AXLE WESTWARDS | | |
|------------------------------|---------------------|---------------|
| Weight (x) | Frequency(f) | fx |
| 2 | 3 | 6 |
| 3 | 6 | 18 |
| 4 | 15 | 60 |
| 5 | 12 | 60 |
| 6 | 9 | 54 |
| 7 | 3 | 21 |
| 8 | 6 | 48 |
| 9 | 2 | 18 |
| 11 | 1 | 11 |
| 12 | 3 | 36 |
| 13 | 2 | 26 |
| 14 | 6 | 84 |
| | 68 | 442 |
| MEAN | 6.5 | 63.74 |
| MAXIMUM | 14 | 137.29 |

| TANDEM AXLE EASTWARDS | | |
|------------------------------|---------------------|---------------|
| Weight (x) | Frequency(f) | fx |
| 6 | 2 | 12 |
| 9 | 5 | 45 |
| 10 | 4 | 40 |
| 11 | 8 | 88 |
| 12 | 8 | 96 |
| 13 | 12 | 156 |
| 14 | 8 | 112 |
| 15 | 2 | 30 |
| | 49 | 579 |
| MEAN | 11.82 | 115.91 |
| MAXIMUM | 15 | 147.1 |

3. Multi-Axle Truck

| 1ST AXLE WESTWARDS | | |
|---------------------------|---------------------|--------------|
| Weight (x) | Frequency(f) | fx |
| 1 | 3 | 3 |
| 3 | 9 | 27 |
| 5 | 12 | 60 |
| 6 | 4 | 24 |
| 7 | 8 | 56 |
| 8 | 1 | 8 |
| | 37 | 178 |
| MEAN | 4.81 | 47.17 |
| MAXIMUM | 8 | 78.45 |

| 1ST AXLE EASTWARDS | | |
|---------------------------|---------------------|--------------|
| Weight (x) | Frequency(f) | fx |
| 5 | 3 | 15 |
| 6 | 1 | 6 |
| 7 | 68 | 476 |
| 8 | 9 | 72 |
| 9 | 2 | 18 |
| 10 | 1 | 10 |
| | 84 | 597 |
| MEAN | 7.11 | 69.73 |
| MAXIMUM | 10 | 98.07 |

| 2ND AXLE WESTWARDS | | |
|--------------------|--------------|---------------|
| Weight (x) | Frequency(f) | fx |
| 5 | 3 | 15 |
| 6 | 6 | 36 |
| 7 | 10 | 70 |
| 8 | 9 | 72 |
| 10 | 1 | 10 |
| 11 | 1 | 11 |
| 12 | 4 | 48 |
| 13 | 1 | 13 |
| 14 | 2 | 28 |
| | 37 | 303 |
| MEAN | 8.19 | 80.32 |
| MAXIMUM | 14 | 137.29 |

| 2ND AXLE EASTWARDS | | |
|--------------------|--------------|---------------|
| Weight (x) | Frequency(f) | fx |
| 7 | 4 | 28 |
| 8 | 1 | 8 |
| 10 | 4 | 40 |
| 11 | 17 | 187 |
| 12 | 16 | 192 |
| 13 | 15 | 195 |
| 14 | 25 | 350 |
| 15 | 2 | 30 |
| | 84 | 1030 |
| MEAN | 12.26 | 120.23 |
| MAXIMUM | 15 | 147.1 |

| TANDEM AXLE WESTWARDS | | |
|-----------------------|--------------|---------------|
| Weight (x) | Frequency(f) | fx |
| 5 | 6 | 30 |
| 6 | 10 | 60 |
| 8 | 5 | 40 |
| 11 | 3 | 33 |
| 12 | 8 | 96 |
| 13 | 4 | 52 |
| 14 | 1 | 14 |
| | 37 | 325 |
| MEAN | 8.78 | 86.1 |
| MAXIMUM | 14 | 137.29 |

| TANDEM AXLE EASTWARDS | | |
|-----------------------|--------------|--------------|
| Weight (x) | Frequency(f) | fx |
| 7 | 2 | 14 |
| 11 | 9 | 99 |
| 12 | 39 | 468 |
| 13 | 15 | 195 |
| 14 | 16 | 224 |
| 15 | 2 | 30 |
| | 83 | 1030 |
| MEAN | 12.41 | 121.7 |
| MAXIMUM | 15 | 147.1 |

B. CESAL values for each axle of each considered vehicle

All CESAL values in the table are expressed in multiples of million.

Table B.1 Calculation of CESAL for Heavy Bus

| Year | Growth Factor | CESAL (msa) | | | | | | | | | | | |
|--------|---------------|-------------|---------|---------|-------|---------|---------|--------|---------|---------|--------|---------|---------|
| | | A | | | B | | | C | | | D | | |
| | | Legal | Average | Maximum | Legal | Average | Maximum | Legal | Average | Maximum | Legal | Average | Maximum |
| 1.000 | 1.000 | 0.442 | 0.897 | 2.964 | 0.233 | 0.396 | 1.035 | 0.370 | 0.641 | 1.671 | 0.873 | 0.683 | 4.953 |
| 2.000 | 2.041 | 0.903 | 1.831 | 6.050 | 0.475 | 0.807 | 2.112 | 0.755 | 1.308 | 3.410 | 1.781 | 1.394 | 10.110 |
| 3.000 | 3.125 | 1.382 | 2.803 | 9.262 | 0.728 | 1.236 | 3.233 | 1.157 | 2.002 | 5.221 | 2.726 | 2.135 | 15.478 |
| 4.000 | 4.253 | 1.881 | 3.815 | 12.606 | 0.990 | 1.682 | 4.400 | 1.574 | 2.724 | 7.106 | 3.711 | 2.905 | 21.066 |
| 5.000 | 5.427 | 2.400 | 4.868 | 16.087 | 1.264 | 2.147 | 5.615 | 2.009 | 3.477 | 9.068 | 4.735 | 3.708 | 26.883 |
| 6.000 | 6.650 | 2.941 | 5.965 | 19.711 | 1.548 | 2.631 | 6.880 | 2.461 | 4.260 | 11.111 | 5.802 | 4.543 | 32.938 |
| 7.000 | 7.922 | 3.504 | 7.107 | 23.483 | 1.845 | 3.134 | 8.196 | 2.932 | 5.075 | 13.237 | 6.913 | 5.412 | 39.242 |
| 8.000 | 9.247 | 4.090 | 8.295 | 27.410 | 2.153 | 3.658 | 9.567 | 3.423 | 5.924 | 15.451 | 8.069 | 6.317 | 45.805 |
| 9.000 | 10.626 | 4.700 | 9.532 | 31.498 | 2.474 | 4.204 | 10.994 | 3.933 | 6.808 | 17.755 | 9.272 | 7.259 | 52.636 |
| 10.000 | 12.062 | 5.335 | 10.820 | 35.754 | 2.809 | 4.772 | 12.479 | 4.465 | 7.727 | 20.154 | 10.525 | 8.240 | 59.748 |
| 11.000 | 13.556 | 5.996 | 12.161 | 40.184 | 3.157 | 5.363 | 14.025 | 5.018 | 8.685 | 22.651 | 11.829 | 9.261 | 67.151 |
| 12.000 | 15.112 | 6.684 | 13.556 | 44.796 | 3.519 | 5.978 | 15.635 | 5.594 | 9.681 | 25.251 | 13.186 | 10.324 | 74.857 |
| 13.000 | 16.732 | 7.400 | 15.009 | 49.597 | 3.896 | 6.619 | 17.311 | 6.193 | 10.719 | 27.957 | 14.599 | 11.430 | 82.880 |
| 14.000 | 18.418 | 8.146 | 16.522 | 54.595 | 4.289 | 7.286 | 19.055 | 6.817 | 11.799 | 30.774 | 16.070 | 12.582 | 91.231 |
| 15.000 | 20.173 | 8.922 | 18.096 | 59.797 | 4.697 | 7.980 | 20.871 | 7.467 | 12.924 | 33.707 | 17.602 | 13.781 | 99.925 |
| 16.000 | 22.000 | 9.731 | 19.735 | 65.213 | 5.123 | 8.703 | 22.761 | 8.143 | 14.094 | 36.760 | 19.196 | 15.029 | 108.975 |
| 17.000 | 23.902 | 10.572 | 21.441 | 70.851 | 5.566 | 9.455 | 24.729 | 8.847 | 15.312 | 39.938 | 20.856 | 16.329 | 118.397 |
| 18.000 | 25.882 | 11.448 | 23.218 | 76.720 | 6.027 | 10.239 | 26.778 | 9.580 | 16.581 | 43.246 | 22.583 | 17.681 | 128.204 |
| 19.000 | 27.943 | 12.359 | 25.066 | 82.830 | 6.507 | 11.054 | 28.910 | 10.343 | 17.901 | 46.690 | 24.382 | 19.089 | 138.414 |
| 20.000 | 30.089 | 13.308 | 26.991 | 89.190 | 7.006 | 11.903 | 31.130 | 11.137 | 19.276 | 50.276 | 26.254 | 20.555 | 149.043 |

Table B.2 Calculation of CESAL for Heavy Truck

| Year | Estimated Traffic | CESAL (msa) | | | | | | | | | | | |
|--------|-------------------|-------------|---------|---------|--------|---------|---------|-------|---------|---------|--------|---------|---------|
| | | A | | | B | | | C | | | D | | |
| | | Legal | Average | Maximum | Legal | Average | Maximum | Legal | Average | Maximum | Legal | Average | Maximum |
| 1.000 | 1.000 | 0.973 | 1.993 | 6.578 | 0.477 | 0.823 | 2.148 | 0.221 | 0.306 | 0.827 | 0.521 | 0.648 | 1.783 |
| 2.000 | 2.041 | 1.987 | 4.068 | 13.425 | 0.973 | 1.680 | 4.384 | 0.451 | 0.625 | 1.688 | 1.064 | 1.322 | 3.640 |
| 3.000 | 3.125 | 3.041 | 6.228 | 20.553 | 1.490 | 2.572 | 6.712 | 0.690 | 0.957 | 2.584 | 1.628 | 2.024 | 5.573 |
| 4.000 | 4.253 | 4.139 | 8.477 | 27.973 | 2.028 | 3.501 | 9.136 | 0.940 | 1.302 | 3.518 | 2.216 | 2.755 | 7.584 |
| 5.000 | 5.427 | 5.282 | 10.817 | 35.698 | 2.588 | 4.468 | 11.658 | 1.199 | 1.662 | 4.489 | 2.828 | 3.516 | 9.679 |
| 6.000 | 6.650 | 6.472 | 13.254 | 43.739 | 3.171 | 5.474 | 14.284 | 1.469 | 2.036 | 5.500 | 3.465 | 4.308 | 11.859 |
| 7.000 | 7.922 | 7.711 | 15.791 | 52.110 | 3.778 | 6.522 | 17.018 | 1.750 | 2.426 | 6.553 | 4.128 | 5.132 | 14.129 |
| 8.000 | 9.247 | 9.001 | 18.431 | 60.824 | 4.409 | 7.613 | 19.864 | 2.043 | 2.832 | 7.649 | 4.819 | 5.990 | 16.491 |
| 9.000 | 10.626 | 10.343 | 21.180 | 69.895 | 5.067 | 8.748 | 22.827 | 2.348 | 3.254 | 8.789 | 5.537 | 6.884 | 18.951 |
| 10.000 | 12.062 | 11.740 | 24.042 | 79.338 | 5.751 | 9.930 | 25.911 | 2.665 | 3.694 | 9.977 | 6.285 | 7.814 | 21.511 |
| 11.000 | 13.556 | 13.195 | 27.020 | 89.169 | 6.464 | 11.161 | 29.121 | 2.995 | 4.151 | 11.213 | 7.064 | 8.782 | 24.177 |
| 12.000 | 15.112 | 14.709 | 30.121 | 99.402 | 7.206 | 12.441 | 32.463 | 3.339 | 4.628 | 12.500 | 7.875 | 9.790 | 26.951 |
| 13.000 | 16.732 | 16.286 | 33.350 | 110.055 | 7.978 | 13.775 | 35.942 | 3.697 | 5.124 | 13.839 | 8.719 | 10.839 | 29.840 |
| 14.000 | 18.418 | 17.927 | 36.710 | 121.145 | 8.782 | 15.163 | 39.564 | 4.069 | 5.640 | 15.234 | 9.597 | 11.931 | 32.846 |
| 15.000 | 20.173 | 19.635 | 40.208 | 132.690 | 9.619 | 16.608 | 43.334 | 4.457 | 6.178 | 16.686 | 10.512 | 13.068 | 35.977 |
| 16.000 | 22.000 | 21.414 | 43.850 | 144.708 | 10.490 | 18.112 | 47.259 | 4.861 | 6.737 | 18.197 | 11.464 | 14.252 | 39.235 |
| 17.000 | 23.902 | 23.265 | 47.641 | 157.218 | 11.397 | 19.678 | 51.345 | 5.281 | 7.320 | 19.770 | 12.455 | 15.484 | 42.627 |
| 18.000 | 25.882 | 25.192 | 51.588 | 170.242 | 12.341 | 21.308 | 55.598 | 5.719 | 7.926 | 21.408 | 13.487 | 16.767 | 46.158 |
| 19.000 | 27.943 | 27.198 | 55.696 | 183.799 | 13.324 | 23.005 | 60.026 | 6.174 | 8.557 | 23.113 | 14.561 | 18.102 | 49.834 |
| 20.000 | 30.089 | 29.287 | 59.973 | 197.913 | 14.347 | 24.771 | 64.635 | 6.648 | 9.214 | 24.887 | 15.679 | 19.492 | 53.661 |

Table B.3 Calculation of CESAL for Multi Axle Truck

| Year | Estimated Traffic | CESAL (msa) | | | | | | | | | | | |
|------|-------------------|-------------|---------|---------|-------|---------|---------|-------|---------|---------|--------|---------|---------|
| | | A | | | B | | | C | | | D | | |
| | | Legal | Average | Maximum | Legal | Average | Maximum | Legal | Average | Maximum | Legal | Average | Maximum |
| 1 | 1.000 | 0.565 | 2.297 | 6.232 | 0.295 | 1.096 | 2.500 | 0.156 | 0.827 | 2.092 | 0.529 | 4.753 | 11.427 |
| 2 | 2.041 | 1.153 | 4.689 | 12.719 | 0.602 | 2.237 | 5.102 | 0.318 | 1.689 | 4.271 | 1.079 | 9.701 | 23.323 |
| 3 | 3.125 | 1.765 | 7.178 | 19.473 | 0.921 | 3.425 | 7.812 | 0.487 | 2.585 | 6.538 | 1.652 | 14.851 | 35.706 |
| 4 | 4.253 | 2.403 | 9.770 | 26.503 | 1.254 | 4.661 | 10.632 | 0.663 | 3.518 | 8.899 | 2.248 | 20.213 | 48.598 |
| 5 | 5.427 | 3.066 | 12.467 | 33.822 | 1.600 | 5.948 | 13.568 | 0.846 | 4.490 | 11.356 | 2.869 | 25.794 | 62.017 |
| 6 | 6.650 | 3.757 | 15.276 | 41.440 | 1.960 | 7.288 | 16.624 | 1.036 | 5.501 | 13.914 | 3.515 | 31.605 | 75.987 |
| 7 | 7.922 | 4.476 | 18.199 | 49.371 | 2.335 | 8.683 | 19.805 | 1.234 | 6.554 | 16.577 | 4.188 | 37.654 | 90.530 |
| 8 | 9.247 | 5.225 | 21.243 | 57.627 | 2.726 | 10.135 | 23.117 | 1.441 | 7.650 | 19.349 | 4.889 | 43.950 | 105.669 |
| 9 | 10.626 | 6.004 | 24.411 | 66.222 | 3.133 | 11.647 | 26.565 | 1.656 | 8.791 | 22.235 | 5.618 | 50.505 | 121.429 |
| 10 | 12.062 | 6.815 | 27.709 | 75.169 | 3.556 | 13.220 | 30.154 | 1.879 | 9.979 | 25.239 | 6.377 | 57.329 | 137.834 |
| 11 | 13.556 | 7.659 | 31.142 | 84.483 | 3.996 | 14.858 | 33.891 | 2.112 | 11.215 | 28.366 | 7.167 | 64.432 | 154.913 |
| 12 | 15.112 | 8.538 | 34.716 | 94.178 | 4.455 | 16.564 | 37.780 | 2.355 | 12.502 | 31.622 | 7.989 | 71.826 | 172.692 |
| 13 | 16.732 | 9.453 | 38.437 | 104.272 | 4.933 | 18.339 | 41.829 | 2.607 | 13.842 | 35.011 | 8.846 | 79.524 | 191.199 |
| 14 | 18.418 | 10.406 | 42.310 | 114.779 | 5.430 | 20.187 | 46.044 | 2.870 | 15.237 | 38.539 | 9.737 | 87.537 | 210.466 |
| 15 | 20.173 | 11.398 | 46.342 | 125.716 | 5.947 | 22.110 | 50.432 | 3.143 | 16.689 | 42.211 | 10.665 | 95.879 | 230.522 |
| 16 | 22.000 | 12.430 | 50.539 | 137.103 | 6.486 | 24.113 | 54.999 | 3.428 | 18.201 | 46.034 | 11.631 | 104.563 | 251.401 |
| 17 | 23.902 | 13.505 | 54.909 | 148.956 | 7.046 | 26.198 | 59.754 | 3.724 | 19.774 | 50.014 | 12.636 | 113.603 | 273.135 |
| 18 | 25.882 | 14.623 | 59.457 | 161.295 | 7.630 | 28.368 | 64.704 | 4.033 | 21.412 | 54.157 | 13.683 | 123.014 | 295.761 |
| 19 | 27.943 | 15.788 | 64.192 | 174.140 | 8.238 | 30.627 | 69.857 | 4.354 | 23.118 | 58.470 | 14.773 | 132.810 | 319.314 |
| 20 | 30.089 | 17.000 | 69.121 | 187.512 | 8.870 | 32.979 | 75.221 | 4.688 | 24.893 | 62.960 | 15.907 | 143.008 | 343.834 |

